First publ. in: Physiological reviews, Vol. 74, No. 1, January 1994

Chaos and Physiology: Deterministic Chaos in Excitable Cell Assemblies

THOMAS ELBERT, WILLIAM J. RAY, ZBIGNIEW J. KOWALIK, JAMES E. SKINNER, KARL EUGEN GRAF, AND NIELS BIRBAUMER

Institute for Experimental Audiology, University of Münster, Münster, Germany; Department of Psychology, Pennsylvania State University, University Park, Pennsylvania; Baylor College of Medicine, Houston, Texas; and Institute for Medical Psychology, University of Tübingen, Tübingen, Germany

PREFACE

The main impetus for writing this review has been the increasing interest in the field of nonlinear dynamics, or chaos as it is commonly called, and its application to physiology. The approach has generated both excitement and concern. As new information is gained, research may demonstrate that some of the excitement is appropriate and some inappropriate. Some of the present concern results from overstatements or misunderstandings that have polarized parts of the scientific community. We, of course, do not believe that nonlinear dynamics will answer all of our questions. However, we suggest that this approach may help us to answer new questions and to rearticulate old ones.

Presently, there are both promises and problems with this approach. For example, one potential promise is the possibility that nonlinear strategies of data analysis in combination with well-articulated theories will eventually illuminate qualities concerning the dynamics of a generating system, and in this manner venture beyond previous understandings of emerging neural patterns. On the other hand, a current technical problem is whether the algorithms provided by nonlinear systems theory to detect chaos are indeed part of a revolutionary new paradigm shift or just represent another heuristic mathematical transformation adding little new information to our understanding. This is a question yet to be fully answered and one of the questions we approach in this review. Chaos is revolutionary in that

the overall approach requires us to adopt a different frame of reference which, at times, may move us away from previous concerns and methods of data analysis. For example, does a concept such as stationarity have the same meaning and validity in the nonlinear approach? Some would suggest not. However, as we see in this review, we still must proceed cautiously.

Although historically this new approach for understanding complexity in nature has its roots in the work of Newton, Rayleigh, and Poincaré, it has been only recently that the procedures and concepts have been developed to a point where they are beginning to have an important impact on a wide variety of fields including physiology. This approach has drastically modified the manner in which physiological processes are viewed and described. For example, some processes formerly perceived as erratic, or random, are now viewed in terms of patterns and potential lawful relationships. Even the term chaos, itself, has changed in meaning. Previously the term signaled randomness, but it now connotes the idea of underlying structure and the potential for describing a complex system with the aid of relatively simple mathematical formulations. One advantage of the theory of chaos is its ability to define and quantify complexity on an abstract level. However, as we see in this review, it is imperative to determine that the processes described as chaotic reflect actual physiological processes. Thus we now see a variety of procedures for delineating whether frenetic chaotic behavior results from a nonlinear dynamic system with a few degrees of freedom, or whether it is caused by an infinite number of variables, i.e., noise.

In this review, we summarize the nonlinear dynamics approach and describe its application to physiology and neural systems. *1*) We present a general overview of the application of nonlinear dynamical techniques to neural systems. *2*) We describe the principles of nonlinear dynamical systems including the derived analytic techniques. *3*) We examine the application of these to the cardiovascular system. *4*) We approach the applications of nonlinear procedures to the neurosciences. *5*) We overview the problems and promises of this approach. We have tried to make each section self-contained so that the reader can focus on those topics of greatest interest. True to our subject, we have not performed an exhaustive review of the growing literature, but attempted to describe the area with the important underlying principles.

I. INTRODUCTION

A. *Universality of Chaos in Complex Neuronal Networks: an Illustration of Some General Principles*

Historically, the idea of the existence of "chaotic" activities in biological systems, such as the central nervous system (CNS) in particular, is not a new one. However, when thinkers of the presocratic period in ancient Greece and again the first Renaissance scientists, such as Girolamo Cardano, approached the topic, they were unable to formulate mathematical rules for nonpredictable events such as gambling, weather, pendulums, waves, and so forth. Despite the fact that some philosophers and physicists, e.g., Galileo Galilei, considered the presence of chaos in a variety of physical systems such as the weather and planet movements, the application of a chaotic view to biological systems has only recently been seen. This may have resulted partly because cybernetically oriented views have had and still have a persuading explanatory power in physiological regulation.

While the classical "phenomenological" definition of "chaos" means absence of order and unpredictability, the modern definition of chaos is based on nonlinear mathematics whose principles were anticipated during the late 19th century by Poincaré but made mathematically accessible by Lorenz in 1963 in a paper in the *Journal of Atmospheric Sciences* with the title "Deterministic nonperiodic flow" (161). Today, chaos is defined as unforeseen behavior in a deterministic system or to say it in a more colloquial form: Chaos is apparently lawless behavior totally ruled by (deterministic) laws. In 1987, Skarda and Freeman (248) brought the definition down to one phrase when they described chaos as "pseudorandom noise." Generally the word *chaos* refers to a low-dimensional aperiodic signal, while the term *noise* is used to describe behavior resulting from very many degrees of freedom. We shall present the mathematical definition and applications and examples of this definition to physiology later in the review. Before turning to specific examples, some general remarks seem to be justified where the new principles of deterministic chaos depart from or modify our traditional way of thinking about physiological systems.

1. Sensitive dependence on initial conditions

Poincaré suggested in 1903 that "small differences in initial conditions produce very great ones in the final phenomena." This important fundamental characteristic of a chaotic system is referred to as sensitive dependence on initial conditions. This sensitivity to initial conditions also carries with it the dramatic implication of the impossibility of long-term prediction of the system as arbitrary small perturbations may or may not have a consequence. Graphically, this phenomenon also can be viewed as a loss of neighborhood in terms of location. Sensitivity in this case refers to the situation in which two systems are started initially with two arbitrarily close numbers. Following this, their dynamical states will diverge from each other quickly in the phase space such that each has a completely different time series $x(t)$ and represent two separate systems. Thus, in the process of successive iterations, any small difference "explodes" exponentially. To say it mathematically, the image of any finite subinterval will eventually shadow the whole interval. Even if we know the system's equations exactly, the limited precision by which we can spec-

ify the present condition will snowball over time and soon render predictions useless. Furthermore, even if we could know the initial conditions with infinite precision, the computation of the next iteration of the system's equation must lead to minimal errors, which then would grow again exponentially and ultimately destroy long-term prediction. The everyday implications of this principle guarantee that even with the most modern meteorological advances, we will still continue to discuss the weather and its unpredictability. Similarly, we must also realize the limitations of predicting cortical activity or human behavior. However, we may come to a better understanding of the underlying dynamics.

2. *Chaos and homeostasis*

Nonlinear process models, such as the model of olfaction by Freeman and co-workers (69–71, 75, 82), do not necessarily replace classical feedback or reflexology models; they complement them in some very significant ways. No one would deny that self-preservation of living organisms in evolution can be described by positive- and negative-feedback systems. In this sense self-preservation can be seen as the main selection mechanism to keep the energy output of physiological systems within tight limits. In this model, the body is thought to maintain a steady-state equilibrium in its critical variables (e.g., blood pressure, lymphocyte activity) and to respond to perturbations to restore this equilibrium. From this perspective, the elimination of noise can be seen as the main purpose of equilibrium-oriented systems. This is also particularly true for devices using negative feedback to stabilize output, such as thermostats that keep temperature constant by negative feedback. Because irregular behavior of some machines could be disastrous, it is an essential ingredient that mechanisms exist for elimination of noise.

The obvious analogy between machines and organisms blurred our view for mechanisms in adaptive systems such as the CNS which run contrary to homeostatic ones. Adaptive brain processes have to produce body movements oriented toward the anticipation of goals to achieve self-preservation, promote reproduction, and engage in social interaction. To achieve these ultimate aims, organisms have to search, orient, attack, relate, and so forth often under totally new unlearned circumstances. To manipulate the environment, homeostatic and deterministic systems have to be "destabilized" (e.g., Refs. 77, 248) at times to produce entirely new activity patterns (new ideas, creative thoughts, new form of behavior). Although there have been various speculations in terms of anatomy (e.g., Refs. 27, 227), a complete theory must account for the manner in which the chaotic interruption of "old" overlearned activity patterns together with the deterministic formation of new expectancies prepares the sensory and motor system to respond to new environmental demands. A similar question guided Freeman and co-workers' analysis of the olfactory system (69–71, 75, 82), particularly the entorhinal cortex. In any ambiguous or new situation, the brain has to self-produce new activity patterns before it settles down to old (deterministic) ones. Regularly oscillating physiological rhythms are one source for rhythmic changes in motivated behavior (such as eating and drinking cycles). These have been incorporated into homeostatic thinking without particular conceptual problems. The same will also be true for the incorporation of the idea of chaotic oscillations within and across neuronal systems. Even in the context of feedback models, chaos would be expected in highly interconnected and tightly coupled feedback loops found in biosystems. Glass and co-workers (86, 89, 91) found that systems with mixed feedback (both positive and negative feedback) and multiple feedback with different time constants are sources of chaos. An der Heiden (10) describes the organism as a dynamical system with the classical equilibrium as a special case of an attractor. Healthy and pathological states become interpretable as different types of attractors, which may be converted from each other by bifurcations or critical perturbations.

3. *Effects of weak perturbations*

One of the most important aspects of chaotic behavior of physiological processes in the face of new environmental demands is the very fast, often instantaneous, reduction of excitatory thresholds of masses of nerve cell populations not excited in that particular combination before. This phenomenon is referred to as "bifurcations" or a type of "rapid state changes" in deterministic chaos theory. Rapid state changes and bifurcations are characteristic of networks that are sensitive to very weak initial conditions that lead to wide-spread changes in the whole system. On a psychological level, not only the unexpected original idea but also the sudden unpredictable onset of an epileptic seizure in pathophysiology constitute examples of chaotic behavior of neuronal nets. Even a whisper can turn on a full-blown paranoid delusion within a fraction of a second, causing physiological and psychological changes of the whole brain.

Behavioral neuroscience traditionally has had difficulties explaining the formation of new and unlearned concepts and percepts (such as responses to new odors) in the CNS. In a feedback-controlled deterministic system, the appearance of totally new activity patterns out of the existing patterns cannot be described adequately. Naturally, the mathematical approximations used in nonlinear dynamics and the physical models of turbulence cannot predict the exact departure of bifurcations, but these models may help us to determine how many explosive changes can be expected in a time series to particular stimulus conditions. The "basin" of an attractor[1] of a dynamic system allows the definition of the

[1] The attractor basin is defined as the set of all initial points (i.e., the set of all those initial conditions) that reach the attractor after a high enough number of iterations. The trajectory that leads from the initial conditions to the region described by the attractor is accordingly a transient.

point in time at which the system suddenly changes its behavior (an attractor is the "frozen" graphical representation of its activity pattern; for the mathematical definition and examples see Ref. 243). This allows the physiological investigation of critical time regions that may cause unpredictable new behavior of the system. Perceptual phenomena such as the sudden jump of the Necker cube between foreground and background (52), as well as the perception of new odors (248), are examples of such rapid state changes and become accessible to a more detailed physiological analysis by using the graphical representations of the relevant chaotic series, which we describe in section I*A5*.

4. Nonlinear systems theory and the relation between normal and abnormal functioning

Recently, several authors (92, 93, 205, 252) have discussed the question of whether chaotic behavior constitutes evidence for pathology of a system or whether chaos indicates healthy variability universally found in living organisms and the whole of nature in general. Glass and Mackey (90) described the change from order to disorder as "dynamical diseases," thus seeing chaos as a sign of pathology. Dynamical disease denoted situations in which control had been lost and was defined as "a disease that occurs in an intact physiological control system operating in a range of control parameters that leads to abnormal dynamics and human pathology" (90). On the other hand, Goldberger and West (92) proposed the hypothesis that the dynamics of a healthy physiological system would produce apparently highly irregular and highly complex types of variability, whereas disease and even aging is associated with less complexity and more regularity. Indeed, Kaplan et al. (140) have reported that the complexity of heart rate and beat-to-beat blood pressure measures is reduced with aging. Skinner (249, 256) has shown, in both animals and humans, that transient decreases in heartbeat complexity are harbingers of imminent lethal cardiac arrhythmias.

There has been increasing evidence to support the case that chaos plays a positive role in the physiology of the organism. Goldberger and co-workers (92, 93) stated that chaos should be healthy because it provides the organism with an "information-rich (broadband) state" and "spectral reserve." Patients with severe heart failure, for example, show a loss of sinus rhythm (heart rate variability) (255). Likewise, it has been shown for an epileptic seizure that the degree of chaos is significantly changed both before and during a seizure (12, 94, 237). Most examples given in the following review seem to indicate that chaotic behavior is a necessary ingredient of normal functioning. However, there are exceptions found in a variety of fields including our own magnetoencephalogram (MEG) studies of tinnitus (148). With progress in the field, more exceptions will most likely be brought forth.

However, it is also possible to demonstrate how different kinds of behavior emerge from the same set of systems equations. Prominent examples are Cheyne-Stokes respiration (a special kind of irregular breathing pattern) and fluctuations in peripheral white blood cell counts in chronic granulocytic leukemia. For both of these processes there exist mathematical models that show how the system is able to change its pattern. In the future it may even be possible to devise therapies for disease by manipulating control parameters back into the normal range.

The broad answer to the larger question of chaos and disease depends on our understanding and interpretation of a particular physiological or behavioral system. Neither nonlinear theory nor conventional homeostatic analysis can, nor should, free us from our scientific logical analysis of the observed data. Chaos procedures do not automatically create the correct theory. Therefore, it will not be surprising to find chaotic processes in the behavior of both abnormal and healthy systems.

5. Analyzing time series

Research in physiology often involves the interpretation of signals reflected in time series that are irregular. One source of continuing frustration has been our ability to visually recognize patterns within these irregular time series which have proven impossible to systematically detect with our current statistical techniques. In the 1980s, one answer was presented to this problem. It was suggested that this discrepancy was the result of examining the time series in terms of static rather than dynamic behavior. That is to say, our techniques had not taken into account nonlinear relationships. Traditional signal-processing procedures decompose, through Fourier analysis or a similar technique, the component frequencies in the signal and thus reflect a limited amount of information (one dimensional). In contrast, the dynamic view suggests that a time series may be seen to reflect the marks of all other variables participating in the dynamics of the system. Overall, the theoretical aspect of this possibility is based on a variety of mathematical theorems (262). Given that complex dynamic systems (such as the human nervous system) have an enormous number of interrelated dependent variables that are impossible to measure directly, the theorems suggest that if we can measure any single suitable variable with sufficient accuracy, sufficiently often, and for sufficiently long periods of time, then it is possible to make quantitatively meaningful inferences about the dynamic structure of the entire system from the behavior of that single variable. From this perspective we have a theoretical foundation to explain why the nonlinear dynamical or chaotic approach may well offer a characterization of behavior that is far richer than that obtained by classical measures (218). Of course, there exists considerable discussion concerning parameters such as what would constitute sufficient accuracy, how often the signal should be sampled, as well as how long data segments should be.

One breakthrough has been the ability to project the dynamics of a system (i.e., a state space) onto a static diagram (e.g., a phase-space diagram). Although we describe this procedure in greater detail in section II, let us conceptually overview this procedure as well as introduce some important terms that we discuss later in this review. The initial question we wish to ask is: What are the underlying dynamics that are produced by this system? To answer this question we follow the Newtonian idea of creating a phase space, a space which is spanned by the system's variables. As is usually the case in physiology, we do not know the system's variables; thus we must reconstruct the phase space from the time series observed. A point in this space represents a momentary state of the system. A sequence of such states followed in time defines the phase-space trajectory. If the dynamics of the underlying system can be reduced to a set of deterministic laws, then the phase-space trajectory may converge toward a subset of the phase space. This invariant subset is referred to as an attractor. Given a particular time series, the initial question one asks concerns the possibility of identifying an attractor. If the answer is yes, then it is possible to view the series as a manifestation of a deterministic dynamic system (albeit possibly a very complex one). An important measure of interest is dimensionality, referred to as D. A periodic oscillation (e.g., a sine wave) would have a dimension of one. A quasiperiodic oscillation (e.g., 2 incommensurate frequencies) would result in a dimension of two. If the system has a dimension larger than two and is not an integer (i.e., it is a fraction), then we would expect the system to exhibit chaotic oscillations (e.g., the Lorenz attractor with a dimension of $\sim$2.08). One further asks about the minimal dimensionality of the phase space within which the attractor is embedded, which defines the minimum number of variables that must be considered in the description of the underlying dynamics. If the evolution of a system is dominated by a strange attractor with fractal dimension D, then the minimum number of ordinary differential equations needed to describe the system's evolution is the smallest integer greater than D.

Dimensionality is one of the basic quantitative measures of a complex dynamical system. The classic definition of dimension refers to the minimal number of independent variables (or directions) in a set. This definition has been generalized to include both higher dimensions and fractal dimensions. Although beyond the scope of this brief introduction, it should be pointed out that in this newly developing literature, the term dimension does not always have an absolute technical meaning. For example, when different mathematical procedures used to compute the fractal dimension are applied to the same data set, different values may result. These differences may result because the data are finite, and the measures presume infinite data length, or the data are nonstationary, and the measures presume that the data generator does not change. Therefore, relative differences in dimension between conditions, or within the same condition, may be of more practical interest than any inaccurate estimate of the absolute value. Another important measure that we describe in section II is entropy. This is a measure of complexity which reflects loss of information or inversely the amount of information needed to describe the future state of a system. The more complex the system (with noise being the most complex), the greater the entropy. As valuable as these techniques are proving to be, there are many additional questions that should be considered in applying such measures to actual physiological systems.

To briefly summarize, the major feature of a chaotic system is the sensitivity to initial conditions, which implies intrinsic unpredictability. The butterfly-shaped Lorenz attractor illustrates this condition. The exact trajectory (depending on initial conditions) is different each time it is generated (see Fig. 3). It is impossible to predict when a shift from one side of the Lorenz "butterfly" to the other will take place. Chaos theory offers a means of measuring and quantifying complexity through such measures as those of dimensionality and entropy. Although these measures work within strict mathematical contexts, the broad question exists as to whether it is appropriate and if so, under what conditions, to apply these models to a physiological system. The potential benefit of such an application is that deterministic measures of a deterministic (especially of a chaotic) system may be inherently more accurate in tracking the output of the system. Before considering the measures themselves, let us delineate a variety of successful applications.

B. Sinusoidally Forced Squid Membrane: an Illustration of Deterministic Chaos

Although they may not be governed by very complicated laws, neurons in general are prominent candidates for producing complex patterns because of their pronounced nonlinearity. One of the most investigated of these neurons in physiology is the giant axon of the squid *Doryteuthis bleekeri*, which is known for the rapid transmission of solitary action potentials. If we view the axon of a single neuron as a structure specialized for the transmission of information over a distance, we can further inquire as to the dynamical mechanisms generating these signals and how these vary parametrically in terms of input. In 1952, Hodgkin and Huxley (123) presented their well-known model of the squid axon. Using four simultaneous, first-order differential equations, Hodgkin and Huxley (123) described the time course and voltage dependence of the membrane ionic currents flowing in the giant axon of the squid and thus provided a quantitative model for action potential generation. This model involves three voltage-dependent gating variables, the sodium and potassium activation variables and the sodium inactivation variable, and a fourth variable involving the membrane potential.

Although the isolated giant axons of the squid are silent, it is possible to introduce a self-sustained peri-

odic activity by choosing a mixture of natural seawater and 550 mM NaCl (e.g., 9:1) as the external medium surrounding the axon. In this solution the axon behaves as a nonlinear neuronal oscillator with natural frequency (f_n). The membrane potential can be recorded through a pair of glass pipette Ag-AgCl electrodes (see Ref. 4, p. 251).

The standard method of analyzing the signal-handling characteristics of such a system is to apply a cyclic sinusoidal driving function with $A \sin(2\pi f_s t)$, where A is amplitude, f_s is stimulating frequency, and t is time, being the simplest case of a repetitive input. A spike train gives similar results in most cases. Differential results can be found in both the model and the axon preparation by varying two parameters, A and f_s of the driving function. In principle, five types of dynamic behavior can be observed and distinguished: periodic oscillation, quasiperiodic oscillation, intermittency, chaotic behavior, and stochastic behavior.

The simplest case of the system's reaction to periodic entrainment is given when f_s is close to f_n, or combined frequencies having the ratio of 2:3 or 3:4, and so forth. In this case, the system mode locks to f_s. This results in the action potentials always occurring at specific phase angles of the forcing cycle. Again, if f_s and f_n are different but approximately commensurable, i.e, a pair of integers m and n exists with $m > n$ such that $f_s - F(m,n)f_n$, the result will be n action potentials being generated at locked phases during m cycles of the sinusoidal forcing function. Figure 1*A* shows a motion (which could be also intermittent), close to a one-fourth synchronized oscillation in squid giant axons. A similar phenomenon can be observed in the Hodgkin-Huxley model (Fig. 1*B*; Ref. 5).

It is possible to describe the time evolution of a system by making observations at discrete times with the period T_s ($= 1/f_s$), similar to stroboscopic illumination. Starting with an initial point represented by P_0, the successive points obtained by the stroboscopic representation can be denoted by P_i ($i = 1,2,\ldots$), and the transfer function P_i versus P_{i+1} can be plotted (Ref. 138, p. 57; Fig. 1*B*). Viewing a plot in which one point is identical to the next (i.e., perfect synchronization in which $f_n = f_s$), we would expect the behavior to be frozen. Similarly, a limited set of m points in the plot implies that after m periods of the forcing function, the values of the system will repeat such that we have a $F(n,m)$ synchronized periodic system. (The value of n cannot be determined from such a plot.)

When the frequencies f_s and f_n are irrationally related, the resulting type of behavior is a quasiperiodic oscillation. Its prominent feature is a never-repeating time series [Fig. 1*C* (2) for the giant axon and Fig. 1*D* (5) for the model]. Thus the system will always produce new and different points, and consequently, the transfer function (Fig. 1*D*; Ref. 5) in principle consists of an infinite number of points. However, these points are visually ordered in a simple fashion in that they all lie on a closed curve.

Until the 1980s, the well-known phenomenon that under certain periodic forcing conditions the axon responds with an irregular behavior (Fig. 1*E*; Ref. 173) was discussed in terms of "irreducible noise components" in the system (124). Matsumoto et al. (173) were the first to show that this peculiar behavior results from a deterministic system. The complicated structure in Figure 1*E* is obviously different from both the picture of a quasiperiodic motion (which is a simple closed curve, Fig. 1*D*) and the picture of a stochastic motion (which will fill the plane without a structure). As with the real axon, the model also behaves in a chaotic fashion under certain conditions (Fig. 1*E*, see also Ref. 5 and Fig. 9, *A* and *C*, therein).

Let us now summarize two important points: *1*) the irregular behavior of the axon is not due to a noise component in the membrane but results from a deterministic system, and *2*) for the giant axon of the squid there exists a powerful model (the 4 Hodgkin-Huxley equations) that is able to generate all the types of oscillations known from the experimental observations of the axon. Even specific ways to move the system from regular to chaotic behavior (so-called "routes to chaos") can be identified in both actual axon behavior and the model (2-4, 6). Thus the Hodgkin-Huxley model can be seen as a prototype of a new strategy of investigation, that of modeling the dynamical behavior of a system. However, because these self-sustained oscillations were induced experimentally in a nonnatural solution, there still existed the crucial question as to whether the chaotic oscillation could also exist in naturally occurring physiological systems. This was answered in 1987 by Matsumoto and co-workers (174, 176) when they demonstrated chaotic oscillations by applying periodic trains of current pulses to the silent axon immersed in normal seawater. Thus it became clear that axons in particular and neurons in general could produce chaotic behavior under natural conditions.

C. Chaotic Homeostasis: Why Nonlinear Systems Analysis Might Prove to be a Useful Tool in Physiology

Traditionally, physiological control systems have been viewed as governed by homeostasis. In such a view, the body is thought to maintain a steady state in each of its critical variables. When perturbations are experienced, the body responds to this change by restoring equilibrium. This concept of homeostasis has emerged from negative-feedback models popular in engineering that suggest a machine only works well by maintaining critical values. In such a system oscillations or erratic behavior are viewed as disastrous. The traditional mathematical approach describes this system in a linear manner, such that the number and frequency of oscillators can be adequately determined from the peaks in the power spectrum.

It has now been realized that this concept may be inappropriate when modeling biological systems, such as the example presented in the previous section. Using such a model with physiological variables that are gener-

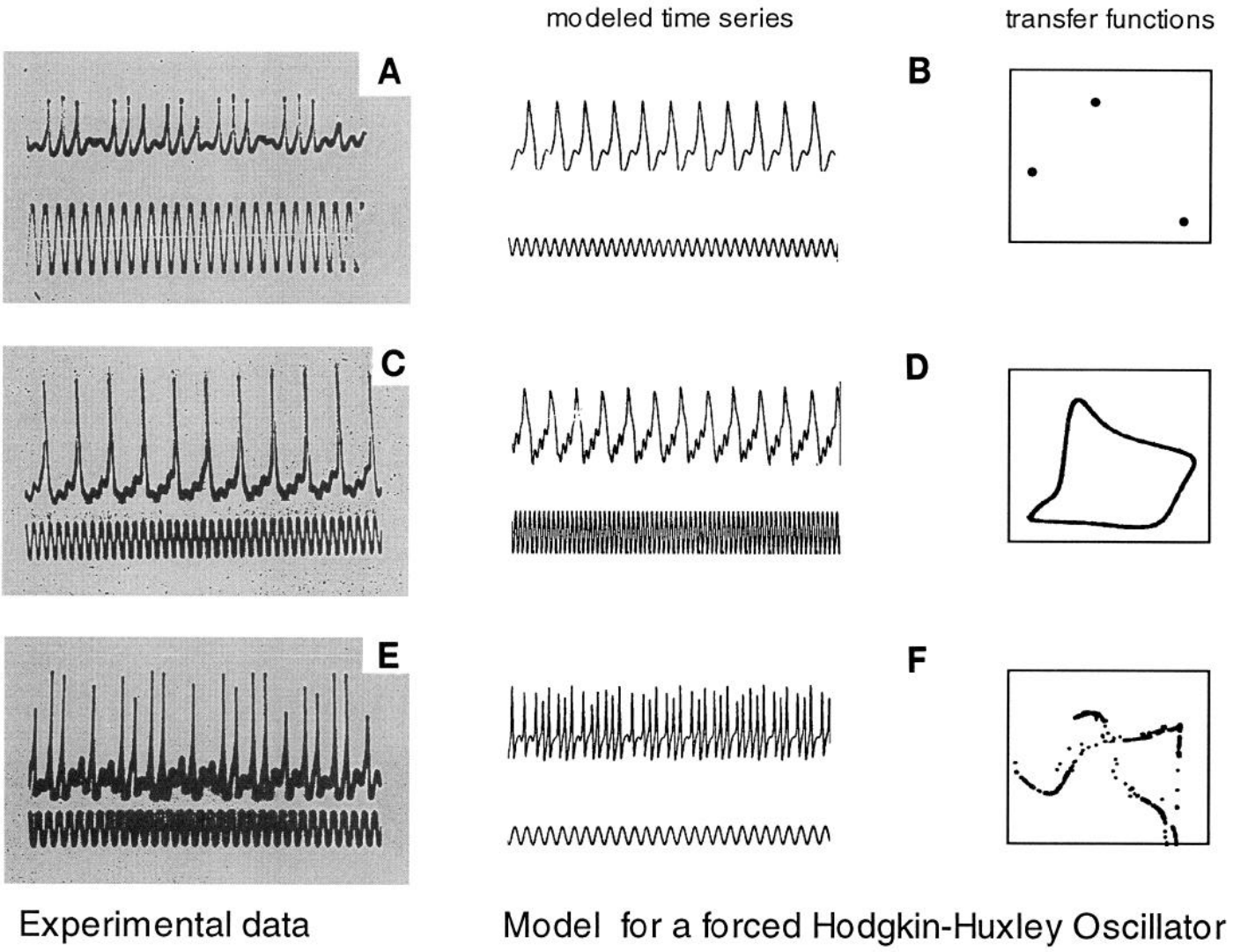

FIG. 1. *A*: a subharmonically synchronized oscillation [the naturally oscillating frequency (f_n) = 180 Hz, the stimulating frequency (f_s) = 254 Hz, and the amplitude (A) of the stimulating current = 2 mA]. Waveform of membrane potential (*top trace*) and that of stimulating current (*bottom trace*) are shown. Length of bar corresponds to 80 mV, 4 mA, and 20 ms for membrane potential, the stimulating current, and time, respectively. [Adapted from Aihara et al. (5).] *B*: one-third synchronization in the forced Hodgkin-Huxley oscillator (A = 40.0 mA/cm^3, f_s = 500.0 Hz). *Left*: waveform of membrane potential (*top trace*) and that of stimulating current (*bottom trace*). *Right*: transfer function consisting of 3 points. *C*: quasiperiodic oscillation in forced squid giant axons; f_n = 187 Hz, f_s = 800 Hz, and A = 2 mA. Waveforms of membrane potential (*top trace*) and stimulating current (*bottom trace*) are shown. Length of bar corresponds to 60 mV, 12 mA, and 15 ms. *D*: quasiperiodic oscillation in forced Hodgkin-Huxley oscillator (A = 100 mA/cm^2 and f_s = 1 kHz). *Left*: waveforms of membrane potential (*top trace*) and stimulating current (*bottom trace*). *Right*: transfer function forming a closed curve asymptotically. *E*: chaotic oscillation in forced squid giant axons (f_n = 228 Hz, f_s = 332 Hz, and A = 4 mA). Waveforms of membrane potential (*top trace*) and stimulating current (*bottom trace*) are shown. Vertical bar stands for 20 mV and 4 mA. Horizontal bar denotes 10 ms. *Right column* in *F* shows corresponding transfer function, which is a complicated structure. *F*: chaotic oscillation in forced Hodgkin-Huxley oscillator (A = 40 mA/cm^2 and f_s = 100 Hz). *Left*: waveforms of membrane potential (*top trace*) and stimulating current (*bottom trace*). *Right*: a transfer function forming a complicated portrait.

ally oscillatory (body temperature, blood pressure, levels of hormones and transmitters), we would expect that interoceptors would habituate to a constant environment, and thus the result would be a drift rather than a constant range of the variable under control (45). Because nonlinearity is ubiquitous in living systems, it is now apparent that complex dynamical systems better describe biological regulation. If this is the case, then we must utilize tools specialized to detect nonlinear relationships.

Apart from the analysis of normal states, nonlinear systems theory may also provide new insights into disturbances of dynamical behavior as reflected in pathological processes. As previously illustrated with the squid membrane, the same system can exhibit very different kinds of behavior, ranging from the normal to the

dysfunctional. Because it is the environment of a system that determines the particular mode via the control parameters, abnormal oscillations may not result solely from pathological systems; rather, some unexpected change in the environment may cause an intact system to switch to a qualitatively different dynamical pattern.

As discussed previously, whether chaos indicates pathological or normal functioning has been debated vigorously. While the initial introduction of the term *dynamical disease* in 1977 equated chaos with illness, more recent evidence suggests that chaos may play a positive role in the survival of the organism. As we can see, chaos implies unpredictability, which in turn can be an important feature in animal and human behavior. For example, the flight of a butterfly or the zig-zag of a rabbit must be unpredictable to avoid being caught by a predator. Likewise, cognitive functions such as searching in memory for a concept or the creative solution of a problem cannot be described in a linear fashion. Freeman (77) speculates that chaos underlies the brain's ability to respond flexibly to the external world and that these novel brain patterns are experienced as "fresh ideas." Chaos may also help us to understand how the brain is able to organize itself and be directed by that organization. To adequately describe these processes, models involving simple oscillations do not provide enough flexibility.

II. BASIC PRINCIPLES OF THE THEORY OF DYNAMIC SYSTEMS

A. *What Comes Next?: the Difference Equations*

By definition with linear systems, the output is proportional to the input; that is, by manipulating an input variable by a certain amount leads to a change in the output variable proportional to that amount. These situations can typically be described by simple equations that result in simple graphic plots. Thus, in the case of linear systems, we always know what comes next. This is not the case with nonlinear systems. Although the equations that describe the dynamical system may at first appear simple, the result may not be so. In this section we point out how even a simple equation can be used to describe an immensely rich process in which we cannot know what comes next. Unlike linear systems in which stability is produced, nonlinear models produce a variety of outcomes that in the physical world can result in qualitatively different behaviors. In this manner we want to underscore that this is true not only for mathematical systems but for also a variety of phenomena from physics to physiology.

In 1845, P. F. Verhulst examined the question of how the population of a single species in a closed well-defined environment might change over generations. In his first model, he required that generations not overlap as would be the case with seasonally breeding insects. Two constraints characterize the model. The first is that the (relative) number of the individuals (x_t) in the year t should give rise to a proportional number of offspring in the next year.[2] We can think of this proportion as birthrate, which we refer to as r. For example, if r were 2, then a population of 100 would be followed the next year by a population of 200, then the next year by a population of 400, then 800, and so on. The second constraint is a control factor (e.g., depletion of feeding grounds), which would restrict unlimited growth; that is, there should be a restriction of the population proportional to the remaining area $(1 - x_t)$. In the resulting equation, x is normalized such that it lies between zero and one. Thus x is expressed as a fraction and represents the maximal number of individuals that the resources could maintain. Given x_t, we now can calculate the number of individuals in the next generation

$$x_{t+1} = rx_t(1 - x_t) \qquad (1)$$

Equation 1 shows the mathematical model, known as a "logistic" or "quadratic" map, and is one of the simplest nonlinear difference equations (177). The control parameter r is determined by the biological system (i.e., it depends on fertility, on available resources) Mathematically, we know that if we multiply x_t times $(1 - x_t)$, then we arrive at the resultant x_t minus $(x_t)^2$, which graphs as a parabola. Thus, as a function of x_t, x_{t+1} is simply a parabola (Fig. 2*A*) attaining a smooth round maximum value of $r/4$ at $x = 1/2$, with the parameter r controlling the height and steepness of the hump. The variable r must remain in the interval $0 < r \leq 4$ or the time series will "explode" to infinity.

Using traditional linear thinking in determining the population, one might expect that the built-in feedback mechanism forces the population toward a predetermined size. This, however, is not necessarily so. Depending on the value of r, simple nonlinear models are capable of producing an astonishing variety of qualitatively different behaviors. If $r < 1$, as can be easily derived from *Equation 1*, subsequent x values will become smaller and smaller, and the species will quickly vanish. In this case, all trajectories are attracted to $x = 0$, the only stable fixed point. A fixed point (fp) is defined as $x_{fp} \equiv f(x_{fp})$. Whatever starting point is chosen (after a transient phase), the population reaches a constant nonzero value only when $1 < r < r_1$, with $r_1 = 3$ for the quadratic map (*Eq. 1*). That is to say, if we chose the birthrate to be below three (but above one), we find that the resulting population moves toward two-thirds the size of the original population. Because any number we chose in the one to three range will result in the same population size, we can see the value of two-thirds of the original population as an attractor on our map. Thus,

[2] In general, we can write $x_{t+1} = f(x_t)$, meaning that the population at time $t+1$ is strictly determined by the population at time t.

starting at any value that differs from the fixed point, the population will follow a spiraling pattern with the point of intersection of the parabola with the line $x_t = x_{t+1} = y$ (Fig. 2*B*). Using *Equation 1*, we obtain this point of intersection $x = 1-1/r$ (i.e., it increases with increasing r). For r somewhat greater than three ($3 < r < 4$), the system loses its stability. In this case, two new initially stable points of period two are born in an act called pitchfork bifurcation, i.e., the population quantity oscillates between two different values. Then a cycle of period four is reached, and further slight increases in r yield cycles of period 8, 16, and so on.[3] This is also referred to as period doubling. However, we should note that if r were set at ~3.8, the population would increase for the first 2 yr and decrease in the third in a predictable manner. Such periods of stability in the midst of chaos are referred to as "intermittency." This illustrates an interesting aspect of chaotic systems: the fact that the same system can range in its production from simple order to great complexity.

Studying a variety of systems, Feigenbaum (64) has shown that period doubling at particular transition points is commonly seen as stability changes to chaos. The Feigenbaum scenario, in which a fixed point is followed over a cascade of bifurcations to a point of accumulation yet fails to achieve a definitive period, is one well-known route to chaos (243). This famous scenario is not only found in most low-dimensional mathematical systems but also in physical ones. Some of the earliest physical demonstrations include liquid helium being heated from below and moved through convection (Bénard convection; e.g., Refs. 158, 243), electronic circuits (147), a bouncing ball (203), chemical reactions (Belousov-Zhabotinskij reaction), optically bistable devices, and acoustics in which water is irradiated with sound of high intensity (153, 154). In areas related to physiology, Aihara et al. (5) show that for the periodically forced Hodgkin-Huxley oscillator, successive period-doubling bifurcations are the route to chaos. Aihara and Matsumoto (2) also observed this route in the periodically forced squid axons. Similarly, Guevara and co-workers (107, 108) described the dynamics of cell aggregates taken from the heart of embryonic chickens. Glass and Mackey (90, 166) developed a model of differential-delay equations for the regulation of hematopoiesis. This situation follows a sequence of bifurcations leading to chaos analogous to that found in the logistic map. Periodic fluctuations in circulating levels of platelets, red blood cells, and white blood cells described in the clinical literature (e.g., cyclical neutropenia) also can be understood with such a model. This results from a stable point, the healthy functioning, becoming unstable and giving rise to a periodic solution. Akamatsu et al. (7) proposed such a model for the intrinsic random or pseudo-random mechanism underlying certain types of muscular tremor, specifically a modified quadratic equation. Consequently, such nonlinear dynamical concepts as period doubling, bifurcation points, and chaotic behavior have proven relevant for the understanding of both insect and isometric mammalian types of tremor.

Next, we may ask what will happen when the parameter r becomes greater than r_∞? In this situation, the periodicity is completely lost, and the time series varies chaotically. For this reason, $r_\infty < r < 4$ has been referred to as the "chaotic regime." However, as we briefly noted earlier, this does not mean that all aspects of this region will be chaotic. This structure, however, is a delicate one and in it exists a large number of small, and often microscopic, stable (i.e., attractive) periodic "windows." This situation can be described as follows: *1*) such cycles are of even periods, starting very high and then descending (e.g., left window in Fig. 2); *2*) odd cycles appear ($r > 3.6786\ldots$) also in descending order (e.g., middle and right window in Fig. 2). Generally, these periodic sequences first appear with some basic period n then go through a sequence of period-doubling bifurcations, creating periods $2^k \times n$ ("subharmonics"), with an accumulation point at $k \rightarrow \infty$ ending the particular periodic window. (More strictly speaking, the cascade is over as the stable and unstable solutions, i.e., attractor and repellor, collide). The three widest such windows are (from left to right in Fig. 2) as follows: basic period six ($r = 3.62\ldots$), basic period five ($r = 3.73\ldots$), and basic period three ($r = 3.82\ldots$), with r values noting the origin of the basic periods. All other periodic windows are exceedingly narrow in r, with their periods generally being extremely high (i.e., some thousands of points). Outside of these windows there exist no stable periodic orbits, although there is an infinite number of unstable cycles. Such dynamic behavior is called chaotic.

As discussed in section 1*A1*, small changes in initial conditions result in completely different time series and make long-term prediction impossible. Thus even a sim-

[3] One may ask in which manner this infinite cascade of period doubling takes place in a limited region of r. The range of parameter values wherein any one cycle is stable diminishes in a geometric fashion so that the entire process of bifurcations converges to a point of accumulation at $r_\infty = 3.5700\ldots$ (with period 2^∞). Feigenbaum (64) detected that a universal constant, coined δ (= 4.6692...), governs this cascade of periodic doubling: the ratio of the actually stable range of parameter values to the next stable range, $(r_{n+1} - r_n)/(r_{n+2} - r_{n+1})$, approaches the constant δ as $n > 1$. There is another universal constant: the distance between new twins of a bifurcation should be, on average, $\alpha = 2.5029\ldots$ times smaller than the distance between their parent and its twin. This rule, as the first, also holds with greater and greater accuracy the larger n becomes. These Feigenbaum numbers α and δ and the bifurcation cascade they govern are universal in so far as they apply independently of the detailed functional form of the map as long as it has a single quadratic maximum, e.g., a sinuslike half-wave or an elliptic curve will produce a similar range of dynamics. The long-term behavior depends only on the infinitesimal segment at the crest of the graph and on the maximum itself. The structure of the infinity of bifurcations reflected in α gives rise to a typical phenomenon of nonlinear systems, self-similarity over different scales. Take, for example, as the starting position a 2^8-point cycle and increase the parameter r to get, via bifurcation, a 2^9-point cycle. In this case the cluster of points about $x = 0.5$ (the maximum point) of the first cycle reproduces itself in the next cycle on a scale approximately α times smaller.

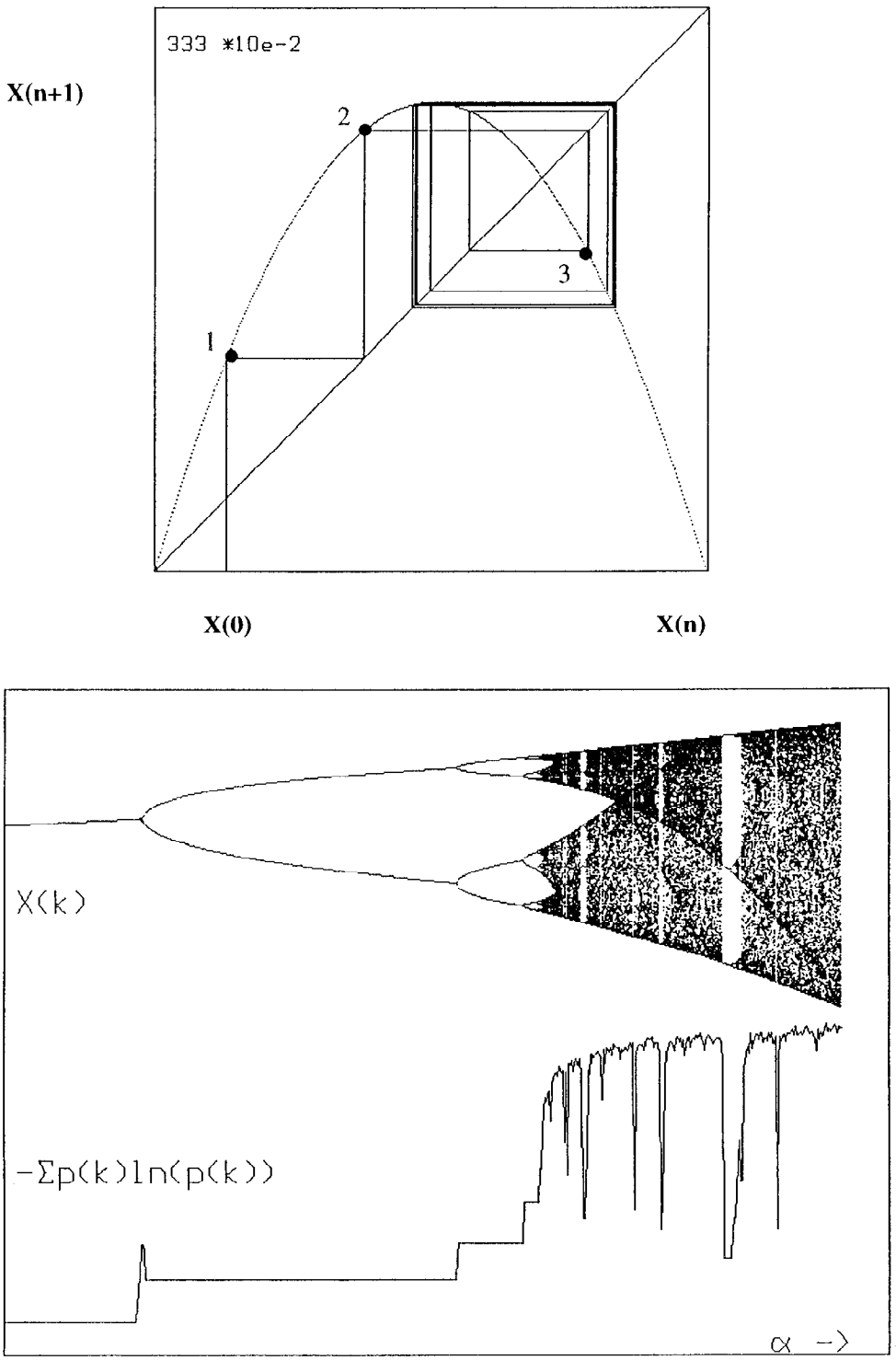

FIG. 2. *Top*: logistic map as detailed in *Equation 1*. Construction of successive time points (1, 2, ...) according to difference *Equation 1* is illustrated. For chosen parameter, $r = 3.33$ time series will oscillate between 4 points (2 pairs of points, located closely together). For a more detailed description of logistic maps, see Reference 20. *Bottom*: route to chaos illustrated for case of logistic map. Instead of using individual diagrams to display behavior of time series for every value of parameter r, information may be assembled in a bifurcation diagram; abscissa includes r values from 2.8 to 4 in *Equation 1*. For each r, all values x are plotted on ordinate, which corresponding time series will assume as time progresses. *Bottom curve* illustrates change in entropy, which system will assume for various choices of r. For $r < 3$, time series will assume only 1 stable point, and entropy will be near 0. As r increases, time series will suddenly start to oscillate between 2 points (first bifurcation), and entropy jumps to a first level. Next jump illustrates transition to period 4, then 8, and so on, in more and more rapid succession, until a first chaotic regimen is reached. There time series becomes totally irregular. Chaotic regions are then interrupted by windows with regular oscillations. Note that entropy drops to lower levels for these parameters r.

ple equation, such as the logistic map, encompasses a surprisingly rich spectrum of dynamical behavior. Depending on the value of the control parameter r, the iterations either converge after a transient phase to a fixed value, converge to cycles of stable points having different periodicity, or most important, the "transients" will never converge, giving rise to an aperiodic, seemingly random (although fully deterministic) behavior that is referred to as deterministic chaos. The only exception to this rule is that of intermittency, a behavior characterized by regular motion interrupted by "random" bursts (170).

To summarize mathematically, the general formula of a one-dimensional difference equation, the logistic equation, is a special case of $x_{fp} = f(x_{fp})$, where $f(x)$ is a scalar function. Typically, $f(x)$ is noninvertible, since,

given x_{t+1}, one cannot uniquely determine x_t. This is due to the fact that for almost each value of x_{t+1} there are at least two possible values of x_t. This results in another restriction, even for deterministic systems; that is, when given a certain segment of the time series, we will be unable to compute its history despite the fact that the system is formally totally deterministic. We likewise cannot predict the long-term future, since the error of our prediction will explode exponentially with time. Now that we have discussed difference equations that represent discrete dynamical systems, we can consider continuous time systems in the next section.

B. Lorenz and Rössler: Famous Attractors and Differential Equations

The counterpart of difference equations with their discrete time steps are systems of (first-order ordinary) differential equations. By letting the time step of the difference equations shrink to zero, the resultant differential equations evolve continuously in time. In physiology as well as in physics, this is the most common way to simulate dynamical systems and hence is used more frequently than difference equations, although difference equations may be easier to study numerically. A differential equation connects the continuous rate of variation of some quantity to that quantity's current size and to the current sizes of some other quantities of the system. Thus a system with m independent variables is fully described by m-coupled differential equations (first order).

The general formula of a system of ordinary differential equations is

$$\mathrm{d}\mathbf{x}/\mathrm{d}t = F[\mathbf{x}(t)]$$

with $\mathbf{x}$ being a vector in an m-dimensional space.

One way to visualize the patterns defined by differential equations is to imagine a multidimensional space in which a moving point constructs a curved line. At any moment, the location of this one point provides complete information about the system's state. Its projections along the various axes (i.e., system's variables) give the values of the relevant quantities that describe this unique state (this space is called the phase space).

For the purpose of a graphical representation of the system's evolution beginning with some initial state $\mathbf{x}(0)$, a state space (phase space) is configured with axes corresponding to the variables of the system. With a phase space, the idea is to mathematically and graphically represent the variables in the system. The state space defines all the possible states of the variables under study. Each state of the system can be completely represented by a point in this space. A particular set of occurrences or points can be connected, e.g., in time, to form an evolution of the system. Common terminology names the continuous curve describing the motion of the system originating from an initial state the trajectory or orbit. The set of orbits originating from all possible initial conditions generates a flow in the state space. Limitations of such a system include the condition that every trajectory must be non-self-intersecting and that different trajectories originating from different initial conditions must not overlap or occupy the same space. This arises from the fact that a point in phase space representing the state of a system is considered to encode all the information about the system, including both its past and future history, which must be unique in a deterministic system. This means that there cannot be two different pathways leading in or out of one point if the system is deterministic. In real dissipative systems (i.e., those subject to friction) with internal friction and ubiquitous noise, trajectories do not move toward filling phase space as conservative systems (i.e., those that conserve energy and thus are not subject to friction), but over time approach a bounded region of the state space. This is a subspace of the total state space with a dimension not greater than the dimension m of the state space. Such a well-defined subspace is called an attractor. An attractor, as the name implies, appears to bring together a variety of nearby trajectories over time. An attractor characterizes the dynamically stable long-term behavior of the system.

There exists a simple hierarchy of types of behavior (attractors) occurring in dissipative systems of differential equations. In one-dimensional systems, the only possible attractor is a stable fixed point (an equilibrium, or resting, state) or a set of such points. In two-dimensional systems, an additional type emerges, the periodic attractor, also referred to as limit cycle, because it is characterized by a closed loop in the phase space. Again, in three-dimensional systems, another type of attractor can be expected. Because of its erratic features it is called, in contrast to traditional "ordinary" attractors, a strange attractor.

Although Poincaré (208) first described the importance of initial conditions for classically deterministic systems in 1892, recent history credits Lorenz in 1963 (161) with first describing a system of ordinary differential equations which exhibit a dynamically stable, but erratic and nonperiodic, behavior. Interested in the problems of long-term weather prediction, Lorenz (161) developed a set of three differential equations modeling a convective process. Simply said, imagine that, as the sun heats the earth, the lower layers of air become warmer and lighter than the upper levels, which results in a upward motion of light warm air and a downward motion of cool dense air. As a result, convection rolls transport warmer air upward and cooler air downward. When heated even more, this laminar state loses its stability and turns into turbulence with the direction of the convection rolls becoming chaotic, i.e., a random-appearing change emerges over time in the spin orientation of the rolls. Lorenz studied this phenomenon in a

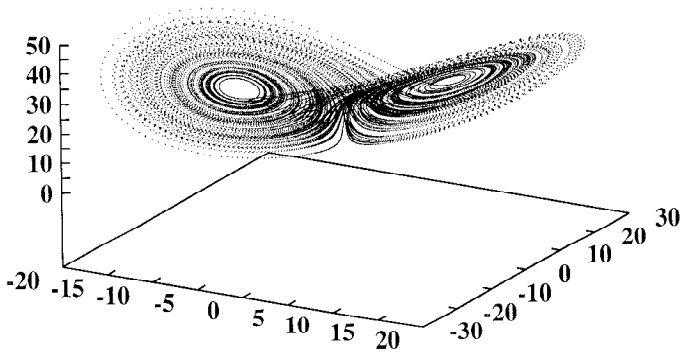

FIG. 3. Lorenz attractor is shown.

three-dimensional space through a set of differential equations. The equations actually arose from a simplification of the Navier-Strokes partial differential equations of fluid dynamics given certain limitations. Today, Lorenz's approach is currently seen as an unrealistic approximation of the phenomenon. However, his work did become a strong argument for the chaotic nature and unpredictability of atmospheric changes.

Figure 3 illustrates the Lorenz attractor. The trajectory spirals around a center and passes back and forth from one spiral to the other without intersecting itself. On the other side, the spiral orbit has some small thickness, inside of which there are an infinite number of closely spaced surfaces with the resultant being that trajectories moving on them will never coincide. Such a complexly structured surface characterizes strange attractors. Looking at two trajectories, starting at initial conditions that can be as arbitrarily close as desired, one can see that the trajectories separate from one another at an exponential rate. As time continues, this leads to totally different futures, previously described as the phenomenon of sensitive dependence on initial conditions. One consequence of this is that a long-term prediction is impossible despite the deterministic nature of the system. For instance, in meteorology, a limited knowledge of initial conditions makes it impossible to predict the weather on a long-term basis. It has even been suggested that such an insignificant event as a butterfly flapping its wings may destroy the predictive validity of such a weather system (referred to as the butterfly effect). Thus, in this model, the flutter of butterfly wings in New York today is seen to affect the weather in Berlin some time later. As Lorenz pointed out (161), two initially very similar conditions, differing by an imperceptible amount, will eventually evolve into two completely different states.

Another famous three-dimensional system of ordinary differential equations is the Rössler attractor. Invented for the purpose of studying complex dynamics, this system may be seen as modeling the flow around one of the loops of the Lorenz attractor. This system has the simplest topology that will still produce a strange attractor.

The three ordinary differential equations that generate this system are as follows

$$dx/dt = -y - z$$
$$dy/dt = x + ay$$
$$dz/dt = b + z(x - c)$$

with parameters set at $a = b = 0.2$.

This set of equations encompasses three system variables (x, y, z) and hence the dynamics can be embedded in a three-dimensional space. There is only one nonlinear term, zx. Varying the control parameter (c) gives rise to rich dynamic behavior. As with the quadratic equation, this system utilizes the period-doubling route to chaos (Fig. 4). The periods 1, 2, 4, . . . can be seen, for example, for c values 2.5, 3.5, and 4.0, . . . , respectively. As c is increased from 2.5 to 14.2, there is a sequence of period-doubling bifurcations from a simple period one oscillation. The onset of chaos takes place at the point of accumulation $c_\infty \sim 4.233$. As c is increased, the single closed line with a relative maxima of 2^n widens into a band of orbits with nonoverlapping trajectories (Fig. 4).

This motion occurs on what is essentially a band formed to a disk. This strange band demonstrates how a sensitive dependence on initial conditions emerges, i.e., how nearby orbits can diverge exponentially while still being confined to a limited region. The unstable steady-state point (0,0,0) serves as a "repeller" such that there is a tendency for an orbit to enhance its distance from (0,0,0) with each pseudo-cycle. This tendency explains the divergence of nearby orbits that are separated by small lateral displacements on the band. However, without a counteracting "force," the spiraling would grow to infinity. The solution comes from topological folding, which acts as a counterpart to the stretching process of the flow's bandwidth. In each pseudo-cycle, orbits from the outer part of the spiral band are folded back into the inner part of the spiral, continuously creating folds within folds ad infinitum. As a result of this, the almost two-dimensional band on which all motion takes place consists de facto of an infinite number of infinitesimally spaced sheets. With each pseudo-cycle the number of sheets grows as an exponent of two. Because the sheets are closely spaced, an experimentalist might conclude that the surface is two dimensional when in fact the actual dimension is greater. Given a compact object composed of an exponential divergence of nearby trajectories, a folding of sheets is the only solution. Otherwise, the repetitive foldings would produce an infinitely large surface of the plane. In this solution exponential divergence is not a global, but a local feature in that two orbits on an attractor cannot diverge exponentially forever. Although orbits diverge and follow increasingly different paths, they eventually must return to nearby regions on different sheets, during which time, even if brief, the distance between them would be insignificant (so-called Poincaré recurrence). In sum, in three and higher dimensions, it is possible to have flows which, in a compact region, continuously expand the volume of phase space in some direction or directions while contracting them in others.

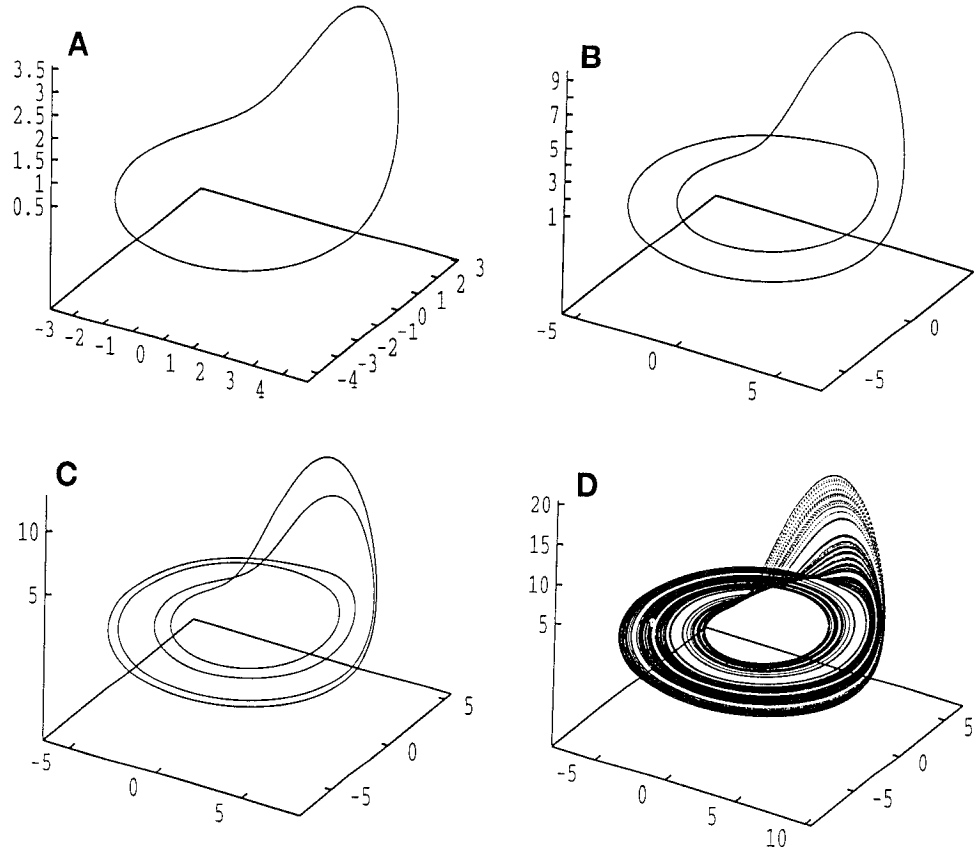

FIG. 4. Four phase portraits of Rössler attractor at different values of c illustrate period-doubling route to chaos. *A–D*: periods 1, 2, and 4, and an example of chaotic attractor are shown, respectively. Note that only *D* plot shows a nonclosed curve and therefore depends on length of trajectory. Motion on band is counterclockwise. Folding happens in area of positive y-values by ascending and afterward descending, both in positive z-direction, whereby trajectories on outer part of band were brought back in inner part of band, enabling further divergence.

C. Poincaré Section and Return Map: Linking Differential and Difference Equations

As mentioned in section II*B*, systems described by difference equations are better classified and easier to study. The question exists as to how we can reduce a system of differential equations to one of difference equations; that is, how can we force a continuous system into discrete states? We answer by describing a Poincaré section.

It was at the end of the last century when the French mathematician and physicist H. Poincaré (208) introduced a method of simplifying phase-space diagrams of complicated systems. He simply sliced the bundle of orbits perpendicular to the flow. Said in more technical terms, a cut is made in the flow of an attractor in the state space of dimension m in an appropriate region with a hyperplane of dimension $(m-1)$ perpendicular to the flow (Fig. 5). The crossing points of the orbit with this hyperplane comprise the Poincaré section (Fig. 5), and the series of these taken at regular intervals, the Poincaré map. The continuous motion of the trajectory in one (pseudo-) cycle is mapped to just one point on the section. It should be further noted that the time interval between two crossings typically will not be a constant, but will vary around an average.

Another way to consider Poincaré sections is to imagine that one is viewing the phase-space diagram utilizing a strobe (20). If the strobe frequency is exactly the same as the frequency of the processes under study, then a single point would result. This is similar to a pendulum or a ball on a string in perfect rotation perpendicular to a strobe of the same frequency. What would be observed would be a single point. If, however, the frequency of the strobe were slightly different from that of the ball, one would see the ball at a slightly different point on the circle at each flash of the strobe. Because in this situation the frequency of the ball and that of the strobe would be incommensurate, the ball would appear as a series of points (i.e., a circle) rather than a single point. If the rotation of the ball were dampened (e.g., the motor controlling the rotation turned off), the rotation would gradually become slower until the ball stopped. In such a system, we would see a movement toward an attractor in both the phase space and the points on the Poincaré section.

In a Poincaré section one dimension is "lost," and the flow discretized. This is because we record only the times the trajectory intersects with some subspace (e.g., a 2-dimensional plane in a 3-dimensional system). A multidimensional periodic attractor can be detected easily in this diagram as a fixed set of d points emerging repeatedly as illustrated by a Poincaré section of the multiperiodic Rössler attractor. With a quasiperiodic motion in which the periodicities are incommensurable, the section appears as an asymptotically infinite number of points which form a closed curve (a "limit cycle" formed by points hopping around). But what about other, more complicated sets of points? To explore this situation it is helpful to remember that the set of points on the surface of the section may be thought of as the graph of a system of $(m-1)$ difference equations. Be-

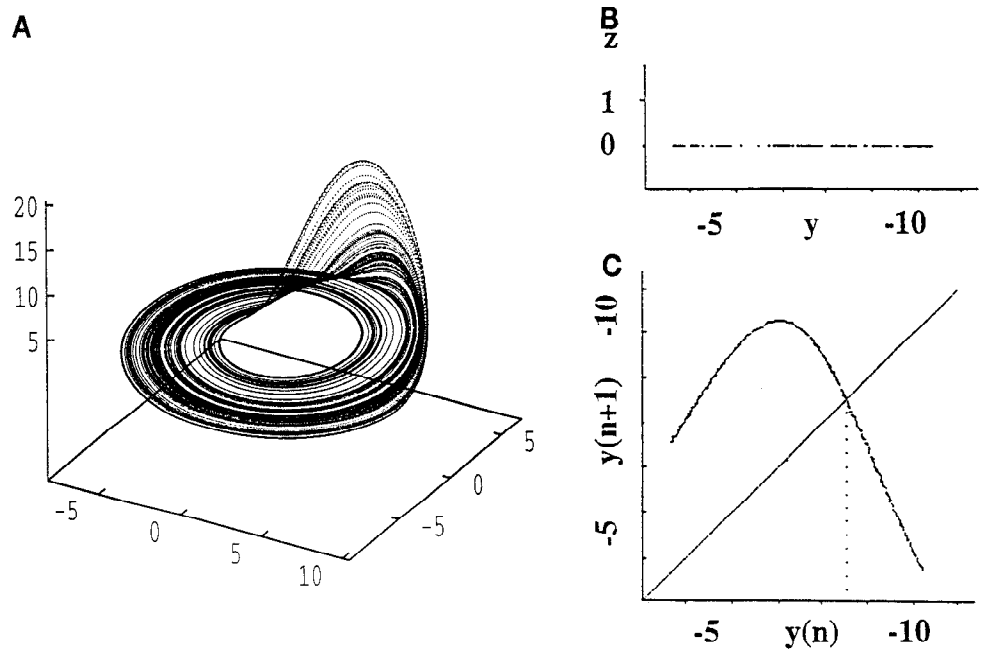

FIG. 5. Poincaré section and return map of Rössler strange attractor ($a = b = 0.2, c = 5.0$). *A*: slicing (transversely cut) of flow in front with a plane at $x = 0$ and $y < 0$. *B*: resulting Poincaré section indicating that all crossing points lie on a line; note that de facto points are not constrained to a simple line but form a package of sheets with some minimal height in z-direction, which only looks like a line under conditions of finite precision in calculation and limited graphical resolution. *C*: corresponding first return map with its striking resemblance to quadratic equation; Rössler described it as a "walking stick" (a smooth bell-shaped curve). Values of y which are lower than crossing point of graph with line $y(i) = y(i + 1)$, forming inner part of spiral in *A*, will be enlarged (exponential divergence of nearby orbits) by next pseudo-cycle but rest on their sheet (i.e., fixed z-value). They are only subjected to stretching process. Other part of y-values, forming outer part of spiral in *A*, in addition to stretching, is folded, resulting in a lowered value of y and in a different value of z; in other words, points return lying on a different (new) sheet. In the course of flow, combination of subsequent folding and stretching acts as a mixing procedure, in which nearby orbits diverge while orbits far away are brought close together.

cause the solution of the differential equations is unique, each crossing point P_i determines the next (P_{i+1}).

In some three or higher dimensional systems such as the Lorenz or the Rössler—strange attractors with their (locally) almost two-dimensional flow—it turns out that all the crossing points essentially lie on a simple line. Consequently, they can be characterized with the help of only one instead of two ($m-1$) variables (Fig. 5). This leads to the result that the system's dynamics can be approximated well by a one-dimensional map. Moving to the next step of analysis, we can plot a graph of the one-dimensional (first) return map (Poincaré map), P_{i+1} vs. P_i (Fig. 5), illustrating the dependence between successive intersection points. This graph allows us to predict the position of the next crossing point by knowing the previous crossing point.

Thus another method of reducing the complexity of the phase space is through the use of a return map. For example, a single variable x can be plotted at regular time intervals such that x is plotted against x_{n+1}. Compared with the often complex flow in phase space, a return map contains only a small portion of the original information; however, it is a highly valid instrument for studying the stable properties of the system because it encapsulates the essential dynamical properties of the flow from which it is extracted. As we pointed out earlier, theorems suggest that given an infinitely long time series of just one variable, a complete description of the total system can be derived.

Based on a theoretical understanding of difference equations, the map can be investigated for the occurrence of chaos. One criterion of chaotic motion is a nonlinear pattern, e.g., a unimodal graph with an absolute slope greater than -1 in almost all parts. In this case stretching and folding should be recognizable in the return map as illustrated by the Rössler attractor (Fig. 5) as well as by examining successive Poincaré sections of the flow. A further significant hint for chaos is the existence of period three in the return map, since it implies period n with $n = 1,2,\ldots$ (Li-Yorke theorem, Ref. 157). Once chaos is identified in the dynamics of the return map, this will also hold for the flow. A theorem of Oseledec (197) ensures that the dynamical properties of the map, e.g., the rate at which nearby orbits diverge, are independent of the choice of the slicing (hyper-) plane.

For the Rössler attractor, a return map is available by reducing the dimension of the system to be investigated to one. However, in many cases this does not hold, and the Poincaré section yields a set of points dispersed in the ($m-1$)-dimensional hyperplane, making the analysis much more difficult. This may also result with the points of the Poincaré section lying on a curve, thus the

return map may fail to show any discernible structure. In higher dimensional systems, such limitations are frequently encountered, causing the technique to be less helpful. Consequently, its major applications are restricted to three-dimensional continuous systems.

An historically popular example of a nonlinear system that may be described by differential equations is the "van der Pol oscillator." Based on work using an electrical feedback system to translate electrical current into tones, this system produces both regularity and chaos. This system has also been modeled such that the theoretical oscillator exhibits all types of nonlinear behavior previously discussed including period doubling routes to chaos, frequency locking, intermittencies, and quasiperiodicity (see, e.g., Ref. 150). The generalized system for such a nonlinear oscillator, together with phase portraits and return maps, is presented in Figure 6. Although there was little understanding of the chaotic nature of the system, this model was used by van der Pol and van de Mark (268) in the 1920s to model the heart as well as to envision explanations for a variety of phenomena including relationships between species, shivering from the cold, menstruation, as well as rhythms of the heart (see Ref. 276).

D. *Getting to the Measure: Fractal Dimension, Metric Entropy, and the Spectrum of Lyapunov Exponents Characterize Attractors*

To date, essentially three different types of measures have been employed to characterize attractors in physiological systems. First, measures of dimension focus on the system's geometric (static) structure. The second type, that of entropy and information, and the third type, the spectrum of Lyapunov exponents, capture the dynamical properties of the system orbiting within the attractor. Roughly speaking, the dimension of a system corresponds to the number of independent quantities needed to specify the state of the system at all given instants. It can also be said that the dimension corresponds to the number of independent quantities (modes or oscillators) inherent in a motion. As we note, it is important to distinguish between the dimension of the phase space (a property of the dynamical system) and the dimension of the attractor in the phase space. In the case of dissipative systems (e.g., those with friction), the first measure should be greater because of the typically wide range of possible initial conditions of the system, whereas the second measure describes any state of the system after it has settled on the subspace of the phase space that is the attractor. Take, for example, a fixed-point attractor, in this case there is no variation in the final phase space position. Its dimension is zero, no matter what the dimension of the phase space is. On the other hand, the dimension of the phase space may be any positive number. For other "simple" attractors, the dimension may be one (e.g., a limit cycle or multiperiodic attractor). A sine wave for example would have a dimension of one. In the case of quasiperiodic attractors with n incommensurable frequencies, the dimension may be any natural number n.

1. *Measuring geometric structure*

Consider a line with a dimension of one. If we were to allow that line to fold back on itself a number of times as one might see with a coastline or what is called a Peano curve in mathematics, the line could begin to fill a plane such that it would appear to be two dimensional. Of course there are a number of figures (e.g., snowflakes) that seem to lie in this area between the one-dimensional line and the two-dimensional plane. To describe these, Mandelbrot (168) introduced the term "fractal," which comes from the Latin fractus and means irregular or fragmented. By definition, a "fractal dimension" is a dimension with noninteger values. In the same way, a point in a phase space folds and refolds with great complexity until a strange attractor is created. How might we describe the dimension of strange attractors with their complicated structure of closely packed sheets, producing a thickened surface as seen with the Lorenz attractor (Fig. 3) for example? We now examine some of the strategies proposed to quantify a strange attractors in terms of dimension or dimensionality (47, 63). Well-known approaches include capacity, Hausdorff-Besicovitch dimension, information dimension, as well as the correlation dimension and its variations.

I) CAPACITY DIMENSION. The simplest of these definitions is that of capacity dimension (63, 146). This same measure is also referred to as Kolmogorow entropy, entropy dimension, metric dimension, logarithmic density, or simply box-counting dimension. To calculate this measure the attractor (constituted by a set of n points) in the phase space of dimension D (the number of equations of the system) is covered by a regular grid of D-dimensional boxes of edge length ϵ (called a coarse-grained partition). The (minimal) number $N(\epsilon)$ of nonempty boxes needed to cover the set is counted. If we have a straight line of length L and $N(\epsilon)$ boxes are required, then $N(\epsilon) = L(1/\epsilon)$. For example, to cover a 10-in. line would require five boxes of 2 in. on a side. For a two-dimensional square, the formula would be $N(\epsilon) = L^2(1/\epsilon)^2$, and for a D-dimensional figure, the formula would be $N(\epsilon) = L^D(1/\epsilon)^D$. Taking the logarithms, we find that D is equal to the log of $N(\epsilon)$ divided by the log of L plus the log of $(1/\epsilon)$. Because L becomes negligible in the limit of small ϵ, the formula is usually written as follows with D replaced by a C

$$C = \lim_{\epsilon \to 0} \left[\frac{\ln N(\epsilon)}{\ln (1/\epsilon)} \right] \tag{2}$$

For practical applications, if ϵ is small enough, the slope of a plot $\ln N(\epsilon)$ against $\ln 1/\epsilon$ will yield the capacity.

For a strange attractor, the capacity dimension will have, in general, a noninteger value reflecting how

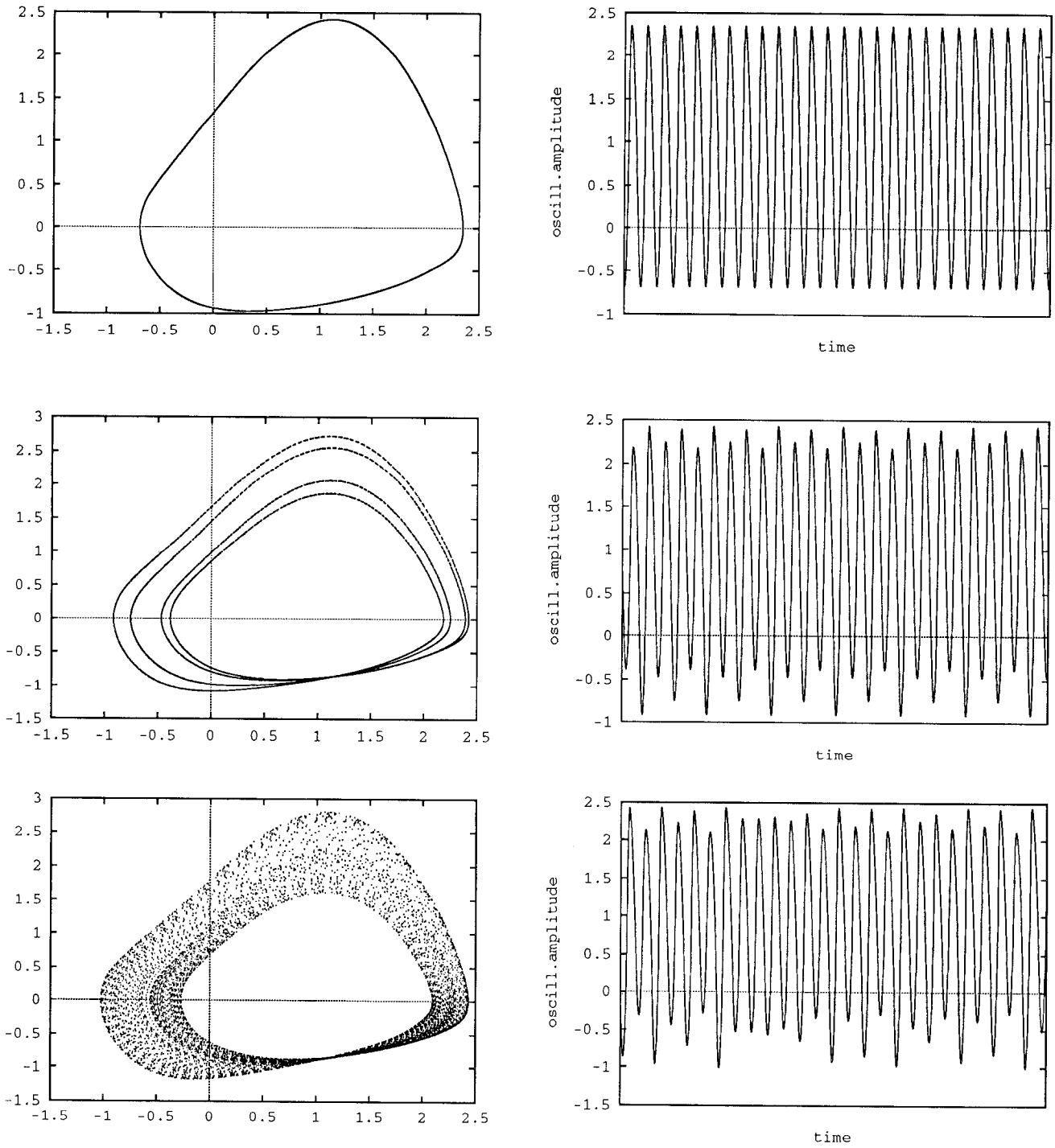

FIG. 6. Route to chaos for a van der Pol-like system according to Kowalik et al. (150). System is described by $\ddot{x} + \dot{x}[c/a + a(1 - \lambda \cos x)] + x + c(x - \lambda \sin x) = -c(A \sin 2\pi ft + B)$, where right side of formula denotes external driving force. One can see that for $c \rightarrow 0$ and $\lambda \rightarrow 2$, above equation in first approximation is just well-known van der Pol equation $\ddot{x} = a\dot{x}(1 - x \times x) - x +$ excitation term. For present estimation (fourth-order Runge-Kutta), parameters were set at $a = 0.8$, $c = 0.25$, $B = 3.1$, and $\lambda = 2.65$. Rows correspond to different choices in frequency parameter (f): *top*, $f = 0.2615$; *middle*, $f = 0.2640$; *bottom*, $f = 0.2650$. *Right column*: waveforms. *Left column*: phase portraits ($\dot{x}$ vs. x).

closely packed the sheets of the attractor are. For example, the Lorenz attractor has a capacity of ~2.08 (99). Loosely speaking, to achieve a result in a whole dimension, points must be infinitely densely packed in that direction. As we require regions of more and more dense packages, the packages of sheets become smaller and smaller. When approaching infinitely dense packed points, the thickness of the respective region approaches zero.

II) HAUSDORFF-BESICOVITCH DIMENSION. The Haus-

dorff-Besicovitch dimension, also called the fractal dimension or simply Hausdorff dimension (112), dates back to the second decade of the 1900s. This measure can be viewed as a generalization of capacity with variable edge sizes instead of fixed ones and a millennium of all possible partitions. In the case of dynamical systems, both will give the same value (63). Again, the practical calculation of capacity is made by a box-counting algorithm based on the definition (236). It becomes increasingly difficult (e.g., prohibitive storage requirements) as the dimension of the phase space increases (>3) (104, but see also Ref. 159).

In "metric" concepts of dimension, only a concept of distance is required (63). A serious problem of these metric concepts of dimension results from the fact that all nonempty boxes are equally important in the formula. Thus, because strange attractors are spatially nonuniform, i.e., certain regions of the attractor are visited more than others, the knowledge of a very long trajectory is needed to ensure that even very improbable boxes are visited. To achieve better convergent behavior for finite trajectories (point sets), definitions of dimension are required that take the different densities on the attractor into account. Therefore, each nonempty box has to be weighted by the relative frequency by which it is visited by a typical trajectory. Farmer et al. (63) called these "probabilistic dimensions." They require both a metric and a probability or "natural" measure (47, 63).

III) INFORMATION DIMENSION. The information dimension δ, originally introduced by Balatoni and Rényi (21), can be understood as a generalization of the capacity by weighing each nonempty cube i with its "mass" (probability) (p_i)

$$\delta = \lim_{\epsilon \to 0} \left[\frac{\sum_{i=1}^{N(\epsilon)} p_i \ln (1/p_i)}{\ln (1/\epsilon)} \right] = \lim_{\epsilon \to 0} \left[\frac{\sum_{i=1}^{N(\epsilon)} p_i \ln p_i}{\ln \epsilon} \right] \quad (3)$$

Theiler (265) suggests that this measure of dimension can also be thought of as how many real numbers or bits of information are needed to specify a point to a certain degree of accuracy. For example, a point on a line can be specified by a single number, whereas a position on a Cartesian plane requires two points. Likewise, a location in a three-dimensional space requires three real numbers. We can further realize that how accurate we locate a point is related to the size of the grid or coordinate system. The more accuracy required (i.e., the finer the grid), the more bits of information needed to specify the position. The numerator of *Equation 3* can also be understood as the number of bits of information required to specify a state of the system within a certain accuracy ϵ. This measure is, in the case of uniform point sets (i.e., each nonempty cube has the same probability p), equal to $\ln N(\epsilon)$ in *Equation 2*. If the points on an attractor are uniformly distributed, then $\delta = C$, and if they are not, then $\delta < C$.

IV) CORRELATION DIMENSION. The most popular attempts to characterize attractors have been based on the correlation dimension ν as proposed by Grassberger and Procaccia (97, 99). It should be noted that the term "correlation" as used in this context can be confusing. However, one way to view this term is to consider a linear system such as represented by a sine wave, which would result in a circular or elipical limit attractor with a dimension of one. Pairs of points chosen along the attractor in the phase space would show a strong correlation. On the other hand, if the attractor is chaotic, then by definition the trajectories would expand exponentially, and pairs of points would not be dynamically correlated.

In determining this measure, pairwise distances are calculated. Unlike methods that partition the phase space with a regular grid of boxes, this method selects spheres centered at randomly chosen reference points on the attractor (Theorem of Young, Ref. 280). The numbers of neighbors falling within a sphere of radius ϵ are counted for successive higher values of ϵ. Experimentally, the slope of a plot of the number of points inside a sphere of radius ϵ, i.e., $C(\epsilon)$ plotted against the radius ϵ (both in logarithmic scales) yields the correlation dimension ν, which is a lower bounds to the fractal dimension such that correlation dimension less than or equal to information dimension less than or equal to fractal dimension. Although there is no standard notation in this field, $C(\epsilon)$ is often written as $C(r)$. The correlation dimension ν is defined as follows

$$\nu = \lim_{\epsilon \to 0} \left[\frac{\ln C(\epsilon)}{\ln \epsilon} \right] \quad (4)$$

The correlation integral $C(\nu)$ defined as

$$C(\epsilon) = \lim_{N \to \infty} \left[\frac{1}{n^2} \times \sum_{i,j=1, i \neq j}^{n} \theta(\epsilon - |\mathbf{x}_i - \mathbf{x}_j|) \right] \quad (5)$$

with the $\theta(x)$ being the Heaviside function (=1 if $x \geq 0$, otherwise = 0), a standard "counting" function. Apart from " . . . ", which is the Euclidean distance (norm) between the vectors $\mathbf{x}_i$ and $\mathbf{x}_j$ (97), the maximum norm (given by the largest difference in any coordinate; Ref. 263) can also be used. Said in simple terms, $C(\epsilon)$ can be viewed as the number of distances less than a given distance ϵ divided by the total number of distances altogether. From this it can be seen that $C(\epsilon)$ can range from zero, in which no points are within ϵ distance of each other, to one, in which all points are within ϵ distance of each other. Thus one way of describing the correlation integral is to see it as the average number of points on the attractor within distance ϵ of each other. If the attractor is fractal, then the log of the correlation integral for a certain range of ϵ will have a linear relationship with the log of ϵ. A physiological example illustrating the steps involved in determing the correlation dimension is illustrated in Figure 7.

V) POINTWISE DIMENSION. With the use of *Equations 4* and *5*, the pointwise dimension D_{2i} (63, 280) will

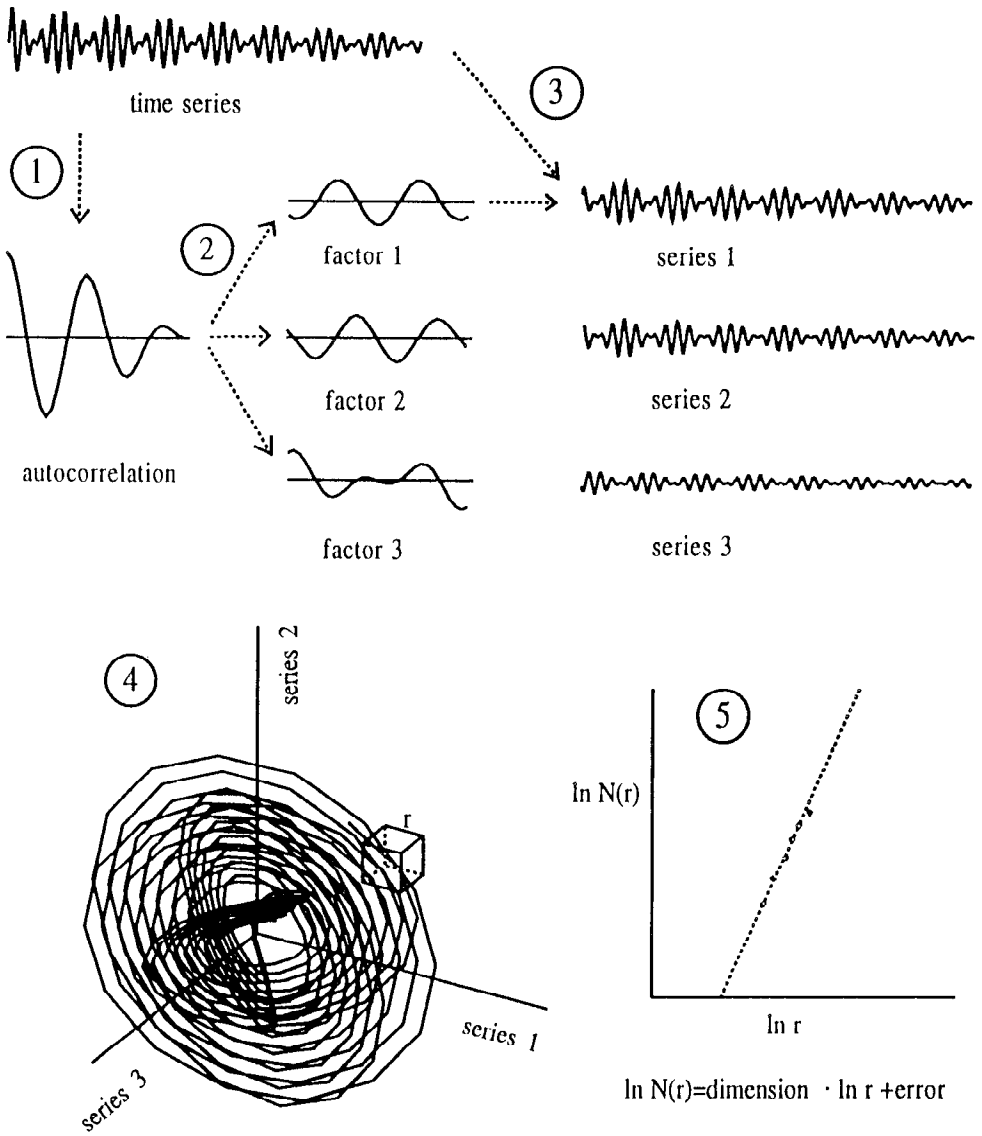

FIG. 7. Schematic description of procedure to estimate dimensional complexity. Autocorrelation function is computed from time series (*1*) then decomposed into its principal components (*2*). For each point a linear sum of these factors is fitted to time series (least square) (*3*). Corresponding weights determine a point in state space (*4*). Moving along time series, a trajectory is created. Dimension of this assembly of trajectories is estimated as dimensional complexity (also called fractal dimension), by the following procedure. Starting with a distinct reference point of electroencephalogram (EEG) time series, number of points $N(r)$, which lie in a hypercube with sides of length r around this chosen point, is counted. This counting is performed for subsequently larger radii until ultimately all points of time series lie within this hypercube. For a single point attractor, number of data points around reference point (hypercube with radius r) will be 0. If attractor is a 1-dimensional line, number of points will increase with r^1; for a 2-dimensional attraction, a plane, number will increase with r^2, and so forth. Generally, number of counted points will increase with r^d, with d denoting fractal dimension of attractor or fractal complexity of EEG. It is estimated as linear slope in (log r/log N) plot (*5*). A detailed description of procedures is provided in text. [Adapted from Elbert et al. (53).]

result simply by taking just one reference point instead of the sum over all the reference points $i = 1, \ldots, n$. This measures how fast the number of neighbor points around the reference point increases as the distance ϵ is increased. For uniform point sets, where the pointwise dimension is independent of the chosen reference point i, ν and D_2 both equal D_{2i} and will yield the same value. This point is supported by a computational argument by Mitra and Skinner (183), who showed that if the sample epoch is adequate (e.g., around 8,000 points for the Lorenz time series, when $\tau = 0.001$), then the pointwise scaling dimension D_{2i} smoothly converges to the correlation dimension D_2. Convergence occurs as the set of vector-difference lengths used to make the log $C(n,\epsilon)$ versus log ϵ plots contains larger and larger numbers from the separate D_{2i} contributions. Intuitively, this makes sense, since given an adequate data string describing a strange attractor, or any other attractor, the estimated dimension based on several orbits around the attractor (i.e., D_{2i}) should give the same approximate estimate as that based on data containing many more orbits (i.e., D_2 at the limit).

VI) POINT D2 CORRELATION DIMENSION. A variation of the pointwise dimension, the "point D2" (PD2) estimate of the correlation dimension has been developed by Skinner and associates (251, 252, 254, 256) The PD2 does not use all possible vector-difference lengths, like the D_2 algorithm of Grassberger and Procaccia (99), nor all vector-difference lengths with respect to a fixed reference vector, like the Farmer et al. algorithm (63). Rather, it seeks stationary subepochs of the same type as the one in which the reference vector is located, then tests and rejects those vectors for which linear scaling and convergence cannot be found (191, 239, 273, 310, 325, 326). This is seen as an advantage over accepting every reference vector as valid, which means erroneously including some vector-difference lengths for which the fundamental scaling relationship that defines dimension does not hold (198, 262).

VII) RELATIONSHIP OF DIMENSIONAL MEASURES.

Confronted with the variety of measures for determining dimensions, two questions arise. First, is it possible to integrate them in a "super" concept of dimension? Second, what about nonuniform point sets (e.g., strange attractors) yielding different pointwise dimensions for different reference points. How is it possible to supersede the local description by a global one?

In 1983, Hentschel and Procaccia (122) and Grassberger (95) introduced the spectrum of Rényi dimensions d_q (originally defined by Rényi; Ref. 225), as an information theoretic concept, in the context of dynamical systems theory. Based on the order q Rényi information

$$I_q = \frac{1}{1-q} \ln \sum_{i=1}^{n(\epsilon)} p_i^q$$

(APPENDIX in Ref. 225), certain scaling exponents d_q ["generalized (Rényi) dimensions of order q"] which depend on a continuous parameter q can be defined

$$d_q = \lim_{\epsilon \to 0} \left(-\frac{I_q}{\ln \epsilon} \right) = \frac{1}{q-1} \times \lim_{\epsilon \to 0} \left[\frac{\ln \sum_{i=1}^{N(\epsilon)} p_i^q}{\ln \epsilon} \right] (q \neq 1) \quad (6)$$

$$\text{For } q \to 1 \; d_1 = \lim_{\epsilon \to 0} \left[\frac{\ln \sum_{i=1}^{N(\epsilon)} p_i}{\ln \epsilon} \right]$$

coincides with *Equation 3*, the information dimension.

For nonuniform point sets ("multifractals"), the d_q values are unequal for different values of q, yielding instead of only one, an infinite number of dimension values. With the aid of this formula, three of the dimension concepts described previously can be placed into a continuum of correlation exponents based on qth moments of the probability distribution of boxes: $d_0 = C$ (or Hausdorff dimension), $d_1 = \sigma$, $d_2 = \nu$ [the sum $\sum_{i=1}^{N(\epsilon)} p_i^q$ characterizes the chance that two arbitrary points on the attractor will have a distance $\leq \epsilon$]. Their order is determined by the fact that, generally, $d_q > d'_q$ for any $q < q'$ (a monotonically decreasing function). For uniform point sets ("single fractals") $d_q = d'_q$. When q is an integer, d_q has a physical meaning.

Interpreting *Equation 6* as a suitable average over the pointwise dimensions, the second question, that concerning nonuniform point sets yielding different pointwise dimensions for different reference points, can also be answered. As q is varied, different subsets, which are associated with different scaling indexes (i.e., pointwise dimensions), become dominant. Large positive values of q emphasize the most concentrated regions of the phase space (small pointwise dimensions), whereas large negative values emphasize the most rarely visited regions (large pointwise dimensions). So the d_q values are able to reflect that an attractor may have regions of different densities and therefore can be viewed as a characterization of the nonuniformity of the point set. The larger the range of d_q values, the more "nonuniform" the point set.

2. Describing the evolution of a system

In describing how often various areas of the phase space are visited (i.e., the density of a region), measures of dimension emphasize the static qualities of the attractor without regard to time. To study the dynamical characteristics, i.e., the evolution of a system, we can utilize measures of entropy and the spectrum of Lyapunov exponents, which help us to understand the manner in which trajectories develop over time. It should be noted that these measures are specific to dynamical systems, whereas the measure of dimension can be defined for any fractal measure (point set).

I) CONCEPT OF ENTROPY. To introduce the concept of entropy, it is useful to recall the information dimension described above. Entropy estimates the (average) information gained by observing a state of the system with precision ϵ. One view of information is to consider the dynamical process as a machine that takes the initial input and generates a string of numbers (245). In the case of a fixed point or periodic orbit (e.g., as generated by a sine wave), each orbit is the same and thus after a time no new information is gained by considering additional orbits. Said in other words, there is no uncertainty in such a system. Thus it is easy to predict the outcome before an observation is made of the next orbit. However, in a chaotic system, each orbit is new to the observer, and thus new information is gained. With new information, prediction before an observation of the next orbit would become more difficult. Such a system can be seen as creating information. The question now becomes how can we measure the amount of information created.

The "dynamical" question, how much information, on average, is gained (or lost) by observing a portion of the system's evolution (i.e., a subset of the full trajectory) can be answered by the metric of Kolmogorov-Sinai (K-S) entropy (146). It measures the degree of "chaoticness" of the system, or the long-time average rate at which information is generated by the system, or equivalently, the rate at which current information about the system is lost. K-S entropy is inversely proportional to the time interval over which the state of the system can be predicted, given that one knows an initial state with precision ϵ as well as the evolution equations of the system.

We know that the trajectories of chaotic systems emerging from nearby (but indistinguishable within a certain limit) initial conditions diverge exponentially and evolve into distinguishable states after a time. Because of this sensitivity to initial conditions, chaotic systems continually generate new information, thus making any long-term prediction impossible. In a chaotic system, if we begin with a certain precision of mea-

surement ϵ, such that two initial conditions appear insignificantly different (i.e., starting in the same box and less than ϵ distance apart), we will discover that these two conditions will become significantly different (i.e., visit 2 different series of box sequences) as the system evolves in time. To be more precise, if we partition the attractor into $N(\epsilon)$ boxes $s_1, \ldots s_N$ with box size ϵ, then m successive measurements, taken at regular time intervals τ, will yield a sequence of boxes $(s_1, \ldots s_N)$ visited by the observed trajectory. Now, let $P(s_1, \ldots s_N)$ be the joint probability of finding the trajectory at time τ in box s_1, at time 2τ in box $s_2, \ldots$, and at time $m\tau$ in box s_m.

The K-S entropy (K) is then defined as (62, 98)

$$K = -\lim_{\tau \to 0} \lim_{\epsilon \to 0} \lim_{m \to \infty} \times \left[\frac{1}{m\tau} \sum_{s_1 \ldots s_m} P(s_1 \ldots s_m) \times \ln P(s_1 \ldots s_m) \right] \quad (7)$$

The time for which the behavior of the system can be predicted is proportional to $1/K$. Thus, if K approaches 0, i.e., no change in information, then the system becomes fully predictable and new measurements provide no additional information. In contrast, in the case in which K approaches infinity, the system becomes a stochastic process. For a chaotic system, however, the metric entropy will have a positive finite value. The greater this value is, the more chaotic the system. For applications with cardiovascular data, Pincus (204) has modified the K-S entropy measure to require less computational resources. The resultant measure, not actually an estimate of K-S entropy, is referred to as approximate entropy. It has been used to measure the amount of regularity in a series of heart beats and other physiological signals.

As in the case of dimensions, entropy can be generalized to a set of order q Rényi entropies (98), the dynamical counterparts of the Rényi dimensions

$$K = -\lim_{\tau \to 0} \lim_{\epsilon \to 0} \lim_{m \to \infty} \times \left[\frac{1}{m\tau} \frac{1}{1-q} \ln \sum_{s_1 \ldots s_m} p^q(s_1 \ldots s_m) \right] \quad (8)$$

and, analogously, K_2 (as for $d_2 = \nu$) is of all K_q the easiest to calculate. K_0 corresponds to the topological entropy, which is the dynamical analog of the Hausdorff-Besicovitch dimension, and K_1 is the K-S entropy K.

An example of estimating the K_2 entropy of spontaneous MEG activity is presented in Figure 8. As can be seen, in the middle of the record the entropy rapidly jumps to a different level, indicating a phase transition in the regulation of neural mass activity.

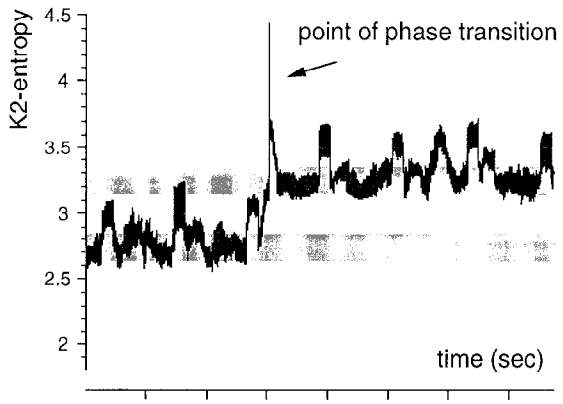

FIG. 8. Example for evolution of K_2 entropy (following *Eq. 8*) for a 15-s magnetoencephalogram (MEG) segment from 1 subject. A 7.5-s time window was chosen for present estimation and scanned across whole interval. MEG was recorded over left temporal region during relaxed waking state with eyes open.

II) LYAPUNOV EXPONENTS. Another very important fundamental measure of a system's dynamic is the spectrum of characteristic Lyapunov exponents (165, 242), which completely describes the characteristics of the trajectories in phase space. In comparison to K-S entropy, which is seen as a measure of the rate of information flow, Lyapunov exponents can be viewed as measuring the rate of exponential divergence of nearby trajectories. As a digression, it should be noted that, whereas trajectories in chaotic systems are sensitive to initial conditions, the overall structure of the attractor tends not to be. In practice, one takes a number of initial conditions spread over the trajectory to calculate the average Lyapunov exponent. The Lyapunov exponent is written as λ and may be negative, zero, or positive. If the exponent λ is negative, the trajectories converge over time, and the system is not chaotic. This represents the condition in which insignificant differences in the initial conditions (e.g., x and $x + \epsilon$) become even less so as the system evolves. If the exponent is positive, then the trajectories diverge; that is, insignificant differences in the initial conditions become significant over time. In this situation, the evolution of the trajectory is sensitive to initial conditions and by definition chaotic. Thus the presence of a positive Lyapunov exponent signifies a chaotic system. For n-dimensional systems there are n Lyapunov exponents such that the spectrum consists of as many exponents as there are dimensions in the phase space (not the attractor). Each exponent measures an average rate of exponential divergence (>0) or convergence (<0) of infinitesimally close trajectories on one specific axis. These orthogonal axes are chosen such that they have a fixed relation to the trajectory, and hence rotate within the phase space, as the system evolves.

Consider, for instance, a continuous dissipative system in a phase space with dimension $D > 2$. According to the definition of an attractor as a bounded subset in the phase space surrounded by a basin of attraction, at least one negative exponent must exist. This reflects the fact that nearby trajectories starting in the basin of an attractor converge on it as time progresses (during which time on the average, their initial distance with regard to at least one direction decreases exponentially). If the attractor is a fixed point, all the exponents would be

TABLE 1. *Spectrum of Lyapunov exponents provides a useful classification of attractors*

Dimension of Phase Space	Spectrum of Lyapunov Exponents	Type of Attractor
1	−	Fixed point
2	−, −	Fixed point
	0, −	Limit cycle (1 torus) or periodic attractor
3	−, −, −	Fixed point
	0, −, −	Limit cycle (1 torus) or periodic attractor
	0, 0, −	Two-torus or quasiperiodic attractor
	+, 0, −	Strange attractor (chaos)

+, Positive exponent; −, negative exponent.

negative. If the attractor is not a fixed point, at least one exponent will be zero, indicating that, in at least one direction of the flow, the distance will not vary exponentially with time for two nearby trajectories. As repeated throughout, a hallmark for a strange attractor is the exponential divergence of nearby trajectories. This phenomenon will result in a positive Lyapunov exponent for the corresponding direction in space, which is the direction transverse to the flow on the attractor. Moreover, the magnitudes of an attractor's positive exponents are measures of the chaoticness of the attractor such that the more positive the exponent(s), the more vigorous is the stretching effect in that particular direction (the folding is not measured by the Lyapunov exponents), and the smaller is the predictability for the evolution of such a system. The spectrum of Lyapunov exponents not only quantifies the behavior of orbits on the attractor, which is described by the nonnegative exponents, but also encompasses the behavior of transient trajectories that approach the attractor through the negative exponents. By the latter, one can think of transients or of perturbations of the system's state. Because of the dissipative nature of the system, the sum of all Lyapunov exponents must be smaller than zero.

As seen in Table 1, the spectrum of Lyapunov exponents can provide a useful classification of attractors. The Lyapunov exponents in the spectrum are presented in decreasing order. It should also be noted that in 4-dimensional space (not shown in Table 1), a new type of behavior, hyperchaos (235), can emerge and is characterized by two positive Lyapunov exponents. It is possible only with at least four dimensions that two positive Lyapunov exponents become possible.

To give a technical mathematical definition of the Lyapunov spectrum, consider a set of initial conditions, starting in an infinitesimally small D-dimensional sphere $B_r(x)$ of radius r around a point x. After a time $t \to 0$, the sphere will be transformed under the action of the nonuniform flow into an ellipsoidal set, the length of which ith semi-axis on the average is approximately $re^{(t\lambda_i)}$ for almost all x in the basin of the attractor. The semi-axes λ_i with $i = 1 \ldots D$, which defines the axes of a local coordinate system, are nothing more than the Lyapunov exponents. They are given by

$$\lambda_i = \lim_{\Delta t \to \infty} \lim_{r \to 0} \left[\frac{1}{t} \ln \frac{r_i(t)}{r} \right] \tag{9}$$

where $r_i(t)$ is the length of the semi-axis i after the time t. If the number two is chosen for the basis of the logarithm, the unit of the exponents will be bits per second, or for a discrete set of points, bits per iteration. The limit $r \to 0$ prevents, in the course of the folding process, the ellipsoid from becoming distorted and maintains orthogonality of its semi-axes. (For a more rigorous definition in terms of the Jacobian matrix, see Refs. 47, 197.) For dissipative systems, the sum over all D exponents is negative, indicating that an initial volume contracts exponentially fast on the average. In contrast, for conservative systems (without friction) the sum becomes zero.

For an analytical system, the whole spectrum can be calculated using the Jacobian matrix of partial derivatives at point x (23, 246). For empirical investigations, it is necessary to reconstruct the attractor from a scalar time series, which is generally noisy and of finite length. Before the 1980s, it was not generally possible to estimate Lyapunov exponents of an experimental system. Only systems that produced a one-dimensional Poincaré (return) map could be analyzed. By 1985, a method to estimate all nonnegative exponents as well as some negative ones was introduced by Eckmann, Ruelle, and coworkers (46, 47; see also Ref. 241). In the same year, Wolf et al. (277) proposed an algorithm to estimate the largest exponent and, in principle, the second exponent as well. As the latter approach proved its superiority over the former (270), it has become widely used. However, Eckman et al. (46) were able to show that the major drawback of the Eckmann-Ruelle algorithm (its dependence on the embedding dimension) suggested in previous work does not exist, at least for an improved procedure. It has also been suggested (39) that, in the original comparison (270) of the two methods, the implementation of the algorithm of Eckmann-Ruelle was flawed. Thus the Eckmann-Ruelle procedure may be of interest, since it provides estimates for a larger part of the spectrum.

In the Wolf et al. (277) procedure, an arbitrarily chosen trajectory, which they refer to as the "fiducial trajectory," is followed in its evolution through an attractor, reconstructed through temporal and/or spatial embedding to the end of the data set. In this procedure, one continuously looks for points in its locally nearest neighborhood and measures the separation of the pairs over time. To avoid folding processes (the spurious element problem, see, e.g., Ref. 261) that would cause an artificial decrease in the distance, a new neighboring point has to be substituted whenever the evolved distance exceeds some specified value. The constraint is that the new point shows approximately the same orientation to the fiducial point as the old one, which avoids contributions from other Lyapunov exponents. For simplicity in actual practice, instead of using a variable time step between two substitutions, one can simply

take a fixed time step. The average divergence rate is then finally computed as follows

$$\lambda_i = \frac{1}{t_m - t_0} \sum_{k=1}^{m} \log \frac{r(t_k)}{r(t_{k-1})} \quad (10)$$

where $r(t_k)$ is the separation that evolved from the initial distance $r(t_{k-1})$ and m indicates the number of replacements made in the time $t_m - t_0$.

The data requirements for low-dimensional systems (dimension <3-5) are between some thousands and ten thousands of points (46, 65, 270, 277). However, for higher dimensional systems, the calculations quickly become unfeasible because the amount of data required grows exponentially with the dimension d of the attractor (i.e., $\sim 10^d$). In a physical system (e.g., Rayleigh-Bénard convection), two positive exponents were obtained applying the Eckmann-Ruelle method with 40,000 points (600 periods of the main oscillation) (46). The Wolf et al. (277) algorithm was able to estimate both positive exponents of Rössler's hyperchaos (dimension 3.005) using ~32,000 points. However, it should be noted that it is not only the number of points but also the total recording time that should be considered (46). Both preceding algorithms are fairly insensitive to variations in the fitting parameters (e.g., time steps τ, critical distance r, and embedding dimension D) (270).

A good survey on the methods described previously is available (39). New algorithms and improvements of the described algorithms are also available (103, 242, 244, 259; together with Ref. 260, where an alternative to Lyapunov exponents is described). Analogous to the scaling function $f(\alpha)$ in the theory of dimension (111), generalized Lyapunov exponents (100) can be defined, and a scaling function for the first (effective) Lyapunov exponent can be derived (18, 96, 240). Experimental examples exist for a laser system (259). The spatial distribution of the local largest Lyapunov exponent of brain activity is presented in section IV (Fig. 15).

There exist relations between Lyapunov exponents and dimensional estimates. Kaplan and Yorke (141) conjectured a relationship between the information dimension σ and the positive exponents

$$\sigma \leq d_{KY} = j + \frac{\sum_{i=1}^{j} \lambda_i}{-\lambda_{j+1}} \quad (11)$$

where we assume the Lyapunov exponents to be ordered, $\lambda_1 > \lambda_2 > \lambda > \lambda_N$ and where j is the largest integer so that $\lambda_1 > \lambda_2 > \lambda > \lambda_j > 0$. The term d_{KY} is sometimes referred to as the Lyapunov dimension. A full discussion is available (61, 63, 97, 99, 149, 156, 187, 236, 263). For analytically defined models, d_{KY} may represent the easiest way for computing the dimension. However, some authors use the Lyapunov dimension as means of determining the upper bounds of the information dimension.

In terms of metric entropy, Pesin's theorem (202) states that under certain preconditions, the sum of the positive exponents is equal to the metric entropy K_1. Thus, for a strange attractor with its spectrum (+, 0, −), the largest exponent coincides with the metric entropy.

E. Comparative Overview of Methods for Calculating the Correlation Dimension

Because a variety of studies, which we discuss in sections II*E3* and II*E4*, emphasize measures of dimensionality, we now present a more procedural understanding of three of these dimensionality measures as applied to physiological signals. These are the correlation dimension (D_2), the pointwise dimension D_{2i} (also called the pointwise scaling dimension (PWSD), and the point-D2 (PD2). In section II*D*, we discussed these measures mathematically. Comparison among the three methods of measuring dimensionality using sine waves, the Lorenz attractor, and the Hénon attractor are shown in Figure 9. Figure 10 graphically illustrates the steps required to move from a physiological signal to the dimensional estimate.

1. Grassberger-Procaccia correlation dimension

The correlation dimension (D_2) of a time series is defined as $C(n,r) \sim r^{D_2}$, where $C(n,r)$ is the cumulative number of all rank-ordered vector-difference lengths within a range (r) and n is the number of vector-difference lengths (the $\sim$ sign means, "scales as") (99, 198, 262). Vector differences (as described in Fig. 10) are made as follows: *1*) a reference vector is constructed that begins at a specific point in the data (the **i** vector, Fig. 10*C*) and takes a specified number (m) of sequential time steps in the data stream that are of a fixed length t (Fig. 10, *B* and *C*); each data value encountered by the time steps is used as one coordinate of the m-dimensional vector (Fig. 10, *C* and *D*); *2*) a different vector (**j** vector, Fig. 10*C*) is then made by beginning at a different starting point, but using the same number of time steps; and *3*) the difference vector is made by subtracting the **i** vector and **j** vector from one another (Fig. 10*D*, *far right*).

Normally the reference **i** vector is kept at a fixed place, while the **j** vectors are made, one for each point throughout the data, except the one where the **i** vector is. The **i** vector is then changed, and the **j** vectors are again constructed by running through the entire data series. The unique feature of the D_2 algorithm is that all possible vector differences (i.e., at a given embedding dimension m) are made. Then the vector-difference lengths (their absolute values) are rank ordered, creating the D_2 set for that embedding dimension ($m = 3$ for the example in Fig. 10*C*, *bottom*).

The next step in the algorithm is to make a log $C(n,r)$ vs. log r plot of this rank-ordered histogram of vector-difference lengths (Fig. 10*E*, *left*); a range value (r) (i.e., bin width) that initially includes only the small-

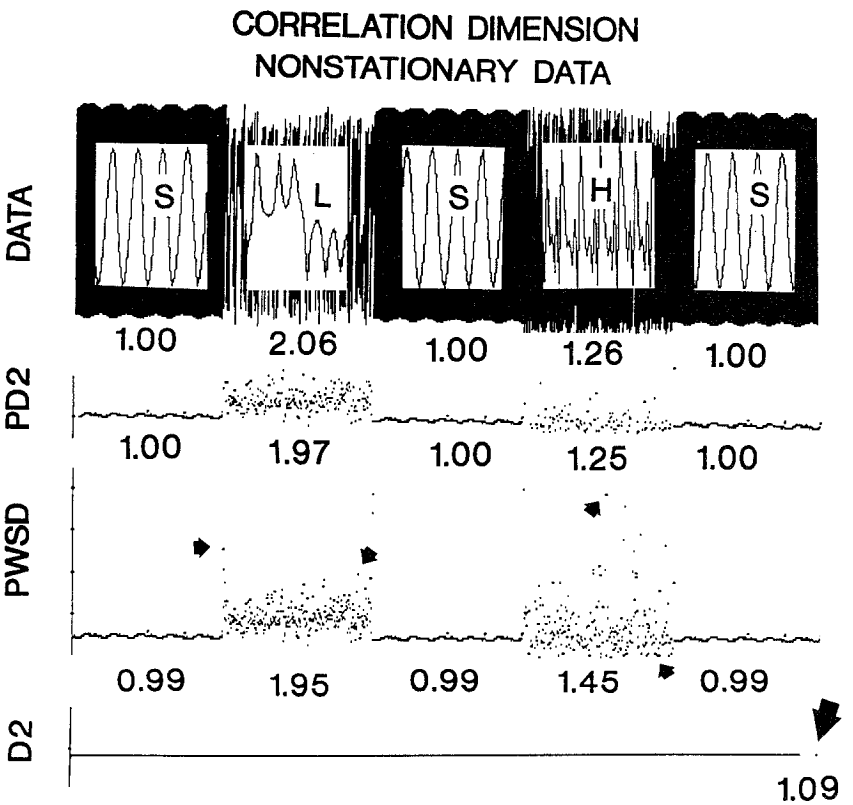

FIG. 9. Comparison of relative accuracies of 3 algorithms [sine (S), Lorenz (L), and Henon (H)] for estimating correlation dimension when used on nonstationary data. Several time series (*top*) with different known (169) dimensions (shown beneath each subepoch) were linked together to make nonstationary time series (6,000 points). "Sampling rate" was adjusted for each subepoch so that same τ step could be used throughout ($\tau = 1$). Subepoch means of point D_2 (PD2; shown as numbers beneath each subepoch) are generally seen to be more accurate than either those of classical D_2 (i.e., a single point, large arrow) or mean "pointwise" scaling dimension (PWSD). Latter shows a larger variance (small arrows), especially at transitions (left small arrow).

est vector-difference length is continuously incremented in size, and the corresponding number (N) of vector-difference lengths in each range are continuously counted. Thus a log-log cumulative histogram is made, C, whose size is related to the values of r and of the total number of vector-difference lengths.

The next step is to measure the slope of the linear region in this log-log plot; this linear region reflects the values of r over which the model $C(n,r) \sim r^{D_2}$, or $D_2 \sim \log C(n,r)/\log r$, is valid. The value of m is incremented and the corresponding slope noted, thus yielding slope and m pairs (Fig. 10*E*, *right*). The values of m are selected to span the size of the expected D^2 value (that is, m ranges from 1 to $2D_2 + 1$). The number of embedding dimensions is relevant up to the point where its increment is no longer associated with increased slope (i.e., it is convergent). D_2 then is the slope of the linear region at the convergent values of m.

2. *Pointwise dimension D_{2i} (also called the pointwise scaling dimension PWSD)*

The pointwise scaling dimension was suggested by Farmer et al. (63) to be an estimate of D_2 that was perhaps less sensitive to nonstationarities (i.e., changes in autocovariation over the time series) because the reference vector ($\mathbf{n}_{ref}$, the current **i** vector) is fixed for each estimate and dominates the calculations. In this procedure, the **j** vectors, which are made with respect to the single reference vector, still span and probe the entire data epoch, but they alone are the basis for the log-log plot and the consequent slope and m pairs. This means that since "$\mathbf{n}_{ref}$" is chosen sequentially for each digitized point in the time series, dimension is estimated as a function of time as well as its position on the attractor.

3. *PD2 algorithm*

The "point-D2" estimate of the correlation dimension (PD2) was developed by Skinner and associates (251, 252, 254, 256).[4] Calculating the PD2 is similar to that of the PWSD; that is, the reference vectors ($\mathbf{n}_{ref}$, the current **i** vectors) remain fixed while the **j** vectors sample the whole data series to make the D_2 sets for each multidimensional (m) phase space. The **j** vectors considered, however, must arise from a subepoch that manifests scaling characteristics similar to those surrounding the **i** vector. Also, the PD2 rejects unsuitable estimates that do not result in linear scaling or clear convergence; these rejections could result from noise or other artifacts in the data, or from an insufficient sample of stationary subepochs. The PD2 does not use all possible vector-difference lengths, like the Grassberger and Procaccia algorithm (D_2), nor all vector-difference lengths with respect to a fixed reference vector, like the Farmer et al. (63) algorithm (PWSD). It seeks its own

[4] The software for the PD2 is available free of charge from Neurotech Laboratories, Box 9797, The Woodlands, TX 77830.

subspecies of stationary data with which to make the vector differences, then it tests and rejects those estimates for which linear scaling and convergence cannot be found. Accepting every data point as a valid coordinate in the reference vector would mean erroneously including those vector-difference lengths for which the relationship $C(n,r) \sim r^{D_2}$ does not hold. The model for the PD2 is $C(n,r,\mathbf{n}^*_{ref}) \sim r^{D_2}$, where $\mathbf{n}^*_{ref}$ is an acceptable reference vector showing scaling within its own subspecies; that is, *1*) linear in the log $C(n,r,\mathbf{n}_{ref})$ versus log r plot, and *2*) convergent in the slope versus m plot. Because each $\mathbf{n}^*_{ref}$ has a new coordinate that could be of any value, the PD2 values are independent of each other, and this justifies using the mean PD2 values over a stationary subepoch as the best estimate of the correlation dimension.

4. Selection of τ

The value of τ is irrelevant if the number of points in the time series is infinite, a condition which is never approached for biological data. A conventional way of determining the size of the τ step is to calculate the first zero crossing of the autocorrelation function of the data (Fig. 10*B*). When multiple peaks are present in the power spectrum (i.e., the fast Fourier transform of the autocorrelation function), as is the case for the Lorenz time series, it is often suggested that τ be selected as the number of digitized values in a quarter-cycle of one of the higher dominant frequencies. One should be cautious about τ selection when nonstationarities arise in finite data. In this case, each subepoch may require a different τ for adequate sampling of the attractor. Thus the autocorrelation function and power spectrum should be evaluated separately for each subepoch.

F. Consideration in the Application to Physiological Time Series

1. Deterministic versus stochastic processes

Measures of system complexity such as dimensionality, entropy, and Lyapunov exponents are useful in describing system properties, but there exist numerous problems in applying these measures to actual physiological data. In fact, it is suggested that major difficulties result from the indiscriminate application of chaotic dynamics (i.e., formulas) to physiological time series before understanding the actual mathematical properties of the signal (204). As can be seen, several authors (e.g., Ref. 196) note that the presence of a fractal dimension alone in a time series is not sufficient to indicate the presence of a strange attractor and, in fact, may have been produced by a filtered stochastic process. They conclude that "observing a finite correlation dimension from experimental data does not necessarily imply the presence of deterministic chaos," since there exist stochastic processes that give such a value also. Theiler (266) has shown how the error of dimensional estimation increases when the sample size is decreased. He (266) has also pointed out the necessity of discriminating low-dimensional chaotic data from filtered high-dimensional noise, which can appear to be low dimensional if filtered enough. Some have addressed this issue statistically, by comparing their dimensional estimates of biological data with those of white noise filtered by the same data acquisition system (e.g., Ref. 254).

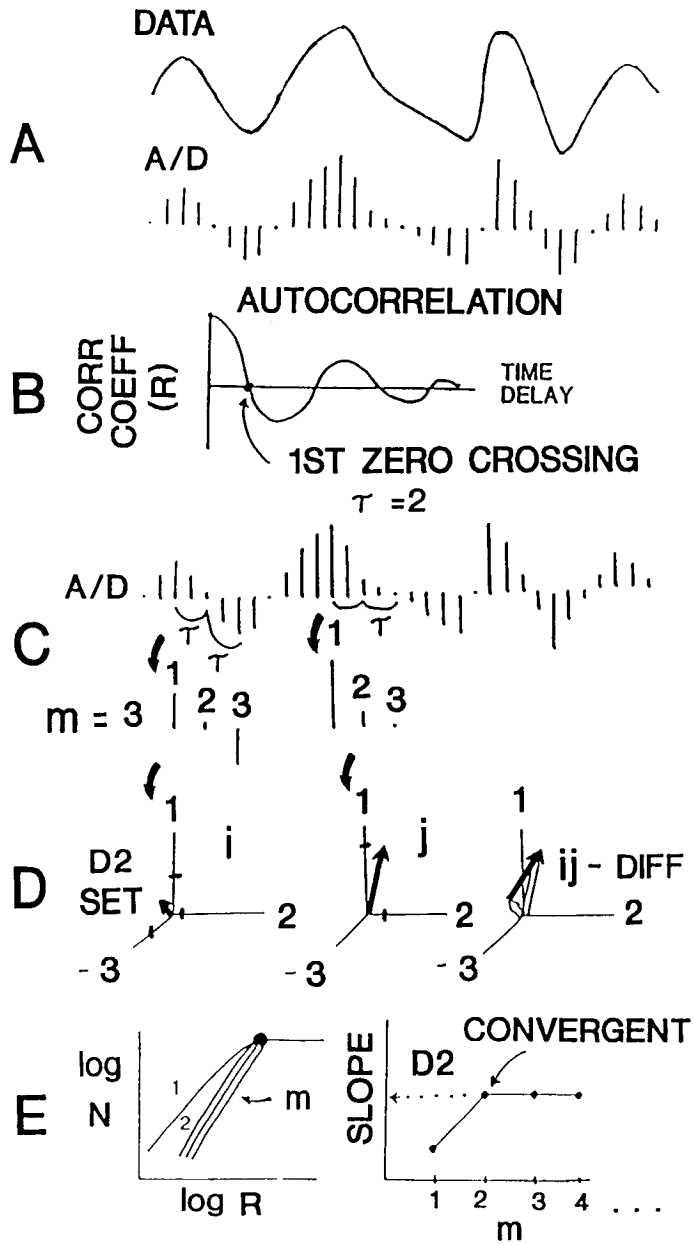

FIG. 10. Calculation of correlation dimension. *A*: raw data and its digitized form (A/D). *B*: autocorrelation function, showing where correlation coefficient (R) crosses 0 point on time-delay axis (i.e., separation of 2 points correlated in time; correlation is 1.0 with a separation of 0 time); τ is found to be 2 digitized values. *C*: τ jumps are used to select digitized voltages to apply as coordinates for an embedding dimension of 3. *D*: plots of selected points result in an **i** vector and a **j** vector; their difference (**ij**-DIFF) makes 1 value in vector-difference length histogram (D2 SET). *E*: plot of log N vs. log r for all embedding dimensions (*left*) and plot of slope found in linear scaling regions for each embedding dimension (*right*); convergence is observed at $m = 2$, and slope (D_2) at this value is indicated by arrow.

Thus an important issue relates to the fact that measures of system complexity do not, in themselves,

give any insight into whether the system under study was the result of a deterministic or a stochastic process. Kaplan and Glass (139) suggest one method for making a determination as to whether the underlying signal is generated by a deterministic or stochastic process. The method is based on an observation by Takens (262, 263) that all the tangents to the trajectory in a given region of phase space generated by a deterministic system will have similar orientations as compared with those generated by a random process. Other techniques will likely be developed for this important concern.

2. *Stationarity and short-term changes in dimension*

By definition, stationarity refers to a property of a time series in which the mean and the variance as well as the autocovariation remain constant over time. This is an important condition for experimentalists, since a variety of signal analytic procedures, including inferential statistics, assume stationarity. Biological signals, such as electroencephalography (EEG), are unlikely to remain stationary over long intervals, especially of the length theoretically considered in the calculation of dimensional estimates. Some investigators (180, 182, 251, 252, 254) have even suggested that such requirements as stationarity represent a fundamental flaw in the application of chaos theory to biological systems.

One solution that has been proposed to this problem is to use short epochs of such signals as EEG. Data lengths varying from 20–30 s to even less than 1 s in the case of evoked potentials have been used. In terms of the 20- to 30-s epochs of EEG, it has been assumed that the error in the dimensional estimate that arises because of the small data samples will be systematic, thus enabling control and experimental comparisons to be made. Thus a measure of dimensional differences between conditions or between subjects should remain useful because the errors will be approximately the same in both cases, and therefore, the results will still be suitable for statistical testing.

In terms of the even smaller epochs of 1 s or less, Skinner and associates (166, 183, 254, 255), using data recorded from the olfactory bulb of the rabbit during behavioral quiescence, reported that epochs as short as 500 ms were necessary to achieve statistical stationarity. After the presentation of a novel odor, the 500-ms epochs still appeared to be stationary within this condition. However, dimensionality (D_2) estimates were observed to be statistically significantly increased compared with control. Similarly, Rapp et al. (218) proposed that human EEG epochs of 1 s would remain stationary, and they found that following a target stimulus the D_2 values were significantly lower than those following a nontarget stimulus.

One problem with these brief-interval studies is that the poststimulus dimensions may appear to be stationary, when actually they are not; that is, the dimensional shift may not change to a new stable state but may actually undergo a variety of rapid nonstationary changes. Most event-related potential studies indicate that indeed a variety of different generators are separately activated within the 500-ms poststimulus interval.

A second approach to solving the problem of data nonstationarity has been to use a method for continuously estimating the dimension, with the expectation that the reference vector, which spans only a short interval, would remain stationary and would dominate the calculations, making the overall estimate less sensitive to nonstationarities (63, 181, 252, 258). Farmer et al. (63) developed the pointwise scaling dimension (referred to above as D_{2i}), which Mayer-Kress et al. (181) report as an improvement over the traditional Grassberger-Procaccia method in a study examining biological data (EEG, EMG, heartbeat intervals). However, errors with this method could arise because the method assumes data stationarity over the whole epoch.

Skinner and associates (250, 252, 255) developed the point-D_2 method, which they believe to circumvent the requirement for data stationarity altogether. As discussed previously, the point-D_2 uses an algorithm in which each reference vector (i.e., the "point") seeks only its own stationary subepochs in which to make the vector-difference lengths that are used to determine the dimensional estimate at that point in the data. When applied to human event-related EEG data of the type previously used by Rapp et al. (218), it was found that the dimension does not appear to shift a unitary value, but rather changes continuously during the 500-ms period following the stimulus. Skinner has argued the PD2 is inherently more sensitive to the output of the underlying biological system than is a stochastic measure [e.g., the signal-averaged mean (183) or the standard deviation (250, 256)] used on the same data. This point is illustrated for the human brain in Figure 11. In Figure 11, he shows that dimensional changes related to differences in instructional set can occur without a change in the actual event-related potentials. This type of sensitivity with the PD2 reveals features in both the nervous system (e.g., sites of single-trial information storage) and heart [e.g., vulnerability to lethal arrhythmias (251)] that have not yet been observed by other methods.

3. *Use of filters and comparison with white and colored noise*

Experimentally, physiological signals are generally filtered in some manner by both analog and digital filters. This has posed the practical problem of how the filtering process itself influences various measures of dimensionality. Some researchers (e.g., Refs. 17, 185) have suggested that if the filter can be described by differential equations, then this will increase the dimensional estimates, although this is not always the case. However, other research suggests that appropriate filters do not necessarily influence estimates of dimensionality (e.g., Ref. 184). Rapp et al. (217) extend this discussion and suggest comparisons with surrogate data sets as one alternative procedure to distinguish between filtered signals and noise.

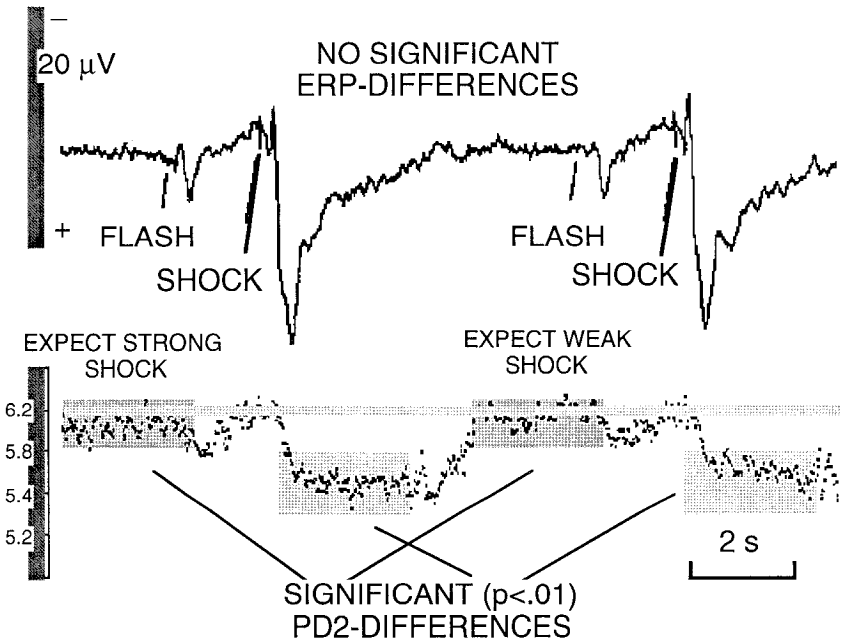

FIG. 11. Effects of instructional set (expectancy) on event-related dimensional response. Subjects (n = 17) were instructed to expect either a strong finger shock (S2) following a dim light flash (S1) or a weak one. The S2 stimuli in both cases were the same. Event-related potentials (ERPs) were recorded from vertex of scalp (Cz). No statistically significant differences were found for any ERP data points (20 trial averages, t tests with protected α-levels) between 2 conditions. PD2 values were calculated for same data, using 20 linked trials within each subject (8,020 data points, at 200 Hz, analog to digital). PD2 values were calculated using $\tau = 6$ in all subjects. Event-related PD2 response showed statistically significant data points using the same statistical method (indicated by dark lines). Resting baseline was found to be lower when expecting a strong stimulus, as was poststimulus drop in dimension. ERP (grand average), left vertical line is 20 μV, and time line is 2 s; PD2 (grand average), left vertical line is 2 dimensions, with baseline drawn through 6.2.

To evaluate a particular physiological signal, many authors have suggested that the obtained results from a particular nonlinear dynamical analysis be compared with that of noise. However, Osborne and Provenzale (196) demonstrated that colored random noise, if analyzed by the Grassberger-Procaccia procedure, may give finite and predictable values of the correlation dimension. Such a result would suggest the presence of a chaotic system, when, in actuality, only noise existed. To test for this possibility, some authors (217) have suggested a shuffle test in which the original data set is shuffled then reanalyzed. A more elegant procedure is suggested by Theiler et al. (267) in which one determines the Fourier transform of the original data set, then randomizes the phases of this transform and produces a second data set by taking the inverse transform. By applying Grassberger-Procaccia to both data sets, it is possible to determine statistically if there exists a difference between the two data sets. In this way, one can evaluate if the actual data set is more than linearly correlated noise. This type of procedure has the additional advantage of establishing an inferential probability in the testing of the null hypothesis (i.e., the signal is not different from that of noise) and is less difficult and has numerous advantages over making the claim that one is measuring dimensionality directly in a particular real world signal. Additionally, if the null hypothesis cannot be rejected, then there would exist no advantage in determining a particular measure of dimensionality. Furthermore, Skinner and co-workers (183, 250, 256) have used the PD2 algorithm to sense and reject bursts of noise (see Fig. 12, N) superimposed upon EEG data. Such noise would markedly increase the subepoch means of the PWSD and the single value for D_2 (i.e., <100 dimensions). For biological data, the PD2 values are found to be significantly smaller and statistically discriminable from white noise passed through the same data acquisition system (254).

III. APPLICATIONS IN CARDIOLOGY: CHAOS IN THE HEART

In this section, we present findings from the behavior in single cardiac cells and also a brief overview of studies investigating the intact heart. Results suggest that low-dimensional chaos can be observed on different levels, in the behavior of single cells, and in the cooperative mass action giving rise to the functioning of a whole organ.

A. Dynamics of Cardiac Cells

Influential work has been carried out by Guevara in his PhD thesis and by Glass and associates (86–89, 91, 108, 110) on aggregates of spontaneously beating, cultured cardiac cells which had been isolated from the ventricles of an embryonic chick heart. In an aggregate, the cells are nearly isopotential, so the choice of the cell to be recorded should not influence the results, i.e., the aggregates are nearly electrically homogeneous. A total of 11 aggregates was investigated. Under several assumptions (201) (mainly that the spontaneous activity of the aggregate can be modeled by a strongly attracting limit cycle attractor illustrated by a trajectory that quickly turns back onto the attractor after a perturbation has been induced), a phase-transition curve can be observed from the reaction of the aggregate to brief pulsatile shocks at different phases of spontaneous, nearly periodic activity of the cardiac cycle. This curve shows the new phase caused by the delivered impulse against the old phase of stimulus presentation. On the basis of the empirically observed phase-transition curve, which is fitted to an analytical function and given certain assumptions, a Poincaré return map consisting of a two-parameter one-dimensional map of the unit circle is derived and iterated to predict the dynamical response of

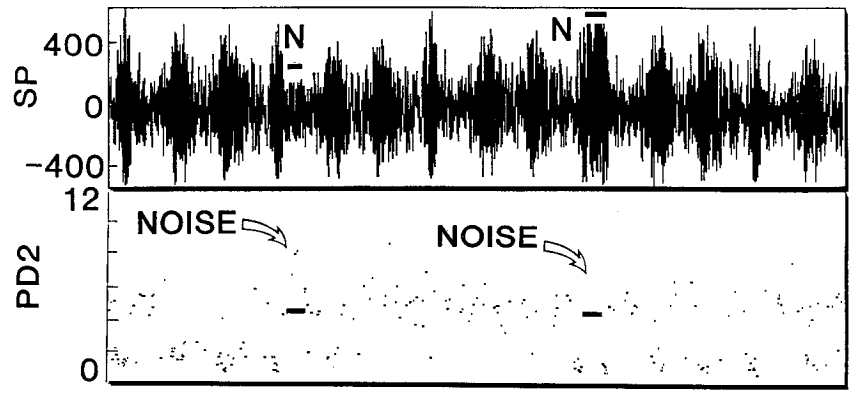

FIG. 12. Dimensional changes (PD2) in surface potentials (SP) recorded from surface of olfactory bulb of awake rabbit. Fusiform bursts of activity are associated with inspiration. White noise of both high and low amplitude (N) is overwritten on data and is either rejected by PD2 algorithm or is high dimensional. Note that low-dimensional changes do not always occur, as seen during inspiratory bursts in middle of record.

the aggregate under periodic stimulation at different amplitudes and frequencies. The results show a bifurcation structure in which the average number of action potentials per stimulus is plotted in a two-parameter (amplitude vs. frequency) space leading to complex behavior of the forced system. Regular (phase locking) as well as irregular (chaotic) activity together with three routes to chaos (period doubling, quasiperiodicity, intermittency) can be predicted for different values of the two stimulation parameters. Presumably, this bifurcation structure is in an analogous sense "universal" for a large class of two-parameter one-dimensional maps (with 2 extrema) in the same manner as the U-sequence is universal for one-parameter one-dimensional maps with one extreme (e.g., the quadratic equation). However, further mathematical research is needed, especially for the zones in which the circle map is noninvertible. Experiments on periodic stimulation of the cardiac cells are, in general, in good agreement with these predictions.

Various periodic zones (phase-locking patterns) and all of the three routes to chaos were confirmed, which strongly supports the usefulness of circle maps for modeling periodically stimulated cardiac cells. Phase-locking patterns that are computed to occupy small regions of the parameter space could not be detected. This failure, however, may be due to experimental noise. The observed dynamics show patterns similar to many cardiac arrhythmias arising from two or more autonomous pacemaking foci (ectopic foci), such as various Wenckebach rhythms, high-grade block, escape rhythms, and pure parasystole. Although highly oversimplified, the aggregate cell model can give valuable insights into cardiac dynamics and may have implications for data obtained from cardiac patients (40, 85).

Similar work has been carried out on periodic stimulation of spontaneous active cardiac Purkinje fibers (109). Chialvo and Jalive and co-workers (37, 38) studied nonspontaneously active Purkinje fibers from sheep driven with periodic current pulse trains. The most striking phenomenon was the observation of various patterns of entrainment in the stimulus strength versus frequency plane, although this did not result from the competition of two oscillators (see Ref. 174 for a comparable behavior in squid axons). Period doubling as well as irregular oscillations were found.

Another experiment examined the action potential propagation along an unbranched Purkinje fiber. When the conduction of the central segment (out of the 3 segments) was slightly impaired by superfusion with an electrical uncoupler or by mechanical compression, the stimulation by regular pulse trains with increasing frequency causes a bifurcation structure in conduction velocity somewhat similar to those of the quadratic equation and consequently suggests chaotic activity. Keener (142) also discussed chaotic dynamics of periodically stimulated, but not spontaneously oscillating, cardiac medium. Driving isolated endocardial right ventricular canine fibers with increasing rates did not produce chaotic activity. However, when ventricular fibrillation was induced with intravenous quinidine (an intoxication which modifies an ionic channel conductance), phase locking, period doubling, and aperiodic dynamics were demonstrated (42).

Chaos appears also to occur in the heartbeat time series. Skinner et al. (252) have applied various methods to the heartbeat following artery occlusion. They report that before the initiation of lethal arrythmogenesis the mutual information increases, the correlation dimension decreases, and the recurrence patterns shift from periodic clustering to local clustering. If true, these results hold exciting clinical promise, since they would offer new tools to monitor the sick or injured heart. Analysis of the dynamic patterns could be easily implemented in standard electrocardiogram monitoring and thus may provide early warning for cardiac problems. A review of the applications of nonlinear dynamical analysis to cardiology is available (41), along with more specialized discussions of chaos and cardiovascular processes that suggest exciting potential applications (252, 255).

B. Low-Dimensional Chaos Prevails in the Intact Heart

Sudden cardiac death is predominantly due to ventricular fibrillation (VF), and it accounts for over 500,000 yearly fatalities in the United States alone (215). A low ventricular ejection fraction or a high degree of premature ventricular complexes observed in a 24-h electrocardiogram are noninvasive indicators of risk. Although their sensitivity in large groups is statistically significant, their predictive power for a given individual (i.e., specificity) is not very good, nor do they suggest

when the lethal event might occur (209). Based on recent insight into the involvement of the autonomic nervous system and higher cortical centers in animal models of sudden cardiac death (84, 200, 253, 257, 271), the relationship of the neurocardiac reflexes to cardiac vulnerability to VF is being closely examined (26, 132). In patients with a myocardial infarction, the standard deviation of spontaneously varying interbeat intervals and the sensitivity of interbeat intervals to forced changes in blood pressure have both been shown to be prospective predictors of mortality (24, 25, 144, 145, 152, 160, 171, 194, 226).

Recently, it has been proposed that fluctuations in the heartbeats manifest deterministic chaos (15, 182, 251); consequently, the use of stochastic predictors, such as the mean and standard deviation, may not be the most accurate way to describe the dynamics of the heartbeat pattern. For example, we could compare two time series of heart rate values, one which alternated between 70 and 90 beats/min (e.g., 70, 90, 70, 90, 70, 90, ...) and another which had the values of 70 and 90 beats/min randomly chosen with a probability of 0.5. Given enough data points, both of these time series would have the same mean and standard deviation. However, the regularity of these two series would be extremely different, one perfectly regular and one random. As introduced previously, Pincus (204) used the measure of approximate entropy (ApEn) as one method for measuring entropy or irregularity in a time series. Consistent with the hypothesis that regularity in neonatal heart rate is a sign of pathology, this author showed that the ApEn measure was lower for a group of sick human babies (in which 3 of 9 died) than for a healthy control group. In other work with aborted sudden infant death syndrome infants (205), and problem labors (206), the ApEn measure was able to detect subtle differences, suggesting its potential usefulness as a practical monitoring procedure.

Using the point correlation dimension (PD2), Skinner and co-workers (15, 182, 251) studied neurocardiac reflex behavior in the conscious pig during experimental myocardial infarction and demonstrated that the PD2 predicted imminent VF, whereas a stochastic measure (i.e., standard deviation) did not; that is, after occlusion of the left anterior descending coronary artery, the mean PD2 values of the interbeat intervals dropped from 2.50 ± 0.81 (SD) dimensions to 1.07 ± 0.18 (SD) some minutes before VF occurred. Occlusions that did not result in VF did not produce low-dimensional shift. Within-subject changes in the standard deviations of the heartbeats before and after occlusion were not significantly different.

A similar decline was found (256) in the PD2 values of the heartbeats in ambulatory electrocardiograms from 10 of 11 human subjects with preexisting coronary heart disease who subsequently experienced VF while being monitored. In 23 of 27 controls, who had severe arrhythmias but no history of VF, the PD2 values did not drop to such low levels. In contrast, the standard deviations of the heartbeat intervals in these same subjects were unable to discriminate the VF patients from their matched controls. Again, support has accrued for the notion that a deterministic measure will be more accurate in tracking the output of a deterministic system (i.e., any system) than a stochastic measure. A deterministic model that may describe how the heartbeat dynamics are produced, both normally (between 2.5 and 3.5 dimensions) and pathologically (<1.2 dimensions), has been discussed recently (249).

IV. APPLICATIONS IN NEUROSCIENCE: CHAOS FROM NEURON TO BRAIN

In this section, we present findings from the different levels at which neural organization is investigated. We begin on the microscopic level with excitable membranes and single neurons (sect. IV*A*) then proceed from multicellular neural systems (sect. IV*B*) to large-scale brain measures and conclude with the study of behavior (sects. IV*C* and IV*D*). In accord with the current state of this field, the review focuses more on research findings than on theoretical models.

A. Dynamics of the Isolated Neuron

The variety of neuron firing patterns offers an opportunity for modeling with nonlinear systems. For instance, West (275, 276) suggests that the behavior of normally silent neurons can be viewed as a fixed point of a dynamical system, that a periodic pulse train can be seen as a limit cycle, and that erratic wave trains can be modeled by chaotic attractors. Individual neurons are characterized by nonlinear elements as indicated by thresholds or refractory periods and, as such, are likely candidates for complex irregular behavior (e.g., the integrate and fire model of a neuron). Evidence for chaotic activity in excitable membranes has been collected in in vitro preparations (see sect. I). In this situation one frequently observes period-doubling cascades as the route to chaos, but intermittency and other routes have also been reported (e.g., Refs. 2, 3, 114). Not all chaotic systems also have nonchaotic states (i.e., routes to chaos). Some, like the EEG-generating system, seem to have continuously chaotic states, at least under nonpathological conditions as described below.

We now present a brief overview of chaotic behavior in cell membranes, which is generally induced by the method of periodic stimulation.

1. Giant internodal cell of the freshwater algae Nitella flexilis (118, 119)

The work of Hayashi et al. (118) was the first to provide evidence for chaotic behavior in cell membranes. These researchers used sinusoidal stimulation, which initially produces entrainment to the stimulation signal. The neuron then loses its entrainment and be-

comes aperiodic. Plotting the membrane potential at the peak of the periodic stimulation against the preceding one shows a single-valued curve with some resemblance to the quadratic map with a period three window (Fig. 2*B*). Thus, using a variety of techniques and the theorem of Li and Yorke (157; "period three implies chaos"), these researchers were able to establish the existence of chaos, although chaos in this case means the existence of aperiodic behavior rather than sensitivity to initial conditions.

2. *Giant neurons (>200 mm diameter) in the isolated esophageal ganglion of Onchidium verruculatum, marine pulmonate mollusk*

There are two types of giant neurons: "silent" ones which need a medium to oscillate as described previously (117) and two pacemaker neurons which spontaneously show periodic activity in artificial seawater (114–116, 135). Both have been shown to produce chaotic activity of various types under period stimulation.

Spontaneous chaotic bursting activity, in the interspike interval as well as in the membrane potential, can be observed in the pacemaker neuron of the mollusk *O. verruculatum* immersed in artificial seawater using a small direct current approaching zero (0.3 nA) (113). In this situation, the input from other neurons of the esophageal ganglion is suppressed by means of carbon dioxide. Chaos was verified through one-dimensional Poincaré return maps using successive interspike intervals, and the attractor was reconstructed from the voltage as a function of time. Chay (36) also detected spontaneous chaotic bursts (with some remarkable resemblance to the Poincaré return map of the interspike intervals) in her three-variable model of an excitable membrane.

3. *Giant axon of squid Doryteuthis bleekeri (2, 4, 6, 60, 173)*

This axon is the subject of a famous mathematical model, the Hodgkin-Huxley differential equations, as described in section I (1, 5, 33, 34, 123, 125, 126) and reviewed in Ref. 127. Many nonlinear features could be found in the model as well as in experiments (1–3, 5, 175, 172). Other types of models based on difference equations, especially circle maps (Ref. 3 and references therein), or based on Eyring multibarrier rate theory (Ref. 35 and references therein) were also capable of chaotic behavior. With one exception (60), a study which uses quantitative measures (Lyapunov exponent and metric entropy) to characterize chaos, these studies used, in addition to power spectra, visual methods of analysis. In general, two-dimensional or three-dimensional phase portraits were reconstructed representing the membrane potential (V) and its (multiple) derivatives (dV/dt). In a few cases, phase portraits were reconstructed by the time lag method, i.e., stroboscopic plots at a fixed phase of the sinusoidal force or Poincaré return maps (see Ref. 128 for an introduction to these methods). An overview of the system's behavior is given by a parameter space composed of the ratio between the forcing and the spontaneous frequency on one axis and the forcing amplitude on the other. In such a plot, the various zones of entrainment and irregularity can be observed (e.g., Refs. 91, 113, 119).

4. *The pond snail Lymnaea stagnalis (129)*

In this early study, the notion and methods of chaos analysis were not yet known. Consequently, the nonperiodic behavior observed was mistakenly described as an effect of "internal noise sources." This work was not on intact central neurons, since the neurons from which the recording took place were not isolated from the brain but were removed from the body.

One problem with some of these studies is that a highly concentrated ionic medium is required to induce self-sustained activity. In addition, a comparatively high-forcing amplitude is required. This problem, however, does not apply to the work of Matsumoto and coworkers (174, 176), who were the first to show chaotic activity under regular trains of current pulses instead of a sinusoidal current. Furthermore, pulse trains also produce chaotic responses in the giant axon of squids (as well as in the Hodgkin-Huxley model) immersed in normal seawater (5). Interestingly, in measuring the correlation dimension at two different points along the axon (30–40 mm distance from one another), they found that chaos is stably propagated ($n = 3.2$ vs. 3.4). This suggests that chaos may be relevant in neural information processing.

Another condition under which chaotic activity can be observed is based on chemical induction. Neurons of the pond snail *L. stagnalis*, in the presence of cocaine, show irregular putative chaotic oscillations (151). Holden and co-workers treated neurons of the same mollusk with high concentrations of aminopyridine (a convulsant drug) (130) and also with menthol-saturated saline (an anesthetic) (120). During prolonged exposure to aminopyridine, the neuron passes through a range of periodic and irregular behaviors in which each state persists for several minutes. Chaotic amplitude modulations are exhibited after the drug has been washed off. Unfortunately, the assessment of chaos in these studies was determined only by visual inspection of the time series.

In conclusion, this brief survey of different cell types and various electrical and/or chemical techniques used to induce phase-locking patterns as well as irregular, chaotic, or chaotic-like oscillations, and the observation of spontaneous chaotic activity, clearly supports the hypothesis that single cells are able to exhibit a variety of behaviors due to their strong nonlinearity. Further insight into the broad spectrum of qualitatively different behaviors can be derived from mathematical models which, in general, are in good agreement with experimental observations. The two-parameter (fre-

quency vs. current amplitude) space with its multiple zones of entrainment and irregularity has proven to be a valuable tool for displaying the results of such dynamical studies. Poincaré return maps and two-dimensional or three-dimensional phase portraits have also been successfully applied, when the dynamics under consideration were of low dimensionality. At this time, the major tools for determining dynamics in the literature are graphical. Unfortunately, quantitative characterizations using fractal dimension, Lyapunov exponents, or metric entropy are not common in the literature. In conclusion, although chaotic irregularity in excitable membranes has been clearly demonstrated for certain conditions, the significance of this behavior for the functioning of a given cell and its interaction with other cells has yet to be determined.

B. Animal Studies: Chaos in Cell Assemblies and Brain Structures

1. Single neurons in the precentral and postcentral gyrus of anesthetized squirrel monkeys

Correlation dimension analyses of the interspike intervals of 10 single neurons in the precentral and postcentral gyri of anesthetized squirrel monkeys have been reported by Rapp and colleagues (219, 220). These studies provide insight into the activity of neurons in their natural environment. Three of the 10 neurons exhibited relatively low fractal dimensions (between 2.2 and 3.5), two presumably gave values between 5 and 7, and the remaining neurons produced behavior that could not be distinguished from random noise. The low-dimensional neurons were slower (17, 21, 32 ms typical interspike intervals) than the higher-dimensional ones (1 ms).[5] This result indicates that low-dimensional chaos can occur in the spontaneous activity of some simian cortical neurons. Because the length of the time series (varying from several hundreds up to ~1,900) is limited, possible higher dimensional chaos could not be detected. Another limitation is that fast-firing neurons (which do not occur normally) could not be detected with the procedures utilized.

2. Bucal ganglion of mollusks

Bucal-cerebral neurons are key neurons in the generation of motor patterns. There exist strong bidirectional connections between these neurons and brain motoneurons that are related to drive and patterned activity. To study chaotic behavior, Mpitsos and co-workers (e.g., Refs. 188, 191–193) deafferented the cerebral ganglion, removing the effects of sensory inputs as well as motoneuron targets in the mollusk *Pleurobranchaea californica*, a sea slug. They recorded two patterns during the generation of rhythmic motor-related activity involving bite-ingestion: the bite-swallow phase of feeding and regurgitation. They found quickly decreasing autocorrelation functions, one-dimensional return maps obtained from Poincaré slices of two-dimensional reconstructed attractors showing folded sheets, correlation dimensions between 1.75 and 2.5, and positive Lyapunov exponents (0.15 up to 0.55 bits/s). All of these findings are suggestive of low-dimensional chaotic behavior during patterned motor activity. One limitation pointed out by Mpitsos (188) is that because of the brief temporal duration and variability of biological actions, such as feeding or regurgitation, attractors that are believed to control these behaviors can be investigated in only a limited manner, since only several cycles are available in the data. Thus a strong claim for chaos in this preparation is difficult to support.

If the motor pattern generation is indeed chaotic, the question arises whether such a signal can be "understood" by other parts of the brain. To approach this question, Mpitsos and co-workers (189, 190) studied a very simple neuronal network with one input unit, one output unit, and four hidden units. They demonstrated that this network was able to distinguish various chaotic signals (98), e.g., the logistic equation and Rössler equation) in the fundamental aspects of the dynamics including the greatest Lyapunov exponent. With this result, one can speculate that the information exchange between various parts of the brain is coded as various degrees of chaos. The meaning of this speculation is that the neural message is not composed of a signal overlapped by noise but lies in the irregularity itself. Different coding mechanisms would allow the simultaneous processing of different tasks but might then also increase the noise for the encoding of information pertaining to concepts of one particular task-related set. This would allow limited parallel processing. Furthermore, the neurons of the motor system are found not to be specialized to produce specific motor patterns but are multifunctional, which means that they are able to produce a variety of behaviors. In this model it would be the reciprocal interaction between the animal and the environment that determines which behaviorally related attractor was selected.

3. Olfactory system of the rabbit

The olfactory bulb is a model neuropil with the same cell types and chemical neuromodulators as the neocortex. Its anatomy and physiology, however, are simpler. Furthermore, the amplitude of the surface potential recorded above a "column" (i.e., a functional unit) is strongly correlated with the firing frequency of the underlying output cell. Because the surface EEG has exactly one-quarter cycle phase lag with the oscillations in the mitral cell firing probability, it is interpreted that the EEG is actually generated by the open-field dipoles

[5] Some of the neurons were firing at a rate of 1,000 Hz. These are dying cortical cells. The average firing rate for a cortical neuron in the conscious brain is ~1.0 Hz.

of the granule cells. The latter are always recurrently activated (i.e., with a quarter cycle lag) when the associated mitral cell fires. Because of the simplicity and knowledge about electrogenesis, it is expected that the study of chaos in the EEG will be easier to interpret for this model neuropil than for the neocortex.

Freeman and associates (66–69, 71, 78, 80, 81, 248, 272), with an overview of their methods (48, 69, 72, 79, 279), thoroughly investigated the perceptive events in the olfactory system of the conscious rabbit (odor recognition and discrimination), and based on this work, they also developed a mathematical model of the bulb that uses nonlinear, coupled, ordinary, differential equations. To extend their findings to sensory processing in the neocortex itself, they also studied the visual system of the monkey (75, 76, 81).

In the rabbit, the surface EEGs were recorded by an 8×8 array of electrodes interspaced at the observed spatial frequency. The array was constructed to cover at least 20% of the bulbar surface. The animals were trained (appetitive conditioning) to respond to two different odors in different ways (i.e., sniffing and licking or sniffing only) (272). It was found that β-receptors must be intact for learning-related changes to occur in the bulbar EEG (101). The terminal endings of the noradrenergic neurons that activate the β-receptors project from the nucleus locus coeruleus to impinge on bulbar locations that regulate the excitability of the mitral cells (162). Based on these biological findings and on the results of simulations in their mathematical model, it was interpreted that during conditioning the main effect was primarily on the potentiation of the mutually excitatory synapses between the mitral cells; that is, these synapses were thought to be subjected to the greatest amount of potentiation according to the Hebbian rule of temporally convergent states of excitation (121). After acquisition, and in the presence of a learned odor, a relatively stable and reproducible distribution of EEG activities was observed that formed a distinctive spatial pattern. This evoked pattern appeared to involve the whole bulbar surface (72, 78, 272), thus leading to the conclusion that the bulb operates as a global dynamical system.

The mathematical model that Freeman developed is based on biology (66, 70, 71, 279) and consists of four interconnected parts, with time delays between them. It is simplified by neglecting the connections to and from the other parts of the brain (248, 279). Four types of activity can be generated by the model that are of the same types actually seen in the rabbit bulb; that is, a time series can be generated by the differential equations (which constitute the model) that resemble the EEG of the bulb observed during four experimental conditions.

The first type of common activity is that of a silent system, which seems to occur under deep anesthesia, and is represented by a fixed point attractor in a time-delayed phase space. A second type is that of normal background EEG observed in the absence of a significant input. Freeman (71) suggests that the bulbar background activity is chaotic, for it has an attractor in phase space that seems to be a point repellor, its power spectrum shows a $1/f$ distribution, its autocorrelation function attenuates rapidly, and its time series is aperiodic. This evidence is further supported by the analysis of the model (71, 248), whose output time series remains statistically indistinguishable from the empirical data. For example, the correlation dimension (106) was calculated for the time series sampled from both the model and the bulb (71, 73), and similar values were obtained: 5.46 (model) and 5.92 (bulb). These values were within the standard error of the measurements. A modified model is also available from this lab (279), yielding significantly lower values of dimension, i.e., between 2.3 and 2.4.

A third type of activity seen in the biological data is the reaction of the system to a learned odor. In this case the surface EEG has an almost coherent series of inspiratory bursts of oscillations, with a narrow spectral distribution, which vanishes during each expiration. Because this seemingly periodic pattern of reaction (248) turned out to be (at least in the model) also chaotic, its time series was thought to be represented by a "near-limit cycle" attractor (71). Because of the requirement for large data sets, Freeman thought dimensional analysis would not be possible for the bulb, but only for the model. Simulations of different "learned" odors produced different time series, each with a different near-limit cycle attractor; the attractors could be easily distinguished from one another and could be distinguished from that of the resting background activity. The dimension decreased from 2.33 in the resting state to 1.13 during the simulated odor (279).

The fourth type of modeled biological activity is that of an epileptic seizure. The seizure results in a paroxysmal discharge which "repeats at a rate of about 3/s for 10–70 s." It is induced biologically by an intense stimulation of the lateral olfactory tract. After temporary cryogenic blockade in the lateral olfactory tract, however, it is considerably easier to initiate the seizure (102). It was interpreted that the seizure results from a disconnected state in which a collapse of transmission occurs between the bulb and other parts of the system (70). In the model, the seizure can be simulated by changing a parameter in the excitatory feedback pathway. This adjustment is thought to produce a Ruelle-Takens-Newhouse route to chaos, via two Hopf bifurcations (195). The resulting chaotic attractor is toroidal shaped (71), with a correlation dimension of 2.52 in the case of the biological system and an average value of 2.76 for the model (73). The recovery from the seizure is not yet understood (74).

Freeman and associates concluded that the dynamical process in the olfactory system of a motivated rabbit is characterized, in the absence of any significant odor, by a spatially and temporally unpatterned chaotic state. Immediately after presenting a learned odor, the system briefly switches to a global odor-specific chaotic state characterized by a single near-limit cycle attractor. They believe that the acquisition of the near-limit

cycle attractor can be understood as a pattern recognition process, which, because of differential conditioning, initiates the required action. Whether the transition to the odor-specific attractor is due to a bifurcation, i.e., to a parameter change in the single system (66, 82, 248), or to a change in the system's state, i.e., the input is switched into the basin of another attractor (19, 71, 279), is not yet clear. In either case, however, they concluded that the learning of a new odor and its subsequent recognition is related to a process involving a change in chaotic dynamics (248).

Using the PD2 algorithm, Mitra and Skinner (183) began to observe new features of the neuropil that could not be seen with the classical D_2 algorithm. This may have resulted from the limited time resolution and data stationarity requirement of the D_2 (183). With each respiratory cycle in the resting state, there was found to be a rapid shift in the PD2 from between six and seven dimensions during expiration to one to two during inspiration. During preodor control epochs there existed a smooth gradient of PD2 values in the spatial array; the mean PD2 values at each point in the array, averaged over 1.3 s (~3 respiratory oscillations), showed a clear spatial pattern. Moreover, the lowest mean dimension in this resting pattern indicated where the future learning-dependent changes in dimension would occur. When a novel odor was presented, it evoked an increase in the mean PD2 values at each point such that all points increased to the same value, again confirming the Freeman idea, based on the change in the surface potential pattern, that the process was global. The dimensional increase occurred primarily during the dimensional "dip" associated with inspiration. After habituation, the odor did not evoke any changes in the spatially distributed mean PD2 values. Comparison of the nonodor gradients before and after the intervening learning (i.e., the habituation), however, showed that small learning-dependent increases in the PD2 values had occurred, in precisely the part of the gradient where the smallest PD2 values had been located. This learning-specific change occurred repeatedly, with additional habituation of new odors; that is, a new low-dimensional trough existed in the resting spatial gradient after each learning episode, which, with new learning, again showed a small dimensional increase during the control condition.

Because no systematic transitions in dimension (i.e., routes to chaos) were noted and because the resting bulb does not seem to be characterized by a single dimension, a shifting among existing attractors or the forming of new ones may best explain the observed PD2 changes rather than the systematic change of a parameter in a single chaotic system (i.e., one that bifurcates to new dynamics with each parameter change). The oscillation of dimension from a higher value to a lower one, which occurs during the evaluation of a set of expected (i.e., habituated) ambient inputs, may be an important part of the sensory process. An example of such data is shown in Figure 12. The observation that all PD2 values rise to the same value during evaluation of a novel odor suggests that a single global dynamic is controlling the bulb at that moment; this, however, is not the case during the background condition, when the spatial distribution of PD2 values is not uniform. The small site-specific increases in dimension that occur with new learning are somehow related to this background gradient, and some are again modified with still newer learning, thus illustrating a "context updating" of the stored information.

The work from the model neuropil indicates that deterministic chaos, of varying dimensional complexity, characterizes its functioning, but why this is the case is still unclear (279). Global higher dimensional attractors characterize the surface potentials only when the bulb is stimulated by new or conditioned odors. Lower dimensional attractors are associated with the evaluation of known, highly habituated (i.e., expected) stimuli. Why these lower dimensions have a graded spatial distribution is unclear. Freeman's mathematical model (e.g., Refs. 66, 69, 78, 248) suggests that chaos enables odor-specific information to be represented by a specific dimension. Although some mathematical models of perception do not require chaos (e.g., Ref. 105), low-dimensional chaos seems to prevail in biological systems. Understanding chaos in the olfactory bulb may be expected to provide a breakthrough in our understanding of how a neuropil works.

4. Dimension evaluations of specific cortical structures in cats

Using chronically implanted electrodes in five cats, Röschke and Başar (228, 230, 231) made dimension evaluations of specific cortical structures. They measured from each of the three structures: the auditory cortex, the hippocampus, and the reticular formation during slow-wave sleep (1–3 Hz) that can be characterized as a state of hypersynchrony over the whole cortex. A total of 15 time series ($7 \times 2{,}048$ points, encompassing ~20 s of time, and $8 \times 4{,}096$ points lasting 41 s) was recorded. The results indicate the presence of various attractors with correlation dimensions in the range of 3.8 and 5.6 for these three structures. Looking at the individual case, a strong relationship was not found between the structures and their fractal dimensions, which was consistent over cases. Likewise, the test-retest reliability from cats with two samples from the same cortical structure was less than moderate. Taking the 15 trials together, the statistically relevant information is that in 86% of the trials the auditory cortex showed the highest correlation dimension (5.06 ± 0.31). Significantly lower were the dimensions of the reticular formation (4.58 ± 0.38) and those of the hippocampus (4.37 ± 0.36). These results can be contrasted with dimension measurements of eight to nine (with a maximal embedding dimension of 10) of an awakened cat determined from spontaneous activity in the auditory cortex.

Also interested in the question of whether chaotic behavior can be detected in a higher frequency window

(between 100 and 1,000 Hz), these authors (232, 233) studied the activity of the inferior colliculus (brain stem) and of the cerebellar cortex in four awake freely moving cats. Different from the above-cited study in which a saturation in the correlation dimension was found in three of four of the cases, in the present study strange attractors could only be observed in one of four of the investigated trials. These results may be partly due to frequent movement artifacts. Thus one might conclude that in this high-frequency window chaotic activity is possible but not the rule. If attractors are observed, their dimensions are 7.05 ± 0.15 for the cerebellar cortex and 6.70 ± 0.20 for the inferior colliculus.

C. *Human Studies: Chaos in Electroencephalograms and Magnetoencephalograms*

While the application of nonlinear analysis techniques to brain processes has been discussed previously, it was Babloyantz et al. (16) who first published results on the dimensionality of the human EEG. Since that time (1985) more than 50 papers have reported results from EEG analysis using nonlinear dynamical analysis (8, 11-14, 16, 22, 44, 53, 94, 155, 163, 164, 179, 180-182, 186, 223, 239, 247, 255, 258, 273, 274, 278). Many of these papers were demonstrational in nature and presented data from only a few subjects with the EEGs being taken from only one or two sites, making variance estimations and inferential statistical comparison impossible. Additionally, many of these studies only examined resting baseline type measurements or did not specify under what conditions the measurements were made. Although supportive of the potential associated with applying nonlinear techniques to EEG in general, Dvorák and Holden (43a) suggested in 1991 that little had been clearly demonstrated in the reported research up to that time. These authors suggest that this results both from the complexity found in the EEG and the lack of a general theoretical model. More recent research has increased the number of subjects being studied as well as the tasks used. Initial group studies ($n \geq 10$) were those of Shinagawa et al. (247), Pritchard and Duke (211), and ourselves (53, 56, 57, 148, 163, 164, 223) and are discussed in this section.

As discussed previously, one major problem with using methods of nonlinear dynamics to evaluate biological data is the nonstationarity of the signal. It remains unclear as to how long the brain remains in a specific state that would result in a stationary signal governed by a single attractor. Principally, nonstationarity can be induced in two ways: *1*) by a change in the parameter values (these are regulated by the surroundings of the system) and *2*) by a change in the actual values of the variables due to an input, which causes a shift in the trajectory away from the surface of the attractor. It has been suggested that neurotransmitter systems, and hence the excitability of interneural connections, might invoke bifurcations in the system generating the EEG signal (136). Sensory input will cause the second kind of perturbation. Both sources of variation should therefore be held constant during the EEG recording. Tests to measure nonstationarity based on characteristics of the amplitude distribution have not proven to be useful. Only abrupt changes in the dimension can be easily detected as a disturbed scaling behavior in the calculation of the fractal dimension. Unfortunately, there exists no adequate method to measure the nonstationarity, although there have been attempts to extend the correlation dimension as a function of time, a procedure which may maintain accuracy over nonstationary epochs (e.g., Refs. 181, 186, 255) as well as the development of measures that do not demand stationarity of the signal.

Several groups of investigators have studied dimension evaluations of the EEG and MEG from human subjects during various mental tasks (eyes closed, eyes open, quiet and awake, computation, verbal tasks, imagination, meditation, sleep). However, a comparison of the reported values for the dimension of the same task reported in different labs shows little consistency in the results. This may result from a variety of factors including the recording condition of the signal (electrode sites, type of recording, filter, data precision, sampling rate), the processing of the signal (digital filtering, artifact correction), and the algorithm used to estimate the dimension.

The two most commonly used algorithms are the Grassberger-Procaccia (99) and the averaged pointwise dimension, although Pritchard et al. (213) have explored an alternative algorithm based on the work of Ellner (58). The Grassberger-Procaccia algorithm is widely used because of its presumed economy in determining the correlation dimension from the slope of the scaling region. This is determined only once for each embedding dimension. The averaged pointwise dimension is more time consuming, since the scaling region has to be determined for each reference point and each embedding dimension separately, but has other advantages (see Refs. 131, 178 for a comparison). In principle, with very long time series, both algorithms should yield the same dimension value. However, in practice, there exists a tendency for the pointwise dimension to be higher (e.g., 4.3 ± 2.2 vs. 6.4 ± 1.2 for correlation and pointwise dimension, respectively; Ref. 179). Both methods are far from becoming an automatic procedure and have to be applied with care. Some of the parametric considerations are as follows: *1*) the length of the time series to be recorded. In general, the higher the dimension, the longer the time series required (9, 178); however, for biological signals, this demand may be in conflict with conditions of nonstationarity that might suggest shorter time intervals. On the other hand, the error to a large extent is systematic and not random; therefore, comparisons between experimental conditions give valid relative information. As was seen in Figure 8, the average value of K_2 entropy may change rapidly during a period of a few seconds. From Figure 8, it is possible to infer the stationarity of a particular time series. *2*) The time lag for the reconstruction of the phase space is also a parametric consideration. The reconstructed axes of

the phase space should be linearly and nonlinearly independent from one another regardless of the reconstruction methods used [e.g., singular value decomposition (30, 53, 143, 164), also illustrated in Figure 7; multichannel reconstruction (43)]. The mutual information function may be used to estimate the optimal time lag. For the EEG, we have shown that the first minimum (or zero crossing) of the autocorrelation function works equally well (94). *3*) The maximal embedding dimension (32, 179) is also important. There exists a boundary effect for high values that causes a systematic underestimation in dimensional calculations. *4*) The number and selection criterion for the reference points is another parametric consideration. If all points are used as reference points, then the procedure must be specified. *5*) The number and refinement of the radius classes used should be taken into account, as well as *6*) the method to find the scaling region, the size of the fitting interval, and goodness of fit (9).

It should also be noted that quite different and sometimes invalid methods are used to determine the error bars of the dimension. Finally, when plotting the measured slope of the scaling region for increasing embedding dimensions, a visually based decision or a numerical cut-off is required to determine whether saturation is reached or not. To circumvent this problem, some studies take as their measured dimension the average over the highest few embedding dimensions. Because all of these factors may have an influence on the evaluated dimension value and because of the failure of an accepted standard, a direct comparison of the results from different laboratories remains difficult. Only changes in the dimension between different conditions may be replicable in different laboratories. For this reason, we emphasize that one should not seek to measure dimensionality directly but in relation to particular tasks, sites, or subject groups.

Before reviewing various studies, it should be noted that artifacts (e.g., eye movement) in the EEG tend to reduce the determined dimension. Based on studies in our lab and those of others, we presume that the actual dimension of EEG lies well above a value of three and are skeptical about dimension values reported that do not exceed this value. Given a measure of relative dimension, we can now begin to summarize the results from the currently existing studies. If not otherwise stated, the comparison is to a relaxed eyes-closed condition.

The eyes-closed state itself shows different dimensionalities due to the existence (dimension reduction) or absence (dimension enhancement) of α-waves (94, 155, 247). "Pure" α-waves obtained by filtering the α-band yield a much lower dimension than is found with the unfiltered time series (258). Investigations of the resting EEG with open eyes typically indicate a relatively higher dimension than under an eyes-closed condition when the α-rhythm becomes more pronounced. This was originally demonstrated in a study by Pritchard and Duke (212) with 12 subjects. The drop in dimensional complexity associated with closing the eyes was greater over occipital loci. In two of three group studies, however, in which we compared an eyes-open with eyes-closed condition, we did not find consistent lowering of the dimension, although parietal α was significantly enhanced. In one study (unpublished data), we calculated the averaged pointwise dimension (63) with 200 reference points equally distributed over the time series. The time delay for the phase-space reconstruction was generally chosen to have the value where the autocorrelation function is zero. The scaling region was found automatically by fitting a regression line within a range which, beforehand, was visually determined. The length of the time series was 8,192 points with the maximal embedding dimension 40. In another study (53), we investigated the EEG from 12 control and 12 schizophrenic subjects under resting conditions, using the singular value decomposition based on the autocovariance function with time lags ranging from 0 to 32 points. A calculation of the dimension (illustrated in Fig. 7) using the method of pointwise dimension (63) did not produce a significant difference due to eyes open or closed in either of the groups (although α-activity was markedly more pronounced when eyes were closed). With the use of the same methods in a larger sample of student subjects (n = 42), the difference became significant. Similarly, Pritchard and colleagues (212–214) replicated their finding of a systematic difference in EEG dimensional complexity for a resting condition between eyes closed and eyes open. Thus it appears that the "idling state" characterized by α-waves is generally one with a lower dimensionality.

In another study, together with Werner Lutzenberger, we sought to extend previous EEG work in three ways. First, we utilized a variety of tasks that cut across sensory modalities including touch, vision, imagery, and verbal processing. These tasks were chosen to reflect neuropsychological processes that differentially utilize both the frontal and more posterior areas of the cortex. Second, we used measurements from nonlinear systems theory and compared these results with measures derived from conventional Fourier analysis. Third, whereas previous studies have been limited to only one or two electrode sites, we collected data from 15 and 32 electrode sites (164). The outcome showed variations between scalp sites for all measures and also variations between tasks. The brain maps, displayed in Figure 13, illustrate that dimensional complexity provides different information than seen in traditional EEG power frequency bands. The highest dimensions were observed for the imagery tasks, followed by the sensory touching tasks and observational task, and the lowest for the verbal alliteration task. Under the assumption that lower dimensionality dominates during rest rather than during more active engagement, we can conclude that more "attractors" are utilized in the imagery tasks than in those tasks of alliteration or simple observation. We are convinced that "rest" is not a well-chosen control condition, because a very large number of more or less complex brain processes may happen during such an unstructured situation. A simple task like our alliteration

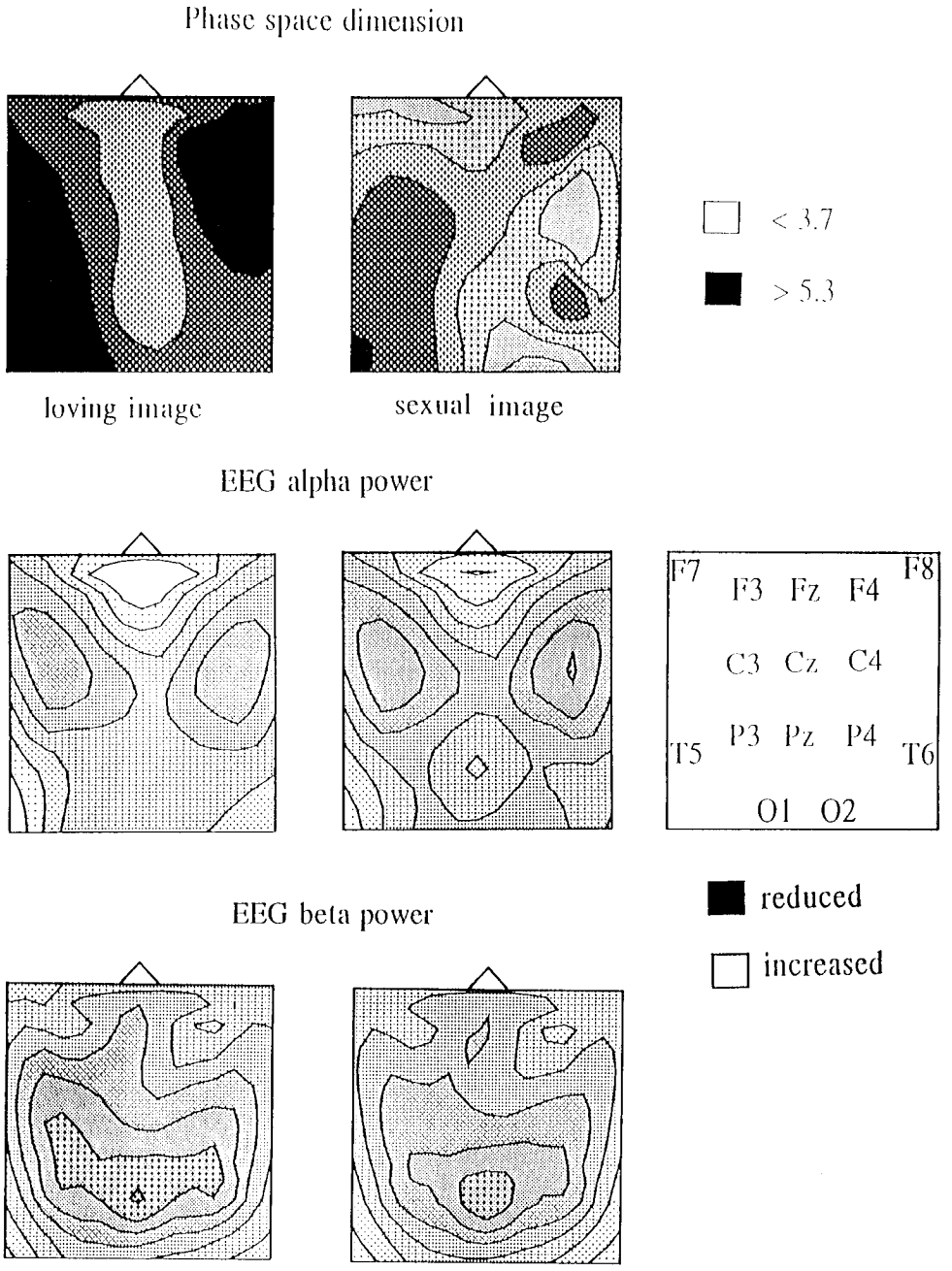

FIG. 13. Brain maps for electroencephalogram (EEG) dimension as well as α- and β-power averaged across 10 subjects. Subjects were asked to imagine and experience an extremely positive time in their past in which they had felt "in love" (*left column*) and to imagine the same type of positive experience which included a sexual experience (*right column*). While maps of α- and β-power do not discriminate 2 types of images, map for dimensional complexity and its mean value differs systematically for 9 of 10 subjects. [Data from Lutzenberger et al. (164).]

task defines the stimulus-response requirements much more precisely and may therefore constitute a more preferable control condition. Although evidence is still preliminary, it seems possible that task performance increases dimensional complexity over those brain areas with little involvement in the task, but reduces the dimensional complexity in those areas in which networks become actively engaged.

One potentially important application of nonlinear measures is in documenting specific states of consciousness such as sleep stages, coma, or hypnosis. For example, Gallez and Babloyantz (83) measured Lyapunov exponents and metric entropy during sleep (stage IV), Creutzfeld-Jakob coma, and an eyes-closed α-condition. Although basically a demonstration study using a single electrode site with a single individual, this study suggests that the dynamical measures used are highest in the α-state, suggesting a more complex system than is present during sleep. Röschke and Aldenhoff (229) extended this work with the first group study ($n \geq 10$) of nonlinear dynamics during sleep. In this study, EEGs were recorded during sleep from 12 young adults. These researchers reported greater differences in dimension between light sleep (stage II) and slow-wave sleep (stage IV). What is impressive is the consistency of results found between subjects. All 12 subjects showed a drop in dimensionality as sleep progressed from stage II to stage III. Likewise, there was a smaller, but statistically significant, drop in dimensionality between stages III and IV. This drop was seen in 11 of the 12 subjects. Fur-

thermore, in every subject the correlation dimension was higher during rapid-eye-movement sleep than during stage IV sleep. More recently, Röschke et al. (234) estimated the largest Lyapunov exponent in sleep EEG, showing its decrement with deepening of slow-wave sleep (stages). However, it should be noted that Principe and Lo (210) point out a variety of difficulties estimating Lyapunov exponents from sleep data.

In terms of hypnosis, work from our lab examined 24 subjects who either easily hypnotized or not during an initial baselines and during an hypnotic induction (224). Differences in both frequency bands (e.g., 4–8 Hz θ) and dimensionality were found between the high and low hypnotic susceptible individuals. However, EEG samples taken at five equal intervals as individuals passed through an hypnotic induction demonstrated changes in EEG frequency bands, especially in the more posterior areas of the brain, as the induction progressed, but showed no differences in dimensionality estimates. In other work, we then asked if individuals prone to dissociative experiences (221), which can range from normal experiences (e.g., absent mindedness) to more pathological processes, would show baseline and task differences in the EEG. Unlike the hypnosis study, there were no EEG differences in either fast Fourier transform frequency bands or estimates of dimensionality between the high and low dissociative subjects. Finally, irrespective of individual differences, overall task differences similar to those found in our previous report (164) were seen. Emotional imagery trials in comparison with mental math trials were characterized by significantly higher dimensional estimates in the more frontal areas (frontal/temporal) as compared with the more posterior ones (parietal/occipital). The entire cortex showed relatively similar dimensional values during the imagery tasks, whereas during the mental math tasks a lower dimensional level was seen in the frontal and temporal areas. These results (222), along with our previous work, build a consistent picture of relatively higher frontal dimensions during imagery and further support the idea that nonlinear dimensional analysis characterizes aspects of brain dynamics not seen in traditional spectral analysis.

As discussed in section II*F3*, there is an emerging trend to move research using chaos methods of analysis toward inferential statistical hypothesis testing. As pointed out by Theiler et al. (267), it is an easier task to reject the null hypothesis that a particular signal is linearly correlated noise than to determine the dimension of the signal. Pijn et al. (207) used a procedure based on an earlier paper of Theiler (264) to compare the EEG of the Wistar rat with that of a control signal. The control signal was computed in three steps: *1*) the actual EEG was Fourier transformed to give an amplitude and phase spectrum, *2*) the phase angle of each frequency component was replaced by a random number, and *3*) an inverse transform of the resulting signal was carried out to create the control signal. This procedure resulted in the actual EEG and the control signal having the same power spectrum. In our own work (164), we used as a control signal computer-generated random series which was filtered to give power spectra identical to the individual EEG traces. At this time there remain a number of technical issues as to the best type of control signal to utilize. Theiler et al. (267) suggest two separate algorithms for generating surrogate data, and this work should be consulted for detailed procedures.

D. Pathological Processes Investigated by Tools Derived From the Theory of Dynamic Systems

The genesis of focal epileptic seizures is often studied using a topical application of convulsants, e.g., penicillin, applied to various cortical structures, especially the hippocampus. Another method is to add a convulsant to the medium of in vitro slice preparations. In both cases, penicillin induces a discharge pattern in the neurons (e.g., CA3 pyramidal cells in the case of the hippocampus) which is quite similar to spontaneously occurring epileptic patterns. In the hippocampus, the structure responsible for this transition consists of a neural circuit of mossy fibers, CA3 pyramidal cells, and inhibitory basket cells. The recurrent inhibitory pathway between pyramidal cells and basket cells is mediated by the inhibitory transmitter γ-aminobutyric acid (GABA). Applying penicillin antagonizes the GABA receptors on the pyramidal cell membrane and weakens inhibition (the network excitability increases), which in turn results in epileptogenic behavior.

In good agreement with experimental data, the neural structure of recurrent inhibition in the hippocampus has been modeled by a neural network (e.g., Ref. 167) with one bifurcation parameter being the amount of convulsant applied. In the latter study, a transition was observed from regular low-frequency burstlike activity with different periodicities to irregular, possibly chaotic, sustained high-frequency firing. By enhancing the time delay as the bifurcation parameter, Kaczmarek and Babloyantz (137), using their early model of recurrent inhibition, found a sequence of qualitatively different dynamical behaviors leading from steady state to chaotic "epileptic" activity. Somewhat different was the study of Ermentrout and Cowan (59) who model tonic-clonic transitions by a bifurcation sequence resulting from an enhancement of the excitability of the neurons. The transition went from a steady state to a high-frequency mode (tonic phase) to a two-frequency mixed mode (transition) to a low-frequency mode (clonic phase). Rapp (216) presents two competitive explanations for the marked depolarization of the membrane potential with its bursts of action potentials induced by a convulsant. The first explanation is the network explanation as described previously with its drug-altered network transmission properties. The second explanation is the thesis of aberrant pacemaker epileptic neurons. These two processes can, in Rapp's view, act together in the clinical state. Rapp (216) further suggests that the epileptic seizure with its massive rhythmic depolarization is not itself a chaotic accident but an "automatic

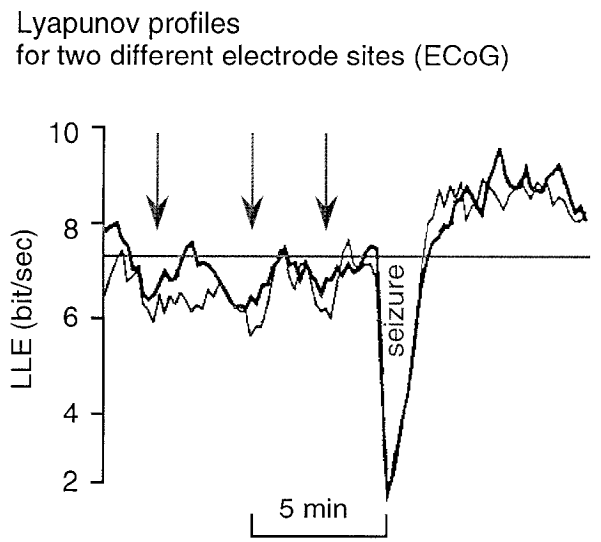

FIG. 14. Human brain not only undergoes a phase transition during an epileptic seizure, as suggested by work of Iasemidis and Sackellares (133), but temporal largest Lyapunov exponent (LLE) profiles indicate phase transitions minutes before seizure onset. Large drop in LLE, prominent at most electrode sites, indicates seizure. Significant reductions can be observed in electrocorticogram (ECoG), minutes before this event. Such attempts to undergo a phase transition are most prominent for electrodes overlying seizure focus (thin line). [Redrawn from Iasemidis and Sackellares (133).]

corrective mechanism that re-establishes neural co-ordination." We previously discussed (see sect. IV*B*) the work of Freeman and colleagues (70, 71, 73) concerning epileptic seizures in the olfactory bulb in which the actual seizure was compared with a mathematical model.

In the literature, there exist several dimension evaluations of epileptic patients during ictal and/or interictal periods as well as comparisons to those of normals. The first dimensional analysis of an epileptic patient undergoing a petit mal seizure was made by Babloyantz and Destexhe (12). Extremely coherent waves lasting 5 s and corresponding to ~18 spike-wave cycles were sampled with a high value of 1,200 Hz and yielded a striking low correlation dimension of only 2.05 ± 0.09. The greatest Lyapunov exponent (2.9 ± 0.6 bits/s) gave further evidence for chaotic behavior. Presumably, the seizure involves the entire cerebral cortex in that the two channels, frontal vs. parietal and vertex vs. temporal, showed equal results. Another study during a seizure (269) reports no significant change in the dimension value but an increase in the metric entropy compared with a normal subject.

Iasemidis and Sackellares and colleagues (133, 134, 237, 238) recorded the electrocorticogram from 16 subdural electrodes covering a relatively larger area over the right mesiotemporal focus of a patient and evaluated the Lyapunov exponent during preictal, ictal, and postictal epochs for three different seizures (an example is provided in Fig. 14). The onset of a seizure is characterized by an abrupt decrease in the exponent solely of the electrodes nearest the focus, so an identification of the epileptogenic focus by means of Lyapunov exponents is possible. As the seizure progresses, the Lyapunov exponent increases and, finally, in the cessation of the seizure, ends with an abrupt decrease in all electrodes. Even though the lowest values of the Lyapunov exponent occurred during the seizure, these were still positive, denoting the presence of a chaotic attractor. Additionally, the Lyapunov values were higher in the postictal state than in the preictal one. These authors (133, 134, 237, 238) conclude that the largest Lyapunov exponent can be useful for seizure detection and localization.

Pijn et al. (207) studied epileptic seizures in male Wistar rats. Using implanted electrodes, these researchers were able to study the seizures over the course of time as well as compare the same brain area under differential behavioral conditions (e.g., restful waking, exploratory locomotion, and seizure). The results showed that as different brain areas were recruited into the seizure activity, there was a corresponding switch in the correlation dimension of the EEG from a high to a low one, suggesting the emergence of chaotic attractors.

In the first step of evaluating the correlation dimension, a marked difference between interictal MEG recordings from four epileptic patients and α-MEG recordings from five normal subjects has been reported by Saermark et al. (239). Instead of the S-like shape in the log C(r) versus log r plot, the curves of epileptics show two inflection points separating three segments of different slopes (the middle part approaches a value of 1). A comparison of the dimension values between the two groups is difficult because different criteria were used to select the leads. The recording sites of the epileptics were chosen to show a clear prominence of 3–6 Hz, whereas the time series of normals come from the auditory cortex and show, at least in the reported case, a prominent α-spectrum. In a study by two of us (94), we could not detect any differences in the averaged pointwise dimension of the seizure-free EEG records from seven epileptic patients compared with two controls. However, for one person undergoing an absent seizure, a dimension reduction of about two was observed.

In the case of Creutzfeld-Jakob disease, the correlation dimension of one patient calculated from various leads shows a relatively wide range from 3.7 to 5.4 (14). This may indicate the coexistence of various attractors in the cortex or is simply due to artifacts. In any case, the dimension lies in between that found with the α-state (~6.1) and an epileptic seizure (~2.05).

It is well known that large doses of anesthetics reduce the EEG to a flat line (fixed point attractor with zero dimension), which suggests the possibility of assessing the depth of anesthesia during a surgical operation by means of the fractal dimension. Mayer-Kress, Layne, and co-workers (155, 180, 182) analyzed the EEG recorded from C_3-T_3, C_4-T_4, P_4-O_2, and P_3-O_1 of one person 5 min before and 10 min during the induction of fluroxene, but got a negative result. The correlation dimension was not sensitive to the depth of anesthesia. The first two locations showed no reaction to fluroxene at all; the second two locations surprisingly showed a

tendency to an increase in the first 5 min (light anesthesia), but remained constant in the following 5 min (medium anesthesia). However, it should be noted that the effects of fluroxene are somewhat different from that of traditional anesthesia. Watt and Hameroff (273, 274) also investigated the effect of anesthetics on the dimension of the EEG (C_3-P_3 lead, 1 person). The anesthetics used isoflurane and Fentanyl, followed by thiopental sodium, the latter one suppressing EEG bursts. The dimension values and embedding dimensions were very low (perhaps due to the short interval length of 4 s) with a slight decreasing tendency from 2.15 (awaking state) to 2.07 (isoflurane and Fentanyl) to 1.90 (thiopental sodium). In summary, the expected relation between the fractal dimension and the depth of anesthesia has not been supported by these preliminary findings.

In a group study, together with Brigitte Rockstroh and Rudolf Cohen (53), we examined the dynamical features of the spontaneous EEG in schizophrenic patients and control subjects under resting conditions. While controls showed about equal dimensional complexities over both central and frontal cortex, schizophrenic patients differed such that the fractal dimension was lower at frontal midline (F_z) than at the central midline (C_z). Two-thirds of the schizophrenic sample exhibited values outside the range of the control group, with one-half of the patients more than three standard deviations above the mean of controls. The observed frontocentral gradients in patients classified as suffering from schizophrenia suggest that the frontal and the central dynamics are dissociated even in the relaxed waking state, whereas a coupling occurs in the control sample. Therefore, we may conclude that the dynamics of the brain regions projecting to these recording sites are different for the two groups.

Using a 37-channel neuromagnetometer, Kowalik et al. (148) measured the spontaneous neuromagnetic activity (MEG) under resting conditions in subjects suffering from tinnitus (ringing in the ears) and normal controls. For all cases, the largest Lyapunov coefficient (LLE), reconstructed from MEG time series, turned out to be positive, a result that strongly supports the conjecture that brain dynamics bear chaotic features. Across channels, the LLE map (as illustrated in Fig. 15) was generally less uniform in the tinnitus sufferers than in controls. Furthermore, in the tinnitus group, LLE peaks tended to be higher than in control subjects. The authors (148) draw the conclusion that tinnitus emerges from a deficit in the regulation of local neuronal excitability in the temporal region. Whether or not such studies will enhance our understanding of cerebral disregulation remains a controversial issue; nevertheless, the work demonstrates the potential usefulness of mapping the LLE for diagnostic purposes.

E. Speculation Concerning Hebbian Cell Assemblies

Historically there have existed two views of the cerebral cortex. The first view divides the cortex into various subsystems and emphasizes the structural diversity of different areas and their short-range connections. The second view describes the brain as a single operating system by emphasizing statistical similarities between the density of synapses, dendrites, and the existence of long-range connectivity and plasticity. As is often the case, the solution to this problem seems to be dialectical in nature. There appears to be some truth to both views. Like an electron, appearing one time as a wave and another time behaving like a particle, we may observe the cortex depending on experimental conditions functioning as a whole system at one time, or separating into subsystems at another time. This hypothesis receives support from the previously cited data by Lutzenberger et al. (164). In this study, resting conditions or imagery of pleasant scenes yielded the same fractal dimensions at every electrode site, whereas specific sensory tasks produced distinct patterns with different fractal dimensions across the scalp, a finding that has been replicated by Ray et al. (222). When such differences are observed, we have reason to assume that the underlying dynamics must differ, thus arising from different systems at work, at least during the time of analysis. This example illustrates that the new methods of looking at brain dynamics might not only extract more information than was previously available, but eventually help us or even force us to create new ideas of brain functioning. However, techniques specifically tailored to study dynamics in neuronal mass action need also to be developed. We conclude this section by presenting some speculation concerning the relationship between nonlinear dynamics and Hebbian cell assemblies.

One major problem in the interpretation of EEG/MEG findings has been the lack of a coherent theoretical approach within which to articulate and test the results from experimental studies. At this time we would like to suggest one such approach that could serve as a working hypothesis for future research. This approach is based on our understanding of how Hebbian cell assemblies are sculptured within a highly interconnected neuropil by the forces of stimulus-evoked activity, forces which include chemical release, synaptic enhancement, and the competition of previously formed cell assemblies.

In the course of this paper we have presented different examples ranging from single-cell firing to complex sleep-waking cycles that all follow deterministic chaotic rules. We believe that some of these applications open a new refreshing view on some well-known, but badly understood, physiological mechanisms. Most of our attention was devoted to the complex behavior of larger interconnected cell masses of the brain and their electrical activity for which nonlinear analysis shows promise. Because most of the work presumes complex neuronal networks functioning according to a connectionistic theory of brain activity, we briefly introduce this view. The connectionistic viewpoint also allows us to understand more clearly the parallel existence of, a continuum of, fully deterministic chaotic activity in the

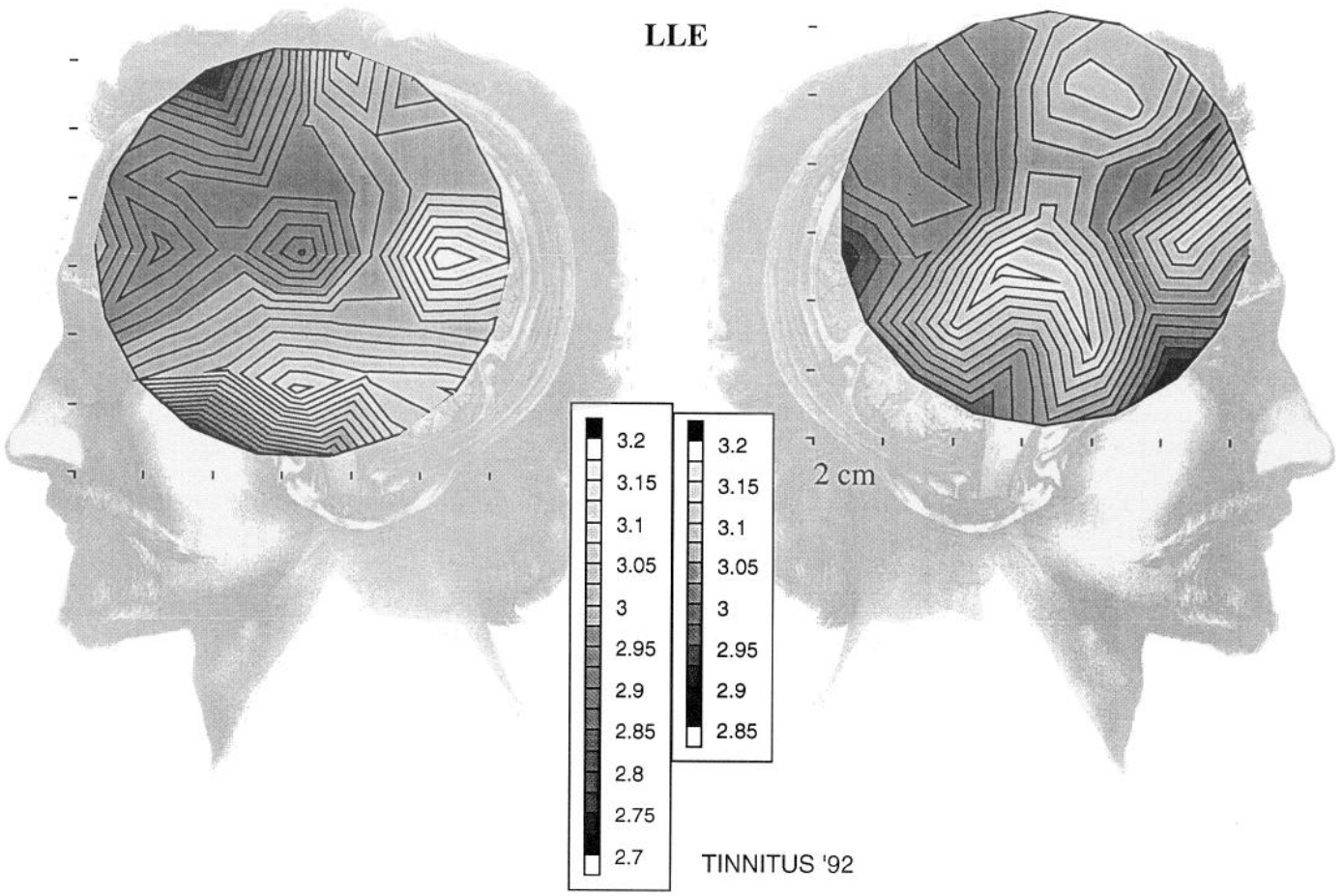

FIG. 15. Brain maps for largest Lyapunov exponents (LLE) for 1 subject. MEG was measured over both temporal regions, and LLE was estimated using a modified algorithm (148) as proposed in Reference 277. For every MEG time segment, change of LLE with number of iterations was estimated. If this value converges, mean across last 20% of iterations was assumed to correspond to LLE. Dark regions refer to valleys; lighter ones describe elevations in LLE. Maximal changes of amplitude on measured surface are in range of ~30%. For all cases, LLE turned out to be positive, a result that strongly supports conjecture that brain dynamics bear chaotic features if we assume that regulation of brain activity is deterministic in nature. [Adapted from Kowalik et al. (148).]

neocortex (49–51, 55, 54). In an earlier paper in this journal (27) we explained some of these interactions.

Let us now consider the competition between neuronal cell assemblies (NCA). The concept of cell assemblies (28, 121) has become fundamental to models concerned with the functioning of the brain, even though many neuroscientists were initially reluctant to accept this position. Hebb in 1949 (121) postulated that short-term memory is represented in reverberatory circuits, as described by Lorente de No in 1943 (160a). Once activated, these circuits can maintain excitation, since they are formed by a set of highly interconnected neurons, each of which receives excitation from, and gives excitation to, other members of the same set. If a sufficiently large number of neurons in one such cell assembly is activated, then the whole set will become active and produce the function for which it has been sculpted, which includes bringing up stored information and outputs to use it.

A key concept related to memory storage is that the structure of these cell assemblies is flexible and can be changed rapidly to update the context of the stored information. This requires the continued strengthening of connections between simultaneously active neurons (Hebb's rule), an assumption which has long been considered the physiological basis for the acquisition of learning and storage of memory. It is thought that increasing the level of postsynaptic activity within neural networks will, in turn, increase the ability of simultaneously active synapses to depolarize the postsynaptic membrane, while insufficient activation is seen to weaken them. Hebbian models of memory were suggested by quite a number of theorists including Palm (199) and more recently Brown et al. (31). The synapses in the assemblies can be upregulated and downregulated by both homosynaptic and heterosynaptic events and by a variety of chemical reactions. Bailey and Kandel (18a) have suggested that the long-term information storage mechanism may involve the modulation of genetic material (i.e., gene expression) to manufacture within the cell a protein that perpetuates or fixes the specific synaptic gain of a particular synapse in the cell.

Probably all of the synapses on dendritic spines are subject to both short-term and long-term modification in their relative gains, a finding which suggests that three of four cortical synapses are plastic (29). The buildup and strengthening of a cell assembly requires that a large portion of synapses in the neuropil that are not relevant for the incoming information event be shut off, otherwise connections would form too randomly. This means that the excitability of the neuropil must somehow be reduced for a fraction of a second or so before a relevant event can be stored (50, 51, 54).

Let us now review the consequences of such a Hebbian view for the interpretation of brain activity, especially that which can be recorded noninvasively as event-related responses and also observed in its behavioral consequences. *1*) The development of cell assemblies depends on plastic ("Hebbian") excitatory cell systems with a rapid rise time for their construction. The system ideally suited for this purpose is the apical pyramidal dendritic trees of the upper neocortical layer.

2) A cell assembly includes sometimes widespread cortical neurons including sensory, cognitive (meaning), and motor functions. Any restrictive separation into highly specialized "modules," as is fashionable in present day neuropsychology, is obsolete; vis-á-vis the fact that every sufficiently large pool of neurons of the cortex is connected to every other neuronal pool, forming the anatomic basis of our illusion of a unified consciousness. The meaning and qualitative nature of an event, an idea, an emotion, or a percept is reflected in the local topography of its connections and firing patterns, so to speak in the topographical "Gestalt" of an assembly in its phase space, not in the properties of its parts, the cells, or its transmitters.

3) This specificity of an assembly is best reflected in the spatial distribution and frequency of fast-changing electrical activities, such as the EEG and event-related components. It has to be fast because assemblies must have the ability to ignite explosively as a whole; a whisper can turn on a full-blown paranoid delusion within a fraction of a second, including all, or nearly all, sensory, motor, and meaning aspects of that delusion.

4) Cell assemblies, and therefore the EEG and event-related or evoked potentials, should have properties of deterministic chaos. They cannot be totally random, since it would be impossible to create new ideas and percepts if assemblies did not generate novel activity patterns within the fraction of a thought. Freeman and Skarda (77, 248) have shown that in the olfactory system of the rabbit chaos becomes more prevalent when there is competition between parts of assemblies, or between several assemblies. We believe that we have hints for a similar mechanism for cognitive processes in the human neocortex (see below).

With increasing competition between different networks in different cortical localizations, the phase space in which a corresponding biological activity of the neurons varies becomes multidimensional. In new situations with multimodel memory demands, the dimensionality (complexity) of the neuronal process should be higher.

5) Whether a given assembly will be ignited and the "contrasts" between assemblies (their foreground-background Gestalt) depends on the threshold of an assembly. Usually assemblies are excited by external or internal stimuli. More frequently, they are primed by conditioned stimuli occurring before a stimulus that ultimately ignites the assembly. In addition to externally controlled threshold regulation, cell assemblies have their own automatic threshold control to, as Braitenberg and Schüz poetically state "discover and isolate ideas..." and to reinforce ideas "and keep them separately" (Ref. 29, p.205). Another main function of automatic threshold control is to prevent the transition from an "Einfall" to an "Anfall" (Ref. 29; transition from an idea to a seizure) in an excitatory neuronal network. Inherent to threshold control is its nonlinear transformation of information. Therefore, we ought to apply principles from nonlinear systems theory (deterministic chaos) to understand the dynamic patterns of threshold regulation.

The chaotic activity has to be deterministic and nonrandom, because living biological systems can only function if held within certain activity limits through feedback of the ongoing activity. On the other hand, nonlinear changes in the state of neuronal cell assemblies is a prerequisite of any living system to generate new sensory-motor patterns that control the environment in a dynamic ever-changing way, which are dependent on slightly different initial conditions and consequences.

As Skarda and Freeman (248) have put it, chaos provides the NCAs with a "deterministic 'I don't know'." Without it, the patterned activity would always return to old, already formed NCAs leading to exhausting repetition. However, it seems as if any group of NCAs can be pressed into limited cycle deterministic activity for a certain time period by highly structured external or internal variations. Some pathological conditions, and repetitive behavior without competitive activity, may fall into this category. Their detection remains an important challenge.

V. SUMMARY

In this review we examined the emerging science of deterministic chaos (nonlinear systems theory) and its application to selected physiological systems. Although many of the popular images of fractals represent fascination and beauty that by analogy corresponds to nature as we see it, the question remains as to its ultimate meaning for physiological processes. It was our intent to help clarify this somewhat popular, somewhat obscure area of nonlinear dynamics in the context of an ever-changing procedural base. We examined not only the basic concepts of chaos, but also its applications ranging from observations in single cells to the complexity of the

EEG. We have not suggested that nonlinear dynamics will answer all of our questions; however, we did attempt to illustrate ways in which this approach may help us to answer new questions and to rearticulate old ones. Chaos is revolutionary in that the overall approach requires us to adopt a different frame of reference which, at times, may move us away from previous concerns and methods of data analysis.

In sections I–IV, we summarized the nonlinear dynamics approach and described its application to physiology and neural systems. First, we presented a general overview of the application of nonlinear dynamical techniques to neural systems. We discussed the manner in which even apparently simple deterministic systems can behave in an unpredictable manner. Second, we described the principles of nonlinear dynamical systems including the derived analytical techniques. We now see a variety of procedures for delineating whether frenetic chaotic behavior results from a nonlinear dynamical system with a few degrees of freedom, or whether it is caused by an infinite number of variables, i.e., noise. Third, we approached the applications of nonlinear procedures to the cardiovascular systems and to the neurosciences.

In terms of time series, we described initial studies which applied the now "traditional" measures of dimensionality (e.g., based on the algorithm by Grassberger and Procaccia) and information change (e.g., Lyapunov exponents). Examples include our own work (53, 148) and that of Pritchard et al. (214), demonstrating that the dynamics of neural mass activity reflect psychopathological states. Today, however, the trend has expanded to include the use of surrogate data and statistical null hypotheses testing to examine whether a given time series can be considered different from that of white or colored noise (cf. Ref. 262).

One of the most important potential applications is that of quantifying changes in nonlinear dynamics to predict future states of the system. For example, Iasemidis and co-workers (133, 134) have reported characteristic alterations in the electrocorticogram before an epileptic seizure. In terms of cardiovascular processes, Skinner et al. (252) suggest that nonlinear dynamics can be used as a basis for future biomedical tests to signal various cardiovascular insults such as a heart failure. If such promises hold, they will have tremendous implications for the understanding of both neurological and cardiovascular pathologies.

We thank Prof. Dr. Manfried Hoke, Prof. Dr. Werner Lutzenberger, Dr. Walter S. Pritchard, Prof. Dr. Brigitte Rockstroh, Prof. Otto E. Rössler, Prof. Robert Wells, and an anonymous reviewer for stimulating discussions and extensive comments on earlier versions of this manuscript.

This work was partially support by the Deutsche Forschungsgemeinschaft Grants SFB 301/B1 (to N. Birbaumer) and Ho 847/6-4 (to M. Hoke and T. Elbert), by a North Atlantic Treaty Organization Collaborative Research Grant (to W. J. Ray and T. Elbert), and by a National Aeronautics and Space Administration grant (to W. J. Ray).

REFERENCES

1. AIHARA, K., AND G. MATSUMOTO. Temporally coherent organization and instabilities in squid giant axons. *J. Theor. Biol.* 95: 697–720, 1982.
2. AIHARA, K., AND G. MATSUMOTO. Chaotic oscillations and bifurcations in squid giant axons. In: *Chaos. Nonlinear Science: Theory and Applications*, edited by A. V. Holden. Manchester, UK: Manchester Univ. Press, 1986, p. 257–269.
3. AIHARA, K., AND G. MATSUMOTO. Forced oscillations and routes to chaos in the Hodgkin-Huxley axons and squid giant axons. In: *Chaos in Biological Systems*, edited by H. Degn, A. Holden, and L. F. Olsen. New York: Plenum, 1987, p. 121–131.
4. AIHARA, K., G. MATSUMOTO, AND M. ICHIWAKA. An alternating periodic-chaotic sequence observed in neural oscillators. *Phys. Lett.* 111: 251–255, 1985.
5. AIHARA, K., G. MATSUMOTO, AND Y. IKEGAYA. Periodic and non-periodic responses of a periodically forced Hodgkin-Huxley oscillator. *J. Theor. Biol.* 109: 249–270, 1984.
6. AIHARA, K., T. NUMAJIRI, G. MATSUMOTO, AND M. KOTANI. Structures of attractors in periodically forced neural oscillations. *Phys. Lett.* 7: 313–317, 1986.
7. AKAMATSU, N., B. HANNAFORD, AND L. STARK. An intrinsic mechanism for the oscillatory contraction of muscle. *Biol. Cybern.* 53: 219–227, 1986.
8. ALBANO, A. M., N. B. ABRAHAM, G. C. DE GUZMAN, M. F. H. TARROJA, D. K. BANDY, R. S. GIOGGIA, P. E. RAPP, I. D. ZIMMERMANN, N. N. GREENBAUM, AND T. R. BASHORE. Lasers and brains: complex systems with low-dimensional attractors. In: *Dimension and Entropies in Chaotic Systems*, edited by G. Mayer-Kress. Berlin: Springer, 1986, p. 231–252.
9. ALBANO, A. M., A. I. MEES, G. C. DE GUYMAN, AND P. E. RAPP. Data requirements for reliable estimation of correlation dimension. In: *Chaos in Biological Systems*, edited by H. Degn, A. V. Holden, and L. F. Olsen. New York: Plenum, 1987, p. 207–220.
10. AN DER HEIDEN, U. Dynamische Krankheiten—Konzept und Beispiele. *Verhaltens Modifikation und Verhaltensmedizin* 14: 51–65, 1993.
11. BABLOYANTZ, A. Strange attractors in the dynamics of brain activity. In: *Complex Systems—Operational Approaches in Neurobiology, Physics and Computers*, edited by H. Haken. Berlin: Springer, 1985, p. 116–122.
12. BABLOYANTZ, A., AND A. DESTEXHE. Low dimensional chaos in an instance of epilepsy. *Proc. Natl. Acad. Sci. USA* 83: 3513–3517, 1986.
13. BABLOYANTZ, A., AND A. DESTEXHE. Strange attractors in the human cortex. In: *Temporal Disorder in Human Oscillatory Systems*, edited by L. Rensing, U. an der Heiden, and M. C. Mackey. Berlin: Springer, 1987, p. 48–56.
14. BABLOYANTZ, A., AND A. DESTEXHE. The Creutzfeld-Jakob disease in the hierarchy of chaotic attractors. In: *From Chemical to Biological Organization*, edited by M. Marcus, S. M. Äller, and G. Nicolis. Berlin: Springer, 1988, p. 307–316.
15. BABLOYANTZ, A., AND A. DESTEXHE. Is the normal heart a periodic oscillator? *Biol. Cybern.* 58: 203–211, 1988.
16. BABLOYANTZ, A., J. M. SALAZAR, AND C. NICOLIS. Evidence of chaotic dynamics of brain activity during the sleep cycle. *Phys. Lett.* 3: 152–156, 1985.
17. BADII, R. Generalized thermodynamic ensembles for fractal measures. *Il Nuovo Cimento* 10: 819–840, 1988.
18. BADII, R., AND A. POLITI. Rényi dimensions from local expansion rates. *Phys. Rev.* 35: 1288–1293, 1987.
18a. BAILEY, C., AND E. KANDEL. Structural changes accompanying memory storage. *Annu. Rev. Physiol.* 53: 397–426, 1993.
19. BAIRD, B. Nonlinear dynamics of pattern formation and pattern recognition in the rabbit olfactory bulb. *Physica* 22: 150–175, 1986.
20. BAKER, G., AND J. GOLLUB. *Chaotic Dynamics*. Cambridge, UK: Cambridge Univ. Press, 1990.
21. BALATONI, J., AND A. RÉNYI. *Selected papers of A. Rényi. 1956*. Budapest: Academiai Budapest, 1976.

22. BAŞAR, E., C. BAŞAR-EROGLU, J. RÖSCHKE, AND J. SCHULT. Chaos and alpha-preparation in brain function. In: *Models of Brain Function*, edited by R. M. J. Corterill. Cambridge, UK: Cambridge Univ. Press, 1989, p. 365–395.
23. BENETTIN, G., L. GALGANI, AND J. M. STRELCYN. Kolmogorov entropy and numerical experiments. *Phys. Rev.* 14: 2338–2345, 1976.
24. BIGGER, J. T., R. E. KLEIGER, J. L. FLEISS, L. M. ROLNITZKY, R. C. STEINMAN, J. P. MILLER, AND M. P.-I. R. GROUP. Components of heart rate variability measured during healing of acute myocardial infarction. *Am. J. Cardiol.* 61: 208–215, 1988.
25. BIGGER, J. T., JR., M. T. LAROVERE, R. C. STEINMAN, J. L. FLEISS, J. N. ROTTMAN, L. M. ROLNITZKY, AND P. J. SCHWARTZ. Comparison of baroreflex sensitivity and heart period variability after myocardial infarction. *J. Am. Coll. Cardiol.* 14: 1511–1518, 1989.
26. BILLMAN, G. E., P. J. SCHWARTZ, AND H. L. STONE. Baroreceptor reflex control of heart rate: a predictor of sudden cardiac death. *Circulation* 66: 874–880, 1982.
27. BIRBAUMER, N., T. ELBERT, A. CANAVAN, AND B. ROCKSTROH. Slow potentials of the cerebral cortex and behavior. *Physiol. Rev.* 70: 1–41, 1990.
28. BRAITENBERG, V. Cell assemblies in the cerebral cortex. In: *Theoretical Approach to Complex Systems*, edited by R. Heim and G. Palm. Berlin: Springer, 1978.
29. BRAITENBERG, V., AND A. SCHÜZ. *Anatomy of the Cortex.* Heidelberg: Springer, 1991.
30. BROOMHEAD, D. S., and G. P. King. Extracting qualitative dynamics from experimental data. *Physica* 20: 217–236, 1986.
31. BROWN, T. H., E. W. KAIRISS, AND C. L. KEENAN. Hebbian synapses: biophysical mechanisms and algorithms. *Annu. Rev. Neurosci.* 13: 475–511, 1990.
32. CAPUTO, I. G., B. MALRAISON, AND P. ATTEN. Determination of attractor dimension and entropy for various flows. In: *An Experimentalist's Viewpoint: Dimension and Entropies in Chaotic Systems*, edited by G. Mayer-Kress. Heidelberg: Springer, 1986, p. 180–190.
33. CARPENTER, G. A. Bursting phenomena in excitable membranes. SIAM. *J. Appl. Math.* 36: 334–372, 1979.
34. CARPENTER, G. A. Normal and abnormal signal patterns in nerve cells. In: *Mathematical Psychology and Psychophysiology*, edited by S. Grossberg. Providence, RI: Am. Math. Soc., 1981, p. 49–90.
35. CHAY, T. R. Abnormal discharges and chaos in a neuronal model system. *Biol. Cybern.* 50: 301–311, 1984.
36. CHAY, T. R. Chaos in a three-variable model of an excitable cell. *Physica* 16: 233–242, 1985.
37. CHIALVO, D. R., AND J. JALIFE. Non-linear dynamics of cardiac excitation and impulse propagation. *Nature Lond.* 330: 749–752, 1987.
38. CHIALVO, D. R., D. C. MICHAELS, AND J. JALIFE. Analysis of chaotic dynamics of excitation and propagation in non-pacemaker cardiac tissues (Abstract). In: *Proc. Annu. Meet. Biophys. Soc. 32nd Phoenix AZ 1988*, p. 158.
39. CONTE, R., AND M. DUBOIS. Lyapunov exponents of experimental systems. In: *Workshop on Nonlinear Evolution Equations and Dynamical Systems Nonlinear Evolutions.* Singapore: World Scientific, 1988, p. 767–780.
40. COURTEMANCHE, M., L. GLASS, M. D. ROSENGARTEN, AND A. L. GOLDBERGER. Beyond pure parasystole: promises and problems in modeling complex arrhythmias. *Am. J. Physiol.* 257 (*Heart Circ. Physiol.* 26): H693–H706, 1989.
41. DENTON, T. A., G. A. DIAMOND, R. H. HELFANT, S. KHAN, AND H. KARAGUEUZIAN. Fascinating rhythm—a primer on chaos theory and its application to cardiology. *Am. Heart J.* 120: 1419–1440, 1990.
42. DENTON, T. A., H. S. KARAGUEUSIAN, AND G. S. DIAMOND. Adequacy and limitations of a non-linear computer model of ventricular myocardial cell membrane. In: *Proc. Natl. Meet. Am. Fed. Clin. Res. 37th Washington DC 1989*, p. 254.
43. DESTEXHE, A., J. H. SEPULCHRE, AND A. BABLOYANTZ. A comparative study of the experimental quantification of deterministic chaos. *Phys. Lett. Appl. Microbiol.* 132: 101–106, 1988.
43a. DVORAK, I., AND A. V. HOLDEN. *Mathematical Approaches to Brain Functioning Diagnostics.* Manchester, UK: Manchester Univ. Press, 1991.
44. DVORAK, I., J. SISKA, J. WACKERMANN, L. HRUDOVA, AND C. DOSTALEK. Evidence for interpretation of the EEG as a deterministic chaotic process with low dimension. *Activ. Nerv. Sup.* 28: 228–231, 1986.
45. DWORKIN, B. Operant mechanisms in physiological regulation. In: *Self-Regulation of the Brain and Behavior*, edited by T. Elbert, B. Rockstroh, W. Lutzenberger, and N. Birbaumer. Heidelberg, Germany: Springer-Verlag, 1984, p. 296–310.
46. ECKMANN, J. P., S. O. KAMPHORST, D. RUELLE, AND S. CILIBERTO. Lyapunov exponents from time series. *Phys. Rev.* 34: 4971–4979, 1986.
47. ECKMANN, J. P., AND D. RUELLE. Ergodic theory of chaos and strange attractors. *Rev. Mod. Phys.* 1: 617–655, 1985.
48. EISENBERG, J., W. J. FREEMAN, AND B. BURKE. Hardware architecture of a neural network model simulating pattern recognition by the olfactory bulb. *Neural Networks* 2: 315–325, 1989.
49. ELBERT, T. Regulation corticaler Erregbarkeit. Im EEG ein deterministisches Chaos? In: *Zugang zum Verständnis höherer Hirnfunktionen durch das EEG*, edited by H. M. Weinmann. Munich: Zuckschwerdt Verlag, 1987, p. 93–107.
50. ELBERT, T. Slow cortical potentials reflect the regulation of cortical excitability. In: *Slow Potential Changes in the Human Brain*, edited by W. C. McCallum and S. H. Curry. London: Plenum, 1992.
51. ELBERT, T. A theoretical approach to the late components of the event-related brain potential. In: *Proceedings of the Ringberg Meeting on Brain Theory.* Heidelberg, Germany: Springer-Verlag, 1992.
52. ELBERT, T., J. HOMMEL, AND L. W. LUTZENBERGER. The perception of the Necker cube reversion interacts with the Bereitschaftspotential. *Int. J. Psychophysiol.* 3: 5–12, 1985.
53. ELBERT, T., W. LUTZENBERGER, B. ROCKSTROH, P. BERG, AND R. COHEN. Physical aspects of the EEG in schizophrenics. *Biol. Psychiatr.* 32: 181–193, 1992.
54. ELBERT, T., AND B. ROCKSTROH. Threshold regulation—a key to the understanding of the combined dynamics of EEG and event-related potentials. *J. Psychophysiol.* 4: 317–333, 1987.
55. ELBERT, T., AND B. ROCKSTROH. Das chaotische Gehirn zur Erfassung nichtlinearer Dynamik aus physiologischen Zeitreihen. *Z. Verhaltensmodifikation Verhaltensmedizin* 14: 80–95, 1993.
56. ELBERT, T., B. ROCKSTROH, M. HOKE, AND Z. J. KOWALIK. Anwendung von Verfahren der nichtlinearen Systemtheorie zur differenzierenden Charakterisierung der Gehirnaktivität bei psychopathologischen und neurologischen Störungen. *DFG Report* 1993.
57. ELBERT, T., B. ROCKSTROH, Z. J. KOWALIK, J. E. SKINNER, M. MOLNAR, AND N. BIRBAUMER. Chaotic brain activity. *J. Electroencephalogr. Clin. Neurophysiol. Suppl.* In press.
58. ELLNER, S. Estimating attractor dimensions from limited data: a new method, with error estimates. *Phys. Lett.* 133: 128–133, 1988.
59. ERMENTROUT, G. B., AND J. D. COWAN. Secondary bifurcation in neuronal nets. SIAM. *J. Appl. Math.* 39: 323–340, 1980.
60. EVERSON, R. M. Quantification of chaos from periodically forced squid axons. In: *Chaos in Biological Systems*, edited by H. Degn, A. Holden, and L. F. Olsen. New York: Plenum, 1987, p. 133–142.
61. FARMER, J. D. Chaotic attractors of an infinite-dimensional dynamical system. *Physica* 4: 366–393, 1982.
62. FARMER, J. D. Information dimension and the probabilistic structure of chaos. *Z. Naturforsch.* 37: 1304–1325, 1982.
63. FARMER, J. D., E. OTT, AND J. A. YORKE. The dimension of chaotic attractors. *Physica* 7: 153–180, 1983.
64. FEIGENBAUM, M. J. The universal metric porperties of nonlinear transformations. *J. Stat. Phys.* 21: 670–706, 1979.
65. FRANASZEK, M., AND Z. J. KOWALIK. Measurement of the dimension of the strange attractor for the Fermi-Ulam problem. *Phys. Rev.* 33: 3508–3510, 1986.

66. FREEMAN, W. J. EEG analysis gives model of neuronal template-matching mechanism for sensory search with olfactory bulb. *Biol. Cybern.* 35: 221–234, 1979.
67. FREEMAN, W. J. Dynamics of image formation by nerve cell assemblies. In: *Synergetics of the Brain*, edited by E. Başar, H. Flohr, H. Haken, and A. J. Mandell. Berlin: Springer, 1983, p. 102–121.
68. FREEMAN, W. J. The physiological basis of mental images. *Biol. Psychiatr* 18: 1107–1125, 1983.
69. FREEMAN, W. J. How the olfactory system generates its chaotic background spontaneous electroencephalographic and unit activity. In: *Olfaction and Taste IX: Ninth Interntional Symposium.* New York: NY Acad. Sci., 1986.
70. FREEMAN, W. J. Petit mal seizure spikes in olfactory bulb and cortex caused by runaway inhibition after exhaustion of excitation. *Brain Res. Rev.* 396: 259–284, 1986.
71. FREEMAN, W. J. Simulation of chaotic EEG patterns with a dynamic model of the olfactory system. *Biol. Cybern.* 56: 139–150, 1987.
72. FREEMAN, W. J. Techniques used in the search for the physiological basis for the EEG. In: *Handbook of Electroencephalography and Clinical Neurophysiology*, edited by A. S. Gevins and A. R. Remond. Amsterdam: Elsevier, 1987, p. 583–664.
73. FREEMAN, W. J. Strange attractors that govern mammalian brain dynamics shown by trajectories of electroencephalography (EEG) potentials. *IEEE Trans. CAS* 35: 781–784, 1988.
74. FREEMAN, W. J. Analysis of strange attractors in EEGs with kinesthetic experience and 4-D computer graphics. In: *Brain Dynamics. Progress and Perspectives*, edited by E. Başar and T. H. Bullock. Heidelberg: Springer, 1989, p. 512–520.
75. FREEMAN, W. J. Perceptual processing using oscillatory chaotic dynamics. In: *Proc. Annu. Int. Conf. IEEE Eng. Med. Biol. Soc. 11th Seattle WA 1989*, p. 2.
76. FREEMAN, W. J. On the problem of anomalous dispersion in chaoto-chaotic phase transitions of neural masses, and its significance for the management of perceptual information in brains. In: *Synergetics of Cognition*, edited by H. Haken and M. Stadler. Berlin: Springer, 1990, p. 126–142.
77. FREEMAN, W. J. The physiology of perception. *Sci. Am.* 264: 78–85, 1991.
78. FREEMAN, W. J., AND V. DIPRISCO. EEG spatial pattern differences with discriminated odors manifest chaotic and limit cycle attractors in olfactory bulb of rabbits. In: *Brain Theory*, edited by G. Palm and A. Aertsen. Berlin: Springer, 1986, p. 97–119.
79. FREEMAN, W. J., J. EISENBERG, AND B. BURKE. Hardware simulation of brain dynamics in learning. In: *Spook Proc. IEEE Annu. Int. Conf. Neural Networks 1st San Diego CA 1987*, p. 435–442.
80. FREEMAN, W. J., AND C. A. SKARDA. A perspective on brain theory: nonlinear dynamics of neural masses. *Brain Res. Rev.* 10: 147–175, 1985.
81. FREEMAN, W. J., AND C. A. SKARDA. Spatial EEG patterns, non-linear dynamics and perception: the neo-Sherringtonian view. *Brain Res. Rev.* 357: 147–175, 1985.
82. FREEMAN, W. J., Y. YAO, AND B. BURKE. Central pattern generating and recognizing in olfactory bulb: a correlation learning rule neural. *Networks* 1: 277–288, 1988.
83. GALLEZ, D., AND A. Babloyantz. Predictability of human EEG: a dynamical approach. *Biol. Cybern.* 64: 381–391, 1991.
84. GILLIS, R. A., P. B. CORR, D. G. PACE, D. E. EVANS, J. DIMICCO, AND D. L. PEARLE. Role of the nervous system in experimentally induced arrhythmias. *Cardiology* 61: 37–49, 1976.
85. GLASS, L., A. L. GOLDBERGER, AND J. BELAIR. Dynamics of pure parasystole. *Am. J. Physiol.* 251 (*Heart Circ. Physiol.* 20): H841–H847, 1986.
86. GLASS, L., A. L. GOLDBERGER, M. COURTEMANCHE, AND A. SHRIER. Nonlinear dynamics, chaos and complex cardiac arrhythmias. *Proc. R. Soc. Lond.* 413: 9–26, 1987.
87. GLASS, L., M. GUEVARA, A. SHRIER, AND R. PEREZ. Bifuraction and chaos in a periodically stimulated cardiac oscillator. *Physica* 7: 89–101, 1983.
88. GLASS, L., M. R. GUEVARA, J. BELAIR, AND A. SHRIER. Global bifurcations of a periodically forced biological oscillator. *Phys. Rev. A* 29: 1348–1357, 1984.
89. GLASS, L., M. R. GUEVARA, AND A. SHRIER. Universal bifurcations and the classification of cardiac arrhythmias. *Ann. NY Acad. Sci.* 584: 168–178, 1987.
90. GLASS, L., AND M. C. MACKEY. Pathological conditions resulting from instabilities in physiological control systems. In: *Bifurcation Theory and Applications in Scientific Disciplines*, edited by O. Gurel and O. E. Rössler. New York: NY Acad. Sci., 1979, p. 214–235.
91. GLASS, L., A. SHRIER, AND J. BELAIR. Chaotic cardiac rhythms. In: *Chaos—Nonlinear Science: Theory and Application*, edited by A. V. Holden. Manchester, UK: Manchester Univ. Press, 1986, p. 237–256.
92. GOLDBERGER, A., AND B. WEST. Chaos in physiology. In: *Chaos in Biological Systems*, edited by A. V. Holden, H. Degn, and L. F. Olsen. New York: Plenum, 1987, p. 1–5.
93. GOLDBERGER, A. L., D. R. RIGNEY, AND B. J. WEST. Chaos and fractals in human physiology. *Sci. Am.* 262: 42–49, 1990.
94. GRAF, K. E., AND T. ELBERT. Dimensional analysis of the waking EEG. In: *Brain Dynamics. Progress and Perspectives*, edited by E. Başar and T. H. Bullock. Heidelberg, Germany: Springer, 1989, p. 174–191.
95. GRASSBERGER, P. Generalized dimensions of strange attractors. *Phys. Lett.* 97: 227–229, 1983.
96. GRASSBERGER, P., R. BADII, AND A. POLITI. Scaling laws for invariant measures on hyperbolic and nonhyperbolic attractors. *J. Stat. Phys.* 51: 135–178, 1988.
97. GRASSBERGER, P., AND I. PROCACCIA. Characterization of strange attractors. *Phys. Rev. Lett.* 50: 346–349, 1983.
98. GRASSBERGER, P., AND I. PROCACCIA. Estimation of the Kolmogorov entropy from a chaotic signal. *Phys. Rev.* 28: 2591–2593, 1983.
99. GRASSBERGER, P., AND I. PROCACCIA. Measuring the strangeness of strange attractors. *Physica* 9: 189–208, 1983.
100. GRASSBERGER, P., AND I. Procaccia. Dimensions and entropies of strange attractors from a fluctuation dynamics approach. *Physica* 13: 34–54, 1984.
101. GRAY, C. M., W. J. FREEMAN, AND J. E. SKINNER. Chemical dependencies of learning in the rabbit olfactory bulb: acquisition of the transient spatial-pattern change depends on norepinephrine. *Behav. Neurosci.* 100: 585–596, 1986.
102. GRAY, C. M., W. J. FREEMAN, AND J. E. SKINNER. Induction and maintenance of epileptiform activity in the rabbit olfactory bulb depends on centrifugal input. *Exp. Brain Res.* 68: 210–212, 1987.
103. GREENE, J. M., AND J. S. KIM. The calculation of Lyaopunov spectra. *Physica* 24: 213–225, 1987.
104. GREENSIDE, H. S., A. WOLF, J. SWIFT, AND T. PIGNATORO. Impracticality of a box-counting algorithm for calculating the dimension of strange attractors. *Phys. Rev.* 25: 3453–3456, 1982.
105. GROSSBERG, S. *The Adaptive Brain.* Amsterdam: Elsevier, 1987, vol. I, II.
106. GUCKENHEIMER, J. Dimension estimates for attractors. *Contemp. Math.* 28: 357–367, 1984.
107. GUEVARA, M. R., AND G. L. GLASS. Phase locking, periodic doubling bifuractions and chaos in a mathematical model of periodically driven oscillator: a theory for entrainment of biological oscillators and the generation of cardiac dysrhythmias. *J. Math. Biol.* 14: 1–23, 1982.
108. GUEVARA, M. R., G. L. GLASS, AND A. SHRIER. Phase locking, period doubling bifuractions, and irregular dynamics in periodically stimulated cardiac cells. *Science Wash. DC* 214: 1350–1353, 1981.
109. GUEVARA, M. R., AND A. SHRIER. Phase resetting in a model of cardiac Purkinje fiber. *Biophys. J.* 52: 165–175, 1987.
110. GUEVARA, M. R., A. SHRIER, AND L. GLASS. Phase-locked rhythms in periodically stimulated heart cell aggregates. *Am. J. Physiol.* 254 (*Heart Circ. Physiol.* 23): H1–H10, 1988.
111. HALSEY, T. C., M. H. JENSEN, L. P. KADANOFF, I. PROCACCIA, AND B. I. SHAIRMAN. Fractal measures and their singularities: the characterization of strange sets. *Phys. Rev.* 33: 1141–1151, 1986.

112. HAUSDORFF, F. Dimension und äußeres Maß. *Math. Ann.* 79: 157–179, 1919.
113. HAYASHI, H., AND S. ISHIYUKA. Chaos in molluscan neuron. In: *Chaos in Biological Systems*, edited by H. Degn, A. V. Holden, and L. F. Olsen. New York: Plenum, 1987, p. 157–166.
114. HAYASHI, H., S. ISHIYUKA, AND K. HIARAWAKA. Transition to chaos via intermittency in the onchidium pacemaker neuron. *Phys. Lett.* 98: 474–476, 1983.
115. HAYASHI, H., S. ISHIYUKA, AND K. HIRAKAWA. Chaotic response of the pacemaker neuron. *J. Phys. Soc. Jpn.* 54: 2337–2346, 1985.
116. HAYASHI, H., S. ISHIYUKA, AND K. HIRAKAWA. Instability of harmonic responses of onchidium pacemaker neuron. *J. Phys. Soc. Jpn.* 55: 3272–3278, 1986.
117. HAYASHI, H., S. ISHIYUKA, M. OHTA, AND K. HIRAKAWA. Chaotic behavior in the onchidium giant neuron under sinusoidal stimulation. *Phys. Lett.* 88: 435–438, 1982.
118. HAYASHI, H., M. NAKAO, AND K. HIRAKAWA. Chaos in the self-sustained oscillation of an excitable biological membrane under sinusoidal stimulation. *Phys. Lett.* 88: 265–266, 1982.
119. HAYASHI, H., M. NAKAO, AND K. HIRAKAWA. Entrained, harmonic, quasiperiodic and chaotic responses of the self-sustained of nitella to sinusoidal stimulation. *Phys. Soc. Jpn.* 52: 344–351, 1983.
120. HAYDON, P. G., W. WINLOW, AND A. V. HOLDEN. The effects of menthol on central neurons of the pond-snail, *Lymnaea stagnalis* (l.). *Comp. Biochem. Physiol. C Comp. Pharmacol.* 73: 95–100, 1982.
121. HEBB, D. O. *The Organization of Behavior.* New York: Wiley, 1949.
122. HENTSCHEL, G. E., AND I. PROCACCIA. The infinite number of gneralized dimensions of fractals and strange attractors. *Physica* 8: 435–444, 1983.
123. HODGKIN, A., AND A. F. HUXLEY. A quantitative description of membrane current and application to conduction and excitation in nerve. *J. Physiol. Lond.* 117: 500–544, 1952.
124. HOLDEN, A. V. *Models of the Stochastic Activity of Neurons. Lecture Notes in Biomathematics.* Heidelberg, Germany: Springer-Verlag, 1976, vol. 12.
125. HOLDEN, A. V. The response of excitable membrane models to a cyclic input. *Biol. Cybern.* 21: 1–7, 1976.
126. HOLDEN, A. V. Autorhythmicity and entrainment in excitable membranes. *Biol. Cybern.* 38: 1–8, 1980.
127. HOLDEN, A. V. The mathematics of excitation. In: *Biomathematics in 1980*, edited by A. C. S. L. Ricciardi. Amsterdam: North-Holland, 1982, p. 15–47.
128. HOLDEN, A. V., AND M. A. MUHAMAD. The identification of deterministic chaos in the activity of single neurons. *J. Electrophysiol. Tech.* 11: 135–147, 1984.
129. HOLDEN, A. V., AND S. M. RAMADAN. The response of a molluscan neurone to a cyclic input: entrainment and phase locking. *Biol. Cybern.* 41: 157–163, 1981.
130. HOLDEN, A. V., W. WINLOW, AND P. G. HAYDON. The induction of periodic and chaotic activity in a molluscan *Lymnaea stagnalis* neuron. *Biol. Cybern.* 43: 169–174, 1982.
131. HOLZFUSS, J., AND G. MAYER-KRESS. An approach to error estimation in the application of dimension algorithms. In: *Dimension and Entropies in Chaotic Systems*, edited by G. Mayer-Kress. Berlin: Springer, 1986, p. 114–121.
132. HULL, S. S., A. R. EVANS, E. VANOLI, P. B. ADAMSON, M. STRAMBA-BADIALE, D. E. ALBERT, R. D. FOREMAN, AND P. J. SCHWARTZ. Heart rate variability before and after myocardial infarction in conscious dogs at high and low risk of sudden death. *J. Am. Coll. Cardiol.* 16: 978–985, 1990.
133. IASEMIDIS, L. D., AND J. C. SACKELLARES. The evolution with time of the spatial distribution of the largest Lyapunov exponent on the human epileptic cortex. In: *Measuring Chaos in the Human Brain*, edited by D. Duke and W. Pritchard. Singapore: World Scientific, 1991, p. 49–82.
134. IASEMIDIS, L. D., J. SACKELLARES, H. ZAVERI, AND W. WILLIAMS. Phase space topography and the Lyapunov exponent of electrocorticograms in partial seizures. *Brain Topogr.* 2: 187–201, 1990.
135. ISHIZUKA, S., AND H. HAYASHI. Chaos in the onchidium pacemaker neuron under sinusoidal stimulation. In: *Proc. Annu. Meet. Physiol. Soc. Japan Tokyo Japan 59th 1982*, p. 351.
136. JANSEN, B. H. On the dimensionality of the human, scalp-recorded EEG. *Chaos Newsletter* 1: 31–33, 1990.
137. KACZMAREK, L. K., AND A. BABLOYANTZ. Spatiotemporal patterns in epileptic seizures. *Biol. Cybern.* 26: 199–208, 1977.
138. KAI, T., AND K. TOMITA. Stroboscopic phase portrait of a forced nonlinear oscillator. *Prog. Theor. Phys.* 61: 54–73, 1979.
139. KAPLAN, D., AND D. L. GLASS. Direct test for determinism in a time series. *Phys.Rev. Lett.* 68: 427–430, 1992.
140. KAPLAN, D. T., M. I. FURMAN, S. M. PINCUS, S. M. RYAN, L. A. LIPSITZ, AND A. L. GOLDBERGER. Aging and the complexity of cardiovascular dynamics. *Biophys. J.* 59: 945–949, 1991.
141. KAPLAN, J. L., AND J. A. YORKE. Chaotic behavior of multidimensional difference equations. In: *Functional Differential Equations and Approximations of Fixed Points*, edited by H. O. Peitgen and H. Walther. Heidelberg, Germany: Springer-Verlag, 1979, p. 204–227.
142. KEENER, J. P. Chaotic dynamics in mathematical aspects of physiology. In: *AMS Lectures in Applied Mathematics*, edited by F. C. Hoppenstedt. Providence, RI: Am. Math. Soc., 1981, p. 299–325.
143. KING, G. P., R. JONES, AND D. S. BROOMHEAD. Phase portraits from a time series: a singular system approach nuclear. *Physics* 2, *Suppl.*: 379–390, 1987.
144. KLEIGER, R. E., J. P. MILLER, J. T. BIGGER, A. J. MOSS, AND M. P.-I. R. GROUP. Decreased heart rate variability and its association with increased mortality after acute myocardial infarction. *Am. J. Cardiol.* 59: 256–262, 1987.
145. KLEIGER, R. E., J. P. MILLER, R. J. KRONE, J. T. BIGGER, AND M. P.-I. R. GROUP. The independence of cycle length variability and exercise testing on predicting mortality of patients surviving acute myocardial infarction. *Am. J. Cardiol.* 65: 408–411, 1990.
146. KOLMOGOROV, A. N. Entropy per unit time as a metric invariant of automorphisms. *Dokl. Akad. Nauk. SSSR* 124: 754, 1959.
147. KOWALIK, Z. J. Nonlinear behavior of Josephson junction PLL analog. *Acta Phys. Polon.* 64: 357–359, 1983.
148. KOWALIK, Z. J., T. ELBERT, AND M. HOKE. Mapping dynamic brain function: the largest Lyapunov exponent derived from multichannel magnetoencephalography. In: *Chaos in the Human Brain*, edited by B. H. Jansen. Singapore: World Scientific, 1993, p. 156–164.
149. KOWALIK, Z. J., M. FRANASZEK, AND P. PIERANSKI. Self-reanimating chaos in the bouncing ball system. *Phys. Rev.* 37: 4016–4023, 1988.
150. KOWALIK, Z. J., N. GOERKE, M. BODE, AND H. G. PURWINS. A period doubling ban in the externally driven van der Pol-like oscillator. *Dynamic Days: Proc. Annu. Workshop 13th Poznan Poland 1992.*
151. LABOS, E., AND E. LANG. On the behavior of snail neurons in the presence of cocaine. In: *Abnormal Neuronal Discharges*, edited by N. Chalayontis and M. Boisson. New York: Raven, 1978, p. 177–188.
152. LA ROVERE, M. T., G. SPECCHIA, A. MORTARA, AND P. J. SCHWARTZ. Baroreflex sensitivity, clinical correlates and cardiovascular mortality among patients with a first myocardial infarction: a prospective study. *Circulation* 78: 816–824, 1988.
153. LAUTERBORN, W., AND E. CRAMER. Subharmonic route to chaos observed in acoustics. *Phys. Rev. Lett.* 47: 1445–1448, 1981.
154. LAUTERBORN, W. Acoustic turbulence. In: *Frontiers in Physical Acoustics*, edited by X. Corso. Bologna, Italy: Soc. Italiana di Fisica, 1986, p. 123–144.
155. LAYNE, S. P., G. MAYER-KRESS, AND J. HOLZFUSS. Problems associated with dimensional analysis of electroencephalogram data. In: *Dimension and Entropies in Chaotic Systems*, edited by G. Mayer-Kress. Berlin: Springer, 1986, p. 246–256.
156. LEDRAPPIER, F., AND L. S. YOUNG. The metric entropy of diffeomorphisms. I. Characterization of measures satisfying Pesin's entropy formula. *Ann. Math.* 122: 509–539, 1985.
157. LI, T. Y., AND J. A. YORKE. Period three implies chaos. *Am. Math. Methods* 82: 985–992, 1975.

158. LIEBCHABER, A., AND J. MAURER. Une experience de Payleigh-Bérnard de Géometrie reduite; multiplication, accrochage et démultiplication des fréquences. *J. Phys. Paris* 41: 3–51, 1980.
159. LIEBOVITCH, L. S., AND T. TOTH. A fast algorithm to determine fractal dimensions by box counting. *Phys. Lett.* 141: 386–390, 1989.
160. LOMBARDI, F., G. SANDORNE, S. PERNPRUNER, R. SALA, M. GARIMOLDI, S. CERUTTI, G. BASELLI, M. PAGANI, AND A. MALLIANI. Heart rate variability as an index of sympathovagal interaction after acture myocardial infarction. *Am. J. Cardiol.* 60: 1239–1245, 1987.
160a. LORENTE DE NO, R. Cerebral cortex: architecture, intracortical connections, and motor projections. In: *Physiology of the Nervous System*, edited by F. J. Fulton. New York: Oxford Univ. Press, 1943.
161. LORENZ, E. N. Deterministic nonperiodic flow. *J. Atmos. Sci.* 20: 130–141, 1963.
162. LOUGHLIN, S. E., S. L. FOOTE, AND F. E. BLOOM. Efferent projections of nucleus locus coeruleus: topographic organization of cells of origin demonstrated by three-dimensional reconstruction. *Neuroscience* 18: 291–306, 1986.
163. LUTZENBERGER, W., N. BIRBAUMER, T. ELBERT, B. ROCKSTROH, AND H. FLOR. Dimensional analysis of the human EEG and intelligence. *Neurosci. Lett.* 143: 10–14, 1992.
164. LUTZENBERGER, W., T. ELBERT, W. J. RAY, AND N. BIRBAUMER. The scalp distribution of the fractal dimension of the EEG and its variation with mental tasks. *Brain Topogr.* 5: 27–34, 1993.
165. LYAPUNOV, A. M. *Lectures on Theoretical Mechanics* (in Russian). Charkov: Naukova Dumka, 1885–1902.
166. MACKEY, M. C., AND G. L. GLASS. Oscillation and chaos in physiological systems. *Science Wash. DC* 197: 287–289, 1977.
167. MACKEY, M. C., AND U. AN DER HEIDEN. The dynamics of recurrent inhibition. *J. Math. Biol.* 19: 211–225, 1984.
168. MANDELBROT, B. B. *Fractals: Form, Chance, and Dimension.* San Francisco, CA: Freeman, 1977.
169. Mandelbrot, B. B. *The Fractal Geometry of Nature.* New York: Freeman, 1983.
170. MANNEVILLE, P., AND Y. POMEAU. Intermittency and the Lorenz model. *Phys. Lett.* 75: 1, 1979.
171. MARTIN, G. J., N. M. MAGID, G. MYERS, P. S. BARNETT, J. W. SCHAAD, J. S. WEISS, M. LESCH, AND D. H. SINGER. Heart rate variability and sudden death secondary to coronary artery disease during ambulatory electrocardiographic monitoring. *Am. J. Cardiol.* 60: 86–89, 1987.
172. MATSUMOTO, G. Long-range spatial interactions and a dissipative structure in squid giant axons and a proposal of physical model of nerve excitation. In: *Nerve Membrane, Biochemistry and Function of Channel Proteins*, edited by G. Matsumoto Kotani. Tokyo: Univ. of Tokyo Press, 1981, p. 203–220.
173. MATSUMOTO, G., K. AIHARA, M. ICHIKAWA, AND A. TASAKI. Periodic and nonperiodic responses of membrane potentials in squid giant axons during sinusoidal current stimulation. *J. Theor. Neurobiol.* 3: 1–14, 1984.
174. MATSUMOTO, G., K. AIHARA, Y. HANYU, N. TAKAHASHI, S. YOSHIZAWA, AND J. NAGUMO. Chaos and phase-locking in normal squid axons. *Phys. Lett.* 123: 162–166, 1987.
175. MATSUMOTO, G., K. KIM, T. UEHARA, AND J. SHIMADA. Electrical and computer simulations upon the nervous activities of squid axons and around the state of spontaneous repetitive firing of action potentials. *J. Phys. Soc. Jpn.* 49: 906–914, 1980.
176. MATSUMOTO, G., N. TAKAHASHI, AND Y. HANYU. Chaos, phase locking and bifurcation in normal squid axons. In: *Chaos in Biological Systems*, edited by H. Degn, A. V. Holden, and L. F. Olsen. New York: Plenum, 1987, p. 143–156.
177. MAY, R. M. Simple mathematical models with very complicated dynamics. *Nature Lond.* 261: 459, 1976.
178. MAYER-KRESS, G. Application of dimension algorithms to experimental chaos directions. In: *Chaos*, edited by H. Bai-Lin. Singapore: World Scientific, 1987, p. 122–147.
179. MAYER-KRESS, G., AND J. HOLZFUSS. Analysis of the human electroencephlaogram with methods from nonlinear dynamics. In: *Temporal Disorder in Human Oscillatory Systems*, edited by L. Rensing, U. an der Heiden, and M. C. Mackey. Berlin: Springer, 1987, p. 57–68.
180. MAYER-KRESS, G., AND S. P. LAYNE. Dimensionality of the human electroencephalogram. In: *Perspectives in Biological Dynamics and Theoretical Medicine*, edited by S. H. Koslow, A. J. Mandell, and M. F. Shlesinger. Heidelberg, Germany: Urban & Schwarzenberg, 1987, p. 62–87.
181. MAYER-KRESS, G., F. E. YATES, L. BENTON, M. KEIDEL, W. TIRSCH, S. J. PÖPPL, AND K. GEIST. Dimensional analysis of nonlinear oscillations in brain, heart, and muscle. *Math. Biosci.* 90: 155–182, 1988.
182. MAYER-KRESS, G., F. E. YATES, L. BENTON, M. KEIDEL, W. TIRSCH, S. J. PÖPPL, AND K. GEIST. Dimensional analysis of nonlinear oscillations in brain, heart, and muscle. *Math. Biosci.* 90: 155–182, 1988.
183. MITRA, M., AND J. E. SKINNER. Low-dimensional chaos maps learning in a model neuropil (rabbit olfactory bulb). *Integrat. Physiol. Behav. Sci.* 27: 304–322, 1993.
184. MITSCHKE, F. Acausal filters for chaotic signals. *Phys. Rev.* 41: 1169–1171, 1990.
185. MITSCHKE, F., M. MÜLER, AND W. LANGE. Measuring filtered chaotic signals. *Phys. Rev.* 37: 4518–4521, 1988.
186. MOLNÁR, M., AND J. E. SKINNER. Low-dimensional chaos in event-related brain potentials. *Int. J. Neurosci.* 66: 263–276, 1992.
187. MORI, H. Fractal dimensions of chaotic flows of autonomous dissipative systems. *Progr. Theoret. Phys.* 63: 1044–1047, 1980.
188. MPITSOS, G. J. Chaos in brain function and the problem of nonstationarity: a commentary. In: *Brain Dynamics. Progress and Perspectives*, edited by E. Başar and T. H. Bullock. Heidelberg, Germany: Springer, 1989, p. 521–535.
189. MPITSOS, G. J., R. M. BURTON, H. C. CREECH, AND S. O. SOINILA. Can chaos provide readable information signals in neural networks. In: *Proc. Annu. Meet. Soc. Neurosci. 18th Toronto Ontario Canada 1988.*
190. MPITSOS, G. J., R. M. BURTON, JR., AND H. C. CREECH. Connectionist networks learn to transmit chaos. *Brain Res. Bull.* 21: 539–546, 1988.
191. MPITSOS, G. J., R. M. BURTON, JR., H. C. CREECH, AND S. O. SOINILA. Evidence for chaos in spike trains of neurons that generate rhythmic motor patterns. *Brain Res. Bull.* 21: 529–538, 1988.
192. MPITSOS, G. J., AND C. S. COHAN. Convergence in a distributed motor system: parallel processing and self-organization. *J. Neurobiol.* 7: 517–545, 1986.
193. MPITSOS, G. J., H. C. CREECH, C. S. COHAN, AND M. MENDELSON. Variability and chaos: neurointegrative principles in self-organization of motor patterns. In: *Dynamics Patterns in Complex Systems*, edited by J. A. S. Kelso, A. J. Mandell, and M. F. Shlesinger. Singapore: World Scientific, 1988, p. 162–190.
194. MYERS, G. A., G. J. MARTIN, N. M. MAGID, P. S. BARNETT, J. W. SCHAAD, J. S. WEISS, M. LESCH, AND D. H. SINGER. Power spectral analysis of heart rate variability in sudden cardiac death: comparison to other methods. *IEEE Trans. Biomed. Eng.* 12: 1149, 1986.
195. NEWHOUSE, S., D. RUELLE, AND F. TAKENS. Strange axiom-A attractors near quasiperiodic flow on T^m $m \leq 3$. *Commun. Math. Phys.* 64: 35, 1978.
196. OSBORNE, A. R., AND A. PROVENZALE. A finite correlation dimension for stochastic systems with power-law spectra. *Physica* 35: 357–381, 1989.
197. OSEDELEC, V. I. A multiplicative ergodic theorem. The Lyapunov characteristic numbers for dynamical systems (English translation). *Trudy Mosk-Mat-Obsc.* 19: 197–210, 1968.
198. PACKARD, N. H., J. P. CRUTCHFIELD, J. D. FARMER, AND R. S. SHAW. Geometry from a time series. *Phys. Rev. Lett.* 45: 712–716, 1980.
199. PALM, G. *Neural Assemblies: An Alternative Approach to Artificial Intelligence.* Berlin: Springer, 1982.
200. PARKER, G. W., L. H. MICHAEL, C. J. HARTLEY, J. E. SKINNER, AND M. L. ENTMAN. Central beta-adrenergic mechanisms may modulate ischemic ventricular fibrillation in pigs. *Circ. Res.* 66: 259–279, 1990.
201. PERKEL, D. H., J. H. SCHULMAN, T. H. BULLOCK, G. P.

MOORE, AND J. P. SEGUNDO. Pacemaker neurons: effects of regularly spaced synaptic input. *Science Wash. DC* 145: 61–63, 1964.
202. PESIN, Y. B. Lyapunov characteristic exponents and smooth ergodic theory. *Usp. Math. Nauk.* 32: 55–68, 1977.
203. PIERANSKI, P., Z. J. KOWALIK, AND M. FRANASZEK. Jumping particle model: a study of the phase space of a nonlinear dynamical system below its transition to chaos. *J. Phys. Paris* 46: 681–686, 1985.
204. PINCUS, S. Approximate entropy as a measure of system complexity. *Proc. Natl. Acad. Sci. USA* 88: 2297–2301, 1991.
205. PINCUS, S., T. CUMMINS, AND G. HADDAD. Heart rate control in normal and aborted SIDS infants. *Am. J. Physiol.* 264 (*Regulatory Integrative Comp. Physiol.* 33): R638–R646, 1993.
206. PINCUS, S., AND R. VISCARELLO. Approximate entropy: a regular measure for fetal heart rate analysis. *Obstet. Gynecol.* 79: 249–255, 1992.
207. PJIN, J. P., J. VAN NEERVEN, A. NOESTT, AND F. H. LOPES DA SILVA. Chaos or noise in EEG signals: dependence on state and brain site. *Electroencephalogr. Clin. Neurophysiol.* 79: 371–381, 1991.
208. POINCARÉ, J. H. *Les Méthodes Nouvelles de la Mécanique Céleste.* Paris: Gauthier-Villars, 1892.
209. Pratt, C. M., P. THEROUX, D. SLYMEN, A. RIORDAN-BENNETT, D. MORIESETTE, A. GALLOWAY, A. SEALS, AND A. HALLSTROM. Spontaneous variability of ventricular arrhythmias in patient at increased risk for sudden death after acute myocardial infarction: consecutive ambulatory electrocardiographic recordings in 88 patients. *Am. J. Cardiol.* 59: 278–283, 1987.
210. PRINCIPE, J. C., AND P. C. LO. Towards the determination of the largest Lyapunov exponent of EEG segments. In: *Measuring Chaos in the Human Brain*, edited by D. W. Duke and W. S. Pritchard. Singapore: World Scientific, 1991, p. 156–166.
211. PRITCHARD, W. S., AND D. W. DUKE. Deterministic chaos and the human EEG (Abstract). *Psychophysiology* 27: 56, 1990.
212. PRITCHARD, W. S., AND D. W. DUKE. Dimensional analysis of no-task human EEG using the Grassberger-Procaccia method. *Psychophysiology* 29: 182–192, 1992.
213. PRITCHARD, W. S., D. W. DUKE, AND K. L. COBURN. Dimensional analysis of topographic EEG: some methodological considerations. In: *Measuring Chaos in the Human Brain*, edited by D. W. Duke and W. S. Pritchard. Singapore: World Scientific, 1991, p. 181–198.
214. PRITCHARD, W. S., D. W. DUKE, AND K. L. COBURN. Altered EEG dynamical responsivity associated with normal aging and probable Alzheimer's disease. *Dementia* 2: 102–105, 1991.
215. RAPAPORT, E. Sudden cardiac death. *Am. J. Cardiol.* 62: 31–61, 1988.
216. RAPP, P. E. Oscillations and chaos in cellular metabolism and physiological systems. In: *Chaos—Nonlinear Science: Theory and Applications*, edited by A. V. Holden. Manchester, UK: Manchester Univ. Press, 1986, p. 179–208.
217. RAPP, P., A. ALBANO, T. SCHMAH, AND L. FARWELL. Acausally filtered noise can mimic low dimensional chaotic attractors. *Phys. Rev.* 47: 2289–2297, 1991.
218. RAPP, P. E., T. BASHORE, J. MARTINERIE, A. ALBANO, I. ZIMMERMANN, AND A. MEES. Dynamics of brain electrical activity. *Brain Topogr.* 2: 99–118, 1990.
219. Rapp, P. E., I. D. ZIMMERMANN, A. M. ALBANO, C. DEGUZMAN, AND N. N. GREENBAUM. Dynamics of spontaneous neural activity in the simian motor cortex: the dimension of chaotic neurons. *Phys. Lett.* 6: 335–338, 1985.
220. RAPP, P. E., I. D. ZIMMERMAN, A. M ALBANO, G. C. DEGUZMAN, N. N. GREENBAUM, AND T. R. BASHORE. Experimental studies of chaotic neural behaviour: cellular activity and electroencephalographic signals. In: *Nonlinear Oscillations in Biology and Chemistry* (Proceedings Utah 1985). Berlin: Springer, 1985.
221. RAY, W., K. JUNE, K. TURAJ, AND R. LUNDY. Dissociative experiences in a college age population: a factor analytic study of two dissociation scales. *Person. Individ. Differ.* 13: 417–424, 1992.
222. RAY, W., R. MORAGA, W. LUTZENBERGER, T. ELBERT, AND N. BIRBAUMER. Non-linear dynamical analysis of the EEG in task and individual differences (Abstract). *Psychophysiology* 30: 53, 1993.
223. RAY, W., R. WELLS, T. ELBERT, W. LUTZENBERGER, AND N. BIRBAUMER. EEG and chaos: dimensional estimation of sensory and hypnotic processes. In: *Measuring Chaos in the Human Brain*, edited by D. Duke and W. Pritchard. Singapore: World Scientific, 1991, p. 199–215.
224. RAY, W. J., R. WELLS, T. ELBERT, W. LUTZENBERGER, AND N. BIRBAUMER. Using chaos to understand EEG measures. *Int. J. Psychophysiol.* 14: 143–144, 1993.
225. RÉNYI, A. *Probability Theory.* Amsterdam: Elsevier North-Holland, 1970.
226. RICH, M. A. W., J. S. SAINI, R. E. KLEIGER, R. M. CARNEY, A. TEVELDE, AND K. E. FREEDLAND. Correlation of heart rate variability with clinical and angiographic variables and late mortality after coronary angiography. *Am. J. Cardiol.* 62: 714–717, 1988.
227. ROCKSTROH, B., T. ELBERT, A. CANAVAN, W. LUTZENBERGER, AND N. BIRBAUMER. *Slow Cortical Potentials and Behaviour.* Heidelberg, Germany: Urban & Schwarzenberg, 1989.
228. RÖSCHKE, J. *Eine Analyse der nichtlinearen EEG-Dynamik.* Göttingen, Germany: Univ. of Göttingen, 1986.
229. RÖSCHKE, J., AND J. ALDENHOFF. A nonlinear approach to brain function: deterministic chaos and sleep EEG. *Sleep* 15: 95–101, 1991.
230. RÖSCHKE, J., AND E. BAŞAR. Is EEG a simple noise or a "strange attractor"? *Pfluegers Arch.* 405: R45, 1985.
231. RÖSCHKE, J., AND E. BAŞAR. The EEG is not a simple noise: strange attractors in intracranial structures. In: *Dynamics of Sensory and Cognitive Processing by the Brain*, edited by E. Başar. New York: Springer, 1988, p. 203–216.
232. RÖSCHKE, J., AND E. BAŞAR. Self-similarity and strange attractors in high and low frequency EEG: 65th meeting of the Deutsche Physiologische Gesellschaft (German Physiological Society). *Pfluegers Eur. J. Physiol.* 411, *Suppl.* 1: R121, 1988.
233. RÖSCHKE, J., AND E. BAŞAR. Correlation dimensions in various parts of cat and human brain in different states. In: *Brain Dynamics. Progress and Perspectives*, edited by E. Basar and T. H. Bullock. Berlin: Springer, 1989, p. 131–148.
234. RÖSCHKE, J., J. FELL, AND P. BECKMANN. The calculation of the first positive Lyapunov exponent in sleep EEG data. *Electroencephalogr. Clin. Neurophys.* 86: 348–352, 1993.
235. RÖSSLER, O. E. An equation for hyperchaos. *AMS Lect. Appl. Math.* 17: 141–156, 1979.
236. RUSSELL, D. A., J. D. HANSON, AND E. OTT. Dimension of strange attractors. *Phys. Rev. Lett.* 45: 1175–1178, 1980.
237. SACKELLARES, J. C., L. D. IASEMIDIS, H. P. ZAVERI, W. J. WILLIAMS, AND T. W. HOOD. Inference on the chaotic behavior of the epileptogenic focus (Abstract). *Epiliepsia* 29: 682, 1989.
238. SACKELLARES, J. C., L. D. IASEMIDIS, H. P. ZAVERI, AND W. J. WILLIAMS. Measurement of chaos to localize seizure onset (Abstract). *Epiliepsia* 30: 663, 1989.
239. SAERMARK, K., J. LEBECH, C. K. BAK, AND A. SABERS. Magnetoencephalography and attractor dimension: normal subjects and epileptic patients. In: *Brain Dynamics: Progress and Perspectives*, edited by E. Başar and T. H. Bullock. Heidelberg, Germany: Springer, 1989, p. 149–157.
240. SANO, M., S. SATO, AND Y. SAWADA. Global spectral characterization of chaotic dynamics. *Prog. Theor. Phys.* 76: 945–949, 1986.
241. SANO, M., AND Y. SAWADA. Measurement of the Lyapunov spectrum from a chaotic time series. *Phys. Rev. Lett.* 55: 1082–1085, 1985.
242. SATO, S., M. SANO, AND Y. SAWADA. Practical methods of measuring the generalized dimension and the largest Lyapunov exponent in high dimensional chaotic systems. *Prog. Theor. Phys.* 77: 1–5, 1987.
243. SCHUSTER, H. G. *Deterministic Chaos.* Weinheim, Germany: Verlag Chemie, 1989.
244. SCHUSTER, H. G., S. MARTIN, AND W. MARTIENSSEN. New method for determining the largest Liaponov exponent of simple nonlinear systems. *Phys. Rev.* 33: 3547–3549, 1986.
245. SHAW, R. Strange attractors, chaotic behavior, and information flow. *Z. Naturforsch.* 36: 80–112, 1981.

246. SHIMADAL, I., AND T. NAGASHIMA. A numerical approach to ergodic problems of dissipative dynamical systems. *Prog. Theor. Phys.* 61: 1605–1616, 1979.
247. SHINAGAWA, Y., K. KAWANO, AND H. MATSUDA. Fractal dimensions on brain. In: *Proc. Annu. Meet. Physiol. Soc. of Japan 66th Okayama Japan 1989*, p. 145.
248. SKARDA, C. A., AND W. J. FREEMAN. How brains make chaos in order to make sense of the world. *Behav. Brain Sci.* 10: 161–195, 1987.
249. SKINNER, J. E. Neurocardiology: brain mechanisms underlying fatal cardiac arrhythmias. *Neurol. Clin.* 11: 325–351, 1993.
250. SKINNER, J. E., C. CARPEGGIANI, C. E. LANDISMAN, AND K. W. FULTON. Low-dimensional chaos in a simple biological model of neocortex: implications for cardiovascular and cognitive diorders. In: *An International Perspective on Self-Regulation and Health*, edited by J. G. Carlson and R. Seifert. New York: Plenum, 1991, p. 95–117.
251. SKINNER, J. E., C. CARPEGGIANI, C. E. LANDISMAN, AND K. W. FULTON. The correlation-dimension of the heartbeat is reduced by myocardial ischemia in conscious pigs. *Circ. Res.* 68: 966–976, 1991.
252. SKINNER, J. E., A. L. GOLDBERGER, G. MAYER-KRESS, AND R. E. IDEKER. Chaos in the heart: implications for clinical cardiology. *Biotechnology* 8: 1018–1033, 1990.
253. SKINNER, J. E., J. T. LIE, AND M. L. ENTMAN. Modification of ventricular fibrillation latency following coronary artery occlusion in the conscious pig: the effects of psychological stress and beta-adrenergic blockarde. *Circulation* 51: 656–667, 1975.
254. SKINNER, J. E., J. L. MARTIN, C. E. LANDISMAN, M. M. MOMMER, K. FULTON, M. MITRA, W. D. BURTON, AND B. SALTZBERG. Chaotic attractors in a model of neocortex: dimensionalities of olfactory bulb surface potentials are spatially uniform and event-related. In: *Brain Dynamics Progress and Perspectives*, edited by E. Başar and T. H. Bullock. Berlin: Springer-Verlag, 1990, p. 119–134.
255. SKINNER, J. E., M. MOLNAR, T. VYBIRAL, AND M. MITRA. Application of chaos theory to biology and medicine. *Integr. Physiol. Behav. Sci.* 27: 39–53, 1992.
256. SKINNER, J. E., C. M. PRATT, AND T. VYBIRAL. Reduction in the correlation dimension of heartbeat intervals precedes imminent ventricular fibrillation in human subjects. *Am. Heart J.* 125: 731–743, 1993.
257. SKINNER, J. E., AND J. C. REED. Blockade of a frontocortical-brain stem pathway prevents ventricular fibrillation of the ischemic heart in pigs. *Am. J. Physiol.* 240 (*Heart Circ. Physiol.* 9): H156–H163, 1981.
258. SOONG, A. C. K., AND C. I. J. M. STUART. Evidence of chaotic dynamics underlying the human alpha-rhythm electroencephalogram. *Biol. Cybern.* 62: 55–62, 1989.
259. STOOP, R., AND P. F. MEIER. Lyapunov exponents and dimensions determined from experimental time series. *Nucl. Phys.* 2, *Suppl.*: 582, 1987.
260. STOOP, R., AND P. F. MEIER. Evaluation of Lyapunov exponents and scaling functions from time series. *J. Opt. Soc. Am.* 5: 1037–1045, 1988.
261. STOOP, R., AND J. PARISI. Calculation of Lyapunov exponents avoiding spurious elements. *Physica* 50: 89–94, 1991.
262. TAKENS, F. Detecting strange attractors in turbulence. In: *Dynamical Systems and Turbulence. Lecture Notes in Mathematics*, edited by D. A. Rand and L. S. Young. Heidelberg: Springer-Verlag, 1981, p. 366–381.
263. TAKENS, F. Invariants related to dimension and entropies. In: *Atas do 13. Coloquio Brasiliero de Matematicas.* Rio de Janeiro: 1983.
264. THEILER, J. Spurious dimension from correlation algorithms applied to limited time-series data. *Phys. Rev.* 34: 2427–2432, 1986.
265. THEILER, J. Estimating the fractal dimension of chaotic time series. *Lincoln Lab. J.* 3: 63–86, 1990.
266. THEILER, J. Statistical precision of dimension estimators. *Phys. Rev.* 41: 3038–3051, 1990.
267. THEILER, J., B. GALDRIKIAN, A. LONGTIN, S. EUBANK, AND J. D. FARMER. Using surrogate data to detect nonlinearity in time series. In: *Nonlinear Modeling and Forecasting*, edited by E. M. Casdagli and S. Eubank. Boston, MA: Addison-Wesley, 1992, p. 163–188.
268. VAN DER POL, B., AND J. VAN DER MARK. The heartbeat considered as a relaxation oscillation, and an electrical model of the heart. *Philos. Mag.* 6: 763–775, 1928.
269. VARGHESE, L., V. P. N. NAMPOORI, AND R. PRATAP. Nonlinear analysis of an electroencephalogram EEG during epileptic seizure. *Curr. Sci. Bangalore* 56: 1039- 1041, 1987.
270. VASTANO, J. A., AND E. J. KOSTELICH. Comparison of algorithms for determining Lyapunov exponents from experimental data. In: *Dimension and Entropies in Chaotic Systems*, edited by G. Mayer-Kress. Berlin: Springer-Verlag, 1986, p. 100–107.
271. VERRIER, R. L., AND B. LOWN. Autonomic nervous system and malignant cardiac arrhythmias. In: *Brain, Behavior, and Bodily Disease*, edited by W. H., M. A. Hofer, and A. J. Stunkard. New York: Raven, 1981, p. 273–291.
272. VIANA DI PRISCO, G., AND W. J. FREEMAN. Odor-related bulbar EEG spatial pattern analysis during appetite conditioning in rabbits. *Behav. Neurosci.* 99: 964–978, 1985.
273. WATT, R. C., AND S. R. HAMEROFF. Phase space analysis of human EEG during general anesthesia. *Ann. NY Acad. Sci.* 504: 286–288, 1987.
274. WATT, R. C., AND S. R. HAMEROFF. Phase space electroencephalography (EEG): a new mode of intraoperative EEG analysis. *Int. J. Clin. Monit. Comput.* 5: 3–13, 1988.
275. WEST, B. J. Fractal forms in physiology. *Int. J. Mod. Phys.* 4: 1629–1669, 1990.
276. WEST, B. J. *Fractal Physiology and Chaos in Medicine.* Singapore: World Scientific, 1990.
277. WOLF, A., J. B. SWIFT, H. L. SWINNEY, AND J. A. VASTANO. Determining Lyapunov exponents from a time series. *Physica* 16: 285–317, 1985.
278. XU, N., AND J. XU. The fractal dimension of EEG as a physical measure of conscious human brain activities. *Bull. Math. Biol.* 50: 559–565, 1988.
279. YAO, Y., AND W. J. FREEMAN. Model of biological pattern recognition with spatially chaotic dynamics. *Neural Networks* 3: 153–170, 1990.
280. YOUNG, L. S. Dimension, entropy and Lyapunov exponents. *J. Ergodic Theory Dynam. Syst.* 2: 109–124, 1982.